January 2012

Statistical Analysis Of Diffusion Bonding Nickel Using Brass Interlayers

Erik Dale Anderson

STATISTICAL ANALYSIS OF DIFFUSION BONDING NICKEL USING BRASS INTERLAYERS

by

Erik Dale Anderson
Bachelor of Science, University of North Dakota, 2010

A Thesis
Submitted to the Graduate Faculty

of the

University of North Dakota

In partial fulfillment of the requirements

For the degree of

Master of Science

Grand Forks, North Dakota
December
2012

This thesis, submitted by Erik Anderson in partial fulfillment of the requirements for the Degree of Master of Science from the University of North Dakota, has been read by the Faculty Advisory Committee under whom the work has been done and is hereby approved.

Dr. Matthew Cavalli

Dr. Brian Tande

Dr. William Semke

This thesis meets the standards for appearance, conforms to the style and format requirements of the Graduate School of the University of North Dakota, and is hereby approved.

Dr. Wayne Swisher
Dean of the Graduate School

Date

PERMISSION

Title Statistical Analysis of Diffusion Bonding Nickel Using Brass Interlayers

Department Mechanical Engineering

Degree Master of Science

In presenting this thesis in partial fulfillment of the requirements for a graduate degree from the University of North Dakota, I agree that the library of this University shall make it freely available for inspection. I further agree that permission for extensive copying for scholarly purposes may be granted by the professor who supervised my thesis work or, in his absence, by the chairperson of the department or the dean of the Graduate School. It is understood that any copying or publication or other use of this thesis or part thereof for financial gain shall not be allowed without my written permission. It is also understood that due recognition shall be given to me and to the University of North Dakota in any scholarly use which may be made of any material in my thesis.

Signature Erik Anderson

Date 12/1/12

TABLE OF CONTENTS

LIST OF FIGURES

LIST OF TABLES

ACKNOWLEDGEMENTS

I wish to express my sincere appreciation to the members of my advisory committee for their guidance and support during my time in the graduate program at the University of North Dakota.

ABSTRACT

The goal of this project is a statistical study of diffusion bonding of commercially pure Ni with a brass interlayer. Four factors were investigated; time, temperature, surface finish, and foil thickness. A Box-Behnken design was selected to analyze the system for composition and strength of the bonded joints. Bonding of the materials was successful. The composition results proved to provide a good model with a fairly low standard error that can accurately predict the composition of the system across the diffusion bond area. The strength model provided two significant terms, and had a very high standard error. This meant that the model was not very good at predicting the strength of the joint because of manufacturing variation and human introduced errors. An attempt was made to combine the composition model with the strength model, but the variation of the strength data allowed no trend to be discerned.

CHAPTER I

INTRODUCTION

Nickel and nickel-based alloys demonstrate a good resistance to corrosion and heat [1]. These materials are used in aerospace, medical, and energy applications [1]. Both the composition and microstructure of components in these environments will affect their service life. Traditional joining techniques, such as fusion welding, will generate heat affected zones that destroy the microstructure, leading to a loss of strength or premature failure [2]. To avoid the degradation of the component, the appropriate microstructure has to be maintained. One method of joining that has the potential do so is diffusion bonding [3]. Diffusion bonding can create a joint between two surfaces through diffusion, rather than bulk melting. The benefit of diffusion bonding is a better ability to maintain the crystal structure throughout the component, eliminating heat affected areas from the joining process that can be detrimental to strength and wear resistance [3]. Because diffusion bonding can create joints that do not have these types of flaws, it is beneficial to determine the optimal conditions for diffusion bonding Ni [4]. Information available in the literature concerning this research is discussed in this chapter including background information on the joining process, the materials used for bonding, and the methods used for joining.

Overview of Joining Methods

When a material is locally heated and melted to cause fusion, the material's has its microstructure is destroyed. The material is thermally stressed on cooling and, typically, the weld area is more brittle than the surrounding material. These heat affected zones typically contain residual stresses and can potentially contain different phases of materials [1, 4, 5]. These features mean that there is an increase in the free energy of the material which can cause it to be more susceptible to a corrosive environment. These features are also problematic in high temperature situations due to the brittle nature of the heat affected zone. Since some of the uses of nickel are for its resistance to corrosion and for its use at high temperatures, joining it in a way that increases the susceptibility to corrosion and premature failure would be a flawed approach.

Traditional Joining of Ni

The key to the success of products that are used in corrosive and high temperature environments can be the ability of these materials to be properly joined [2]. Ni is traditionally joined through the use of conventional welding processes, such as gas tungsten-arc welding (TIG) , gas metal-arc welding (GMAW), flux-cored arc welding, submerged-arc welding, plasma-arc welding, brazing, and soldering [6]. However, certain nickel alloys possess specific characteristics that cause a need for unconventional joining techniques. Utilizing the traditional welding techniques, the joints formed typically have issues with large heat affected zones, improper weld penetration, porosity, an increased prevalence of cracking, and the formation of intermetallic regions [6]. To counter some of the effects of welding, heat treating can be done on welded materials to

potentially remove heat affected zones and dissolve intermetallic phases. The presence of heat affected zones, porosity, and cracks typically lead to increased susceptibility to corrosion. With brazing and soldering, there is better retention of base metal properties and microstructure, but the joints are typically weaker and have a lower resistance to the high temperature and corrosive environments. This is due to the fact that brazed and soldered joints are done at a temperature that can be lower than the use temperature of the Ni alloys. This is typically countered by the use of a filler metal that contains Ni and a melting point depressant. During bonding the filler metal will dissolve away the melting point depressant and leave a more stable joint [3].

Diffusion Bonding

Diffusion bonding and transient liquid phase bonding (diffusion-based bonding) are methods of joining that have the potential reduce corrosion, and high temperature failure of joints [7]. Diffusion bonding (DB) is a solid state joining process in which two materials are placed together, and through temperature or pressure, diffusion of atoms through the interface forms a joint. Initial contact, coalition, and diffusion are the stages of diffusion bonding [3]. Initial contact is the initial contact of the peaks of material based on the surface roughness. Coalition is the closing of the gaps in the surface due to surface roughness. During this stage the voids will finish closing. During the diffusion stage, the material has very minimal voids and begins diffusing from one side to the other. The three stages can be seen in Figure 1.1. This process can be applied to metal-metal, ceramic-ceramic, and metal-ceramic systems [8]. This makes it a desirable bonding method because it allows the engineer to tailor material properties to the system they are designing.

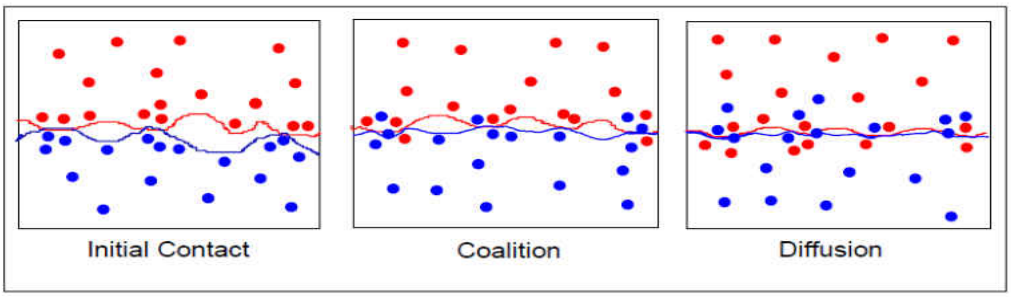

Figure 1.1: Image representing the stages of diffusion. The red and blue materials are being joined together using diffusion bonding. As the bonding progresses, atoms from each material enter the other material until the joint is cohesive.

Transient Liquid Phase Bonding

Transient liquid phase bonding (TLP), also known as diffusion brazing, is a similar process to diffusion bonding; however, it is not a solid state process [9-13]. In transient liquid phase bonding, a thin layer of material at the interface is melted either through a eutectic reaction or through the use of a foil with a lower melting point than that of the bulk material [9, 10, 11]. This liquid phase accelerates inter-diffusion of atoms. By increasing the contact area and promoting the coalescence of voids, it creates a better area of contact to assist in the diffusion process. Diffusion rates are also higher in liquid phases than in solids. A problem with this method is that during the heat up of the system there can be enough diffusion that the interlayer composition changes and the interlayer never reaches the melting point of the system [11].

Typical Experimental Parameters for Diffusion-Based Bonding

The parameters that are typically manipulated for diffusion based bonding are temperature, pressure, time, surface roughness, interlayer material, interlayer thickness and time [3, 4, 6, 8-18]. These variables are easy to control with the correct equipment

setup. Temperature can be controlled by the furnace or heating element, pressure by the load (stress) placed on the jig or sample by the machine applying the load, and time can be controlled by the controller that controls the bonding apparatus. For instance, in a furnace or press a timer can be used so that the temperature or load is applied for a set amount of time. However, variables such as the thickness of the interlayer material and surface roughness are harder to control due to the availability of commercial products and availability of processing equipment. Specific thicknesses of interlayers can be made by deforming sheets of materials or by depositing them onto the end of a specimen. Manipulating the surface finish of a specimen is typically done through polishing and the use of a regulated roughness system. Surface finish is very hard to manipulate to specific values without very specialized equipment.

Other Joining Techniques for Advanced Materials

There exist other methods of manufacturing parts from advanced materials that could be used to make coherent joints with favorable properties and microstructures [2, 7, 8]. Other solid state joining methods of bonding such as roll bonding, extrusion bonding, forge welding, and hot pressure welding, have also shown promise [19, 20, 21]. Production processes such as laser metal deposition are capable of creating coherent parts of amazingly complex geometries with close to the full material properties of the base materials from which they are based [22]. This process is commonly referred to as rapid manufacturing. Current research is being conducted on these methods as replacements to traditional manufacturing methods. However, there will still be a need, at some level, to join even large complex parts together for their end use [2]. Friction stir welding is another potential joining method. It still locally destroys the microstructure, but does not

have a need for alien elements to be introduced to the microstructure [23]. Electron beam melting is possible but it suffers the same limitations as friction stir welding. However, it has a very small heat affected zone in comparison to other techniques [24]. Significant efforts are being made across all industries to develop and characterize bonding methods for advanced materials that will allow for better performing and more efficient parts.

The difficulty with selecting a joining process is the growth of the materials being used across all industries and the new use of materials from one industry to the next. Joining processes need to be cost effective, but each industry has their own definition of what that means. Speed is a large determining factor in determining what bonding method will be used; as the number of materials needing to be joined grows more investigation needs to be done into the processes we have to bond them. Diffusion-based bonding is a method that allows for dissimilar joints to be created and allows for the favorable microstructures of the base materials to be maintained. Joining of materials and their characterization is of growing interest across all engineering industries because to utilize these advanced engineering alloys it is necessary to be able to make parts that have a maximum amount of potential.

The use of interlayers or foils for diffusion-based bonding is necessary because it helps to facilitate diffusion. By utilizing a material that has a high rate of diffusion into the base material, it can be possible to speed up the bonding process. Also, it helps to eliminate any tolerance issues that could have occurred during the preparation phase when the material, is clamped together during bonding. The foil will usually have a lower melting point than the base materials allowing its diffusion rate to increase as well

as its ability to deform to fill any areas of mismatch [1, 3, 8]. Interface thicknesses of 0.025mm have shown to produce the greatest strength [3].

Developing a method that can be used to join two parts together without disruption of their microstructure is of growing interest to engineers across multiple industries [2]. Utilizing diffusion-based joining methods, it is possible to generate a bond that has very little impact on the overall performance of the materials being joined. From previous work, it can be seen that there are difficulties with selecting a system to use for diffusion bonding [3]. Oxide layers and intermetallic regions can disrupt the bond interface and slow down or stall diffusion across it. By selecting materials that do not form intermetallics with the other materials in the system, it is possible to generate a bond that is not disrupted by the elements that surround it. Because of this feature, interlayer selection is of the upmost importance in the experimental design process in the attempt to optimize the bonding parameters.

Materials and Thermodynamics

Nickel-based superalloys are used in turbine blades that need to operate at maximum efficiency [1]. Within gas turbine engines, the parts experience extreme conditions of temperature, stress, and corrosion. The microstructure of the parts needs to be such that the parts do not have a significant increase in their susceptibility to corrosion or failure. The connection from one part to the next, the joint, is often an area where increased susceptibility can occur. This is because in some common joining techniques the desired microstructure is destroyed through melting, leaving in place a heat affected zone that is typically brittle and results in a loss of performance. Diffusion bonding is a method that has been shown to be capable of eliminating this brittle heat affected zone [7]

in nickel and its alloys. Most studies of Ni diffusion bonding involve one of the Ni superalloys; this is because of their high use in engineering applications due to their favorable properties that allow them to withstand extreme environments [10]. Diffusion-based bonding of these nickel alloys is typically done with a Ni-based interlayer with a melting point depressant, such as a Ni-boron material [11]. This type of interlayer is used because the introduction of new materials (materials not present in the bulk material) can have a negative impact on the desired properties and microstructure of the joint. Diffusion-based bonding of pure Ni has been done with several materials: Cu, B, Hf, and several brazing filler metals have been used with pure materials to form successful bonds [9]. Diffusion based bonding of Ni alloys has been done primarily with similar nickel-based brazing filler metals or nickel-based binary alloys [10]. The purpose of the nickel-based interlayers is to utilize a material that is dominant in the bulk material to cause as few disruptions in the microstructure as possible. This should allow for the strongest joints and the best bonding conditions. Transient liquid phase bonding has had great success in joining and repairing Ni-based superalloy components [9, 10, 11].

The use of diffusion-based bonding to generate joints between dissimilar materials is of significant interest because it is then possible to blend material properties to fit the desired operation. For example, a part could be combined to have the abilities of a Ni alloy on the surface of a part to protect from high heat or corrosion, and a copper or aluminum alloy that will allow for the removal of heat from the Ni on the other side. This will protect the Al and Cu alloys from the corrosive environment, but still allow those materials to do the work they would do if they were in close proximity. It is this feature of diffusion bonding that has generated interest in the nuclear power industry,

where the environments that materials can face are some of the most damaging [14]. Another example of this methodology is to use it to strategically reduce the weight of vehicles in the aerospace and automotive industries. Using Mg alloys and Al alloys for their low densities can help save weight on a vehicle; by bonding them with another material we can gain advantages of another material for its desired properties [3]. The use of diffusion bonding in this way opens this process up to a seemingly endless possibilities and combinations to be tailored to almost any specific requirements needed.

Interlayer selection is very important for diffusion bonding because the interlayer serves several purposes. Interlayers can be used when joining dissimilar materials that could form intermetallic phases to stop intermetallic formation. Interlayers can be used to enhance diffusion of elements with low diffusivities. A common example of a material that meets this requirement is a nickel that contains phosphorus because the phosphorus has a very high diffusivity into metallic systems [3]. An interlayer with a lower melting point than the bulk material can help to facilitate diffusion because diffusivity rapidly increases as the material approaches melting or is melted. Ideally, if the interlayer is melted during bonding it will then fill all the voids present in the joint and begin to solidify through diffusion into a new composition with a melting temperature that is higher than the original interlayer material. Interlayers can be identified from the analysis of phase diagrams for simple systems. If a material can absorb a significant amount of the interlayer material and not change its phase then it has the potential to be an acceptable interlayer material. Determining an acceptable interlayer for bonding is a major step in any diffusion-based bonding effort.

Fick's First Law, Equation 1.1, is a model to describe the flux (J), or flow rate, of atoms in a desired direction due to a concentration gradient ($\frac{\partial c}{\partial x}$) and the diffusivity (D) of the solute atom in the solution [6]. This equation stems from the idea of diffusion. Diffusion is driven by free energy and will typically occur from a high concentration to a low concentration. This is the material's effort to reach a lower state of Gibbs free energy. Fick's Second Law, Equation 1.2, is a second-order differential equation of Fick's First Law. It describes the change in concentration versus time (dc/dt) being equal to the second derivative of the concentration gradient. This equation takes into account that the concentration gradient changes with time (changes with diffusion). The diffusivity, D, is based on the base diffusivity, D_0, the activation energy, Q, the gas constant, R, and the absolute temperature, T (eqn. 1.3). The diffusivity is measured in m^2/s. From Equation 1.3, we know that time and temperature will be important in obtaining a strong bond because they will have an impact on the concentration of nickel that is allowed to diffuse through the interlayer and the amount of interlayer material that is allowed to diffuse into the nickel [6]. Figure 1.2 is a schematic of the joint that will be used for this work.

$$J = -D\frac{\partial c}{\partial x} \qquad eq.\ 1.1$$

$$\frac{\partial c_x}{\partial t} = D\frac{\partial^2 c_x}{\partial x^2} \qquad eq.\ 1.2$$

$$D = D_0 e^{-Q/RT} \qquad eq.\ 1.3$$

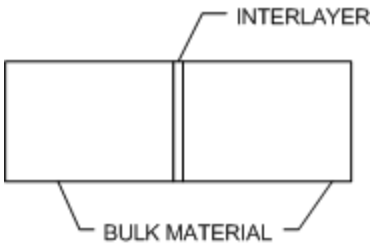

Figure 1.2: Schematic of diffusion bonded joint

Fick's laws have several limitations. There exist different types of diffusion: grain boundary, surface, and volume (bulk) diffusion. For each microstructure a different type of diffusion can dominate the flow of atoms. This knowledge makes Fick's Second Law calculations an initial estimate of diffusion. Another limitation of these preliminary diffusion equations is the assumption of perfect mating of the surfaces which is impossible to achieve with manufacturing techniques. Perfect mating also implies a perfectly clean specimen free of any foreign atoms, and does not take into account for oxidation of the surface of a material. To help determine the importance of contact area, surface finish can be used as a variable for bonding. We understand that the better the finish the more contact area the joint will have, but at what point is the surface finish sufficient to facilitate good bonding. Also, during diffusion bonding the pressure exerted on the specimen could deform the surface of the specimen increasing contact area, but during TLP bonding the bonding pressures can be much lower.

It is important to optimize the variables for diffusion bonding so that the best joints can be made and that the most efficient manufacturing can occur [4]. To investigate the effect of having more mass for diffusion, limitation interlayer foil thickness can be varied. Varying the interlayer thickness can have an impact on the joint. In some cases of TLP bonding, it is possible, with a thin enough interlayer, to diffuse all

of the interlayer material into the bulk material before the interlayer can reach its melting point. It is important to optimize the interlayer thickness for the materials being joined. It has been shown that clamping force and surface roughness can also have an impact on how thick an interlayer must be to facilitate TLP bonding [3].

Conclusion

Due to the increased use of Ni and its alloys, it is important to identify quality joining methods for these materials. Diffusion-based bonding has the potential to be an effective joining method over conventional welding techniques because it avoids the heat affected zones that are a common occurrence with these techniques. It also has potential in the fact that the joint should maintain its strength at the bonding temperature or higher depending on what interlayers are used. It should also have less susceptibility to corrosive environments due to there being no heat affected zone as in most conventional welding techniques. Knowing that there are several factors that can have a significant impact on the joining of Ni through diffusion-based bonding (DB and TLP) can aid us in the selection of experimental variables to study and optimize.

CHAPTER II

METHODS

The chemical properties of Ni are suitable for corrosive and high temperature environments. Because of its properties, Ni is being selected for increased use across many engineering industries. For this project commercially pure Ni (CP Ni) will be joined with the use of an interlayer. A response surface methodology will be applied to the system of several bonding variables to model the concentration at the bond centerline and the strength of the samples. Several interlayers were investigated for their feasibility, commercially pure aluminum (CP Al, 99.99% Al), 96 wt. % Mg 3 wt. % Al 1 wt. % Zn, and 70 wt. % Cu-30 wt. %. Zn (260 Brass). The interlayers for this project will be commercially available foils of varying thickness (Alfa Aesar, USA). The aluminum and the magnesium alloys were selected because of their use in aerospace structural applications due to their material properties. Magnesium and aluminum alloys have low density, high specific strength, and good ductility. The use of these alloys has grown to more commercial applications and offers great value over traditional material selections [3-5]. The brass alloy was selected because of copper's solubility in Ni, and previous research from UND [1].

To obtain the results desired from this research an experimental method was set up to test and compare the effects of time, temperature, surface finish, and interlayer thickness on diffusion bonding of commercially pure Ni using an interlayer. From the

earlier interlayers a single interlayer will be selected based on its viability to generate effective bonds utilizing the equipment at UND. To perform experiments in the most effective manner a design of experiments method is desired. To obtain the necessary data, two sets of experiments will be run. One set will be for composition, the second set will be for strength. Because two sets of data are needed, two specimen geometries were selected. To analyze the strength samples it was decided that tensile tests would be conducted according to ASTM E8 [26]. The composition samples will be analyzed using a Scanning Electron Microscope (SEM) and Energy Dispersive Spectroscopy (EDS). To analyze the data collected from these samples, a Box-Behnken design will be used to generate a response surface that will allow for optimization of the system in the windows that we will investigate.

Specimen Geometry

For this research, the strength test specimens were cut from 1/2" rod stock. The specimens were cut to length and a gauge section was machined out of them. The gauge section was designed according to ASTM-E8 [25]. An image of the final specimen geometry can be found in Figure 2.1. The samples will be sectioned in half and then bonded together in the gage section of the specimen for strength testing.

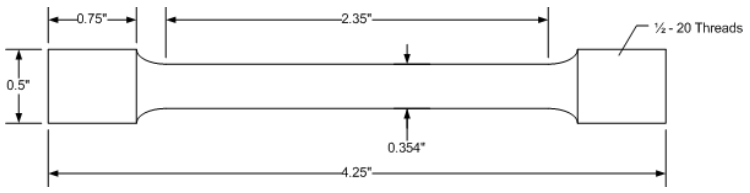

Figure 2.1: Tensile specimen geometry

The microstructure test specimens were cut from ¼"rod stock at a length of .35". To make one sample two pieces need to be cut and polished. The details of preparing each sample will follow in a later section. A schematic of the microstructure sample can be found in Figure 2.2. This figure demonstrates what the final sample will look like. The reason for the size of this sample is to conserve resources, but allow a large enough sample so that it can be easily oriented and polished.

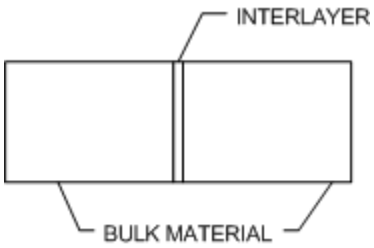

Figure 2.2: Schematic of microstructure joint inside of the jig

Material Selection

The materials to be studied in this research are a commercially pure Ni alloy 270, commercially pure Al, a Mg-Al-Zn alloy, and a 260 Brass alloy. The standard compositions for these alloys can be found in Table 2.1. Using EDS technology we analyzed the materials to determine if their compositions fell within the range of the standardized values of Table 2.1.

Table 2.1: Standard compositions for materials used in wt. %

	Ni	Cu	Zn	Mg	Al	Other
CP Ni	>99	-	-	-	-	<1
CP Al	-	-	-	-	>99	<1
Mg-Al-Zn	-	-	1	96	3	-
260 Brass	-	70	30	-	-	-

Initial investigations into each interlayer were done to allow selection of the best potential foil. As discussed earlier, intermetallics and oxide layers present in both the Al and Mg system are potential areas to avoid [4, 5]. By using vacuum, argon, and temperature we can potentially avoid formation of intermetallics and oxides. A test sample was made for the Ni-Al system and another was made for Ni-(Mg-Al-Zn).

The Al sample presents the problem of the potential to form intermetallic phases and the presence of the oxide layer on the surface of the Al. To reduce the effects of the oxide layer, a bonding temperature above the melting temperature of the bulk Al was selected. This will allow the material to flow more easily around the oxide layer and potentially remove it from the bond line. When analyzing the microstructure of the Ni-Al joint, it was discovered that intermetallic phases were formed. We know from literature that intermetallics and voids at the bond center-line result in a lack of strength of the joint [3-5]. These intermetallics are found to be stable phases on the binary phase diagram Figure 2.3. From the binary phase diagram and the wt. % information provided through the EDS analysis, it can be seen that the phases Al_3Ni_2, Al_3Ni and Al_3Ni_5 are formed in the bond area of the Ni-Al bonded joints.

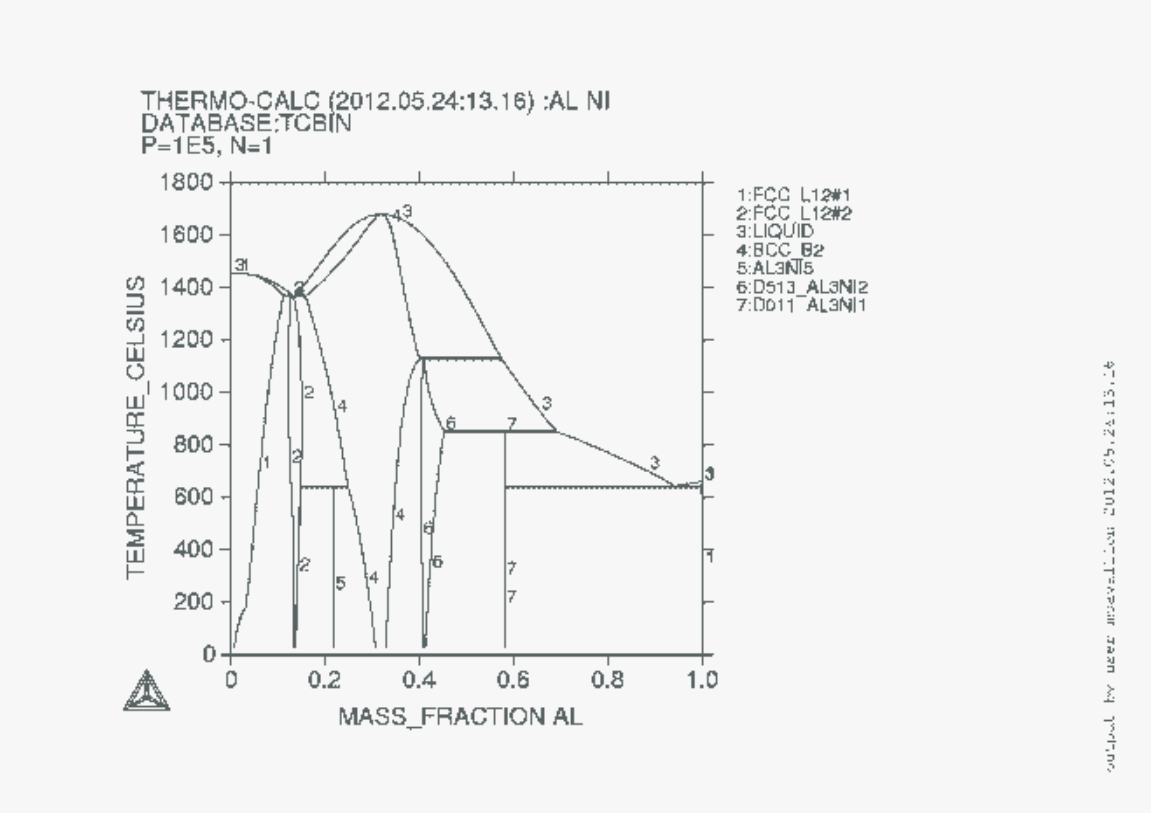

Figure 2.3: Ni-Al binary phase diagram generated from Thermo-Calc software.

The Mg-Al-Zn alloy foil was the next trial sample that was made to check the viability of this foil. The maximum vacuum that can be obtained with the equipment at UND is 0.03 Torr. Even introducing an inert atmosphere of argon in the furnace, enough oxygen was still present to cause the magnesium alloy to oxidize, as seen in Figure 2.4. For this reason, magnesium alloys were determined not valid for further testing. The sample that was made using this method was not acceptable to polish due to the thickness of the oxidation of the foil, and the apparent violence of the oxidation. The foil seems to have melted during bonding and this may have caused the sample to slip in the jig due to the thickness of the foil. Investigations into the phase diagram of the main components of this system (Ni and Mg) showed that bonding has the potential to again produce

intermetallic phases that are detrimental to strength. Phases 4 and 3 are intermetallics in Figure 2.5

Figure 2.4: Ni bonded with a Mg-Al-Zn Alloy specimen size is 0.7" long.

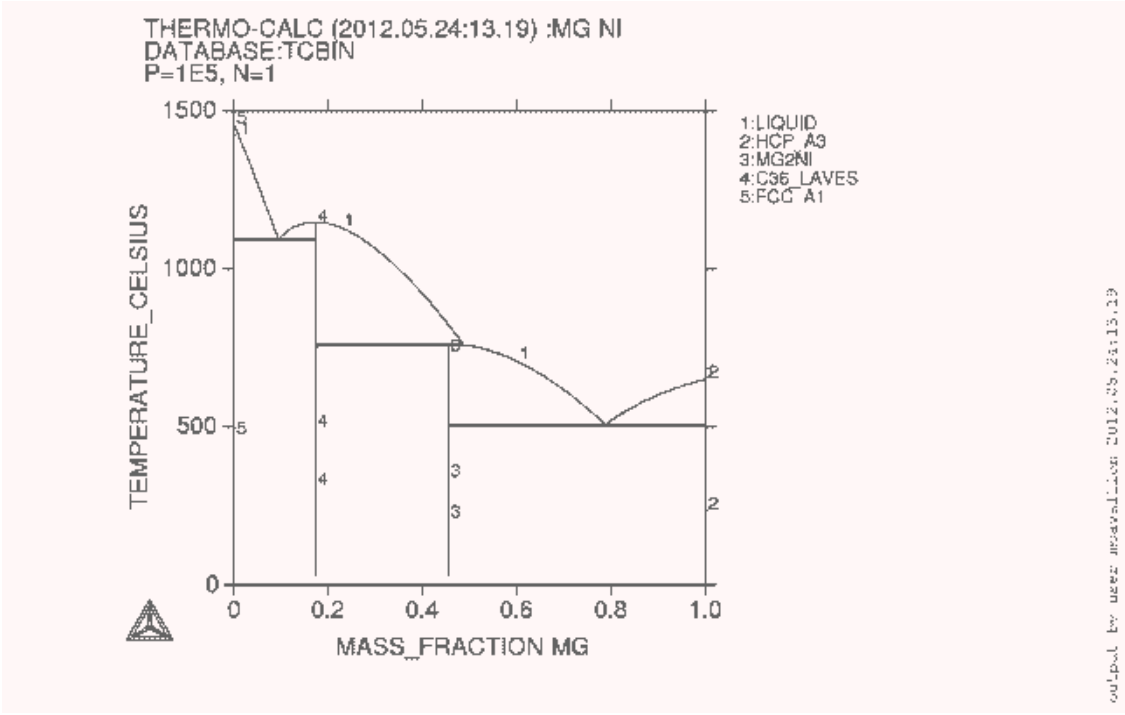

Figure 2.5: Ni-Mg binary phase diagram generated from Thermo-Calc software.

The 260 alloy brass was selected for this study because of previous work done at UND with commercially pure Ni and a commercially pure Cu interlayer. To determine if a Cu based foil would generate adequate bonds, brass and bronze alloys were looked into. Brass was chosen for preliminary investigations because Zn had a higher solubility in Ni

than Sn. The preliminary sample that was made for this testing proved to generate a bond that had very few voids and looked to generate a promising joint.

Experimental Apparatus

The experimental apparatus for this research consists of several different pieces of equipment: a tube furnace, vacuum pump, argon tank, oxygen trap, valves, a thermocouple vacuum gage, pressure regulator, and flow meters. An image of the furnace system for this research can be found in Figure 2.6.

A tube furnace was selected for this study not only for its constant heated zone, but also because it can be easily fitted with a vacuum pump. The ability to apply a constant heat to a known area of the tube means that we can set a temperature and that temperature will be applied to entire specimen. This allows us to heat the entire specimen and not introduce any unnecessary thermal stresses in the form of a thermal gradient along the specimen during bonding. This furnace is also easily calibrated using an offset temperature; this is done to ensure that the measured temperature (temperature that is measured outside the tube) and the temperature inside the furnace are the same. The procedure for furnace calibration can be found in Appendix A. Figure 2.7 shows a cutaway view of the furnace and a representation of a sample in the constant temperature zone.

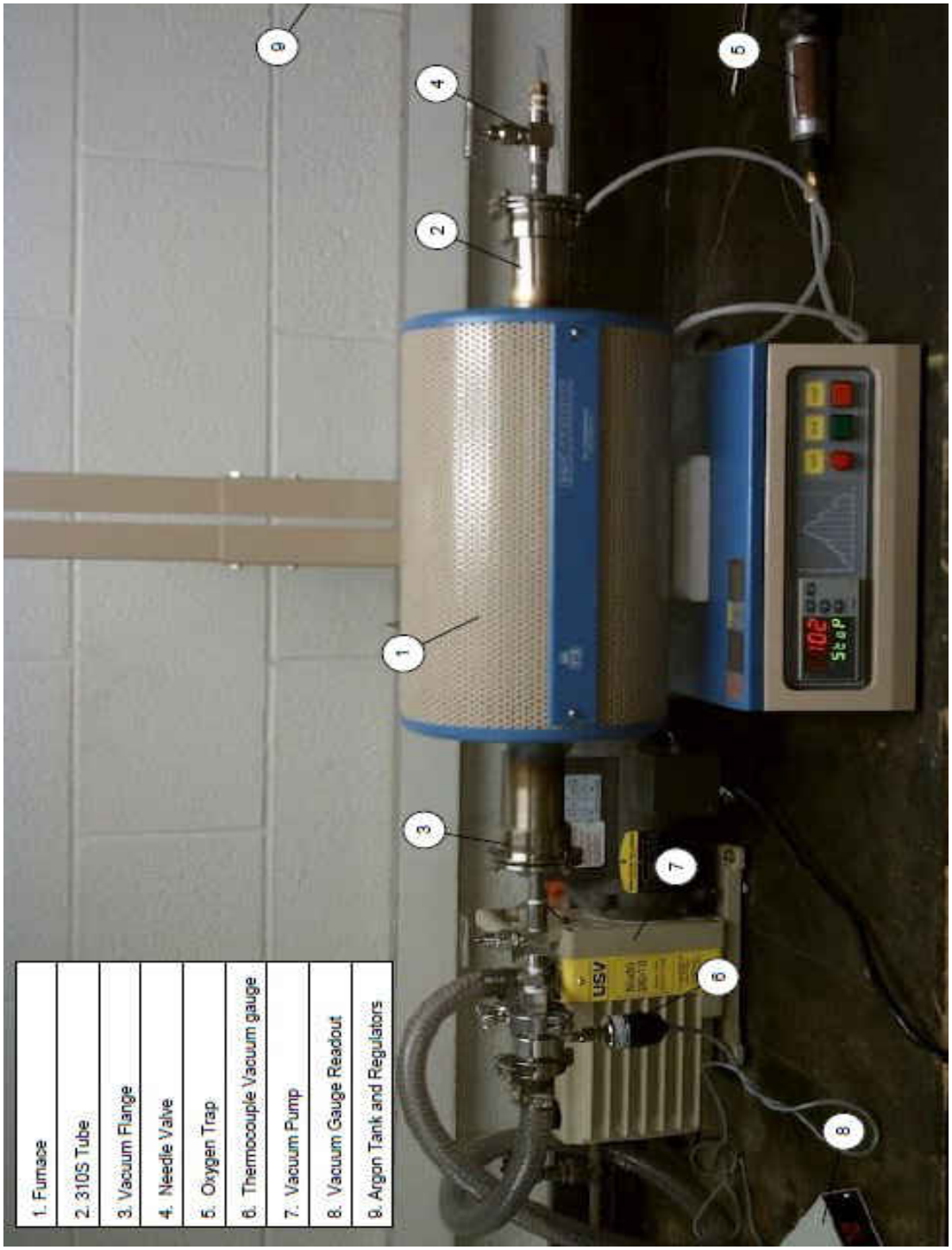

Figure 2.6: Furnace system overview. The samples are placed in the constant heat zone of the furnace. To set up the furnace the sample is sealed in the furnace and purged.

The tube supplied with the MTI GSL-1100X-110V 2" Tube Furnace was a silica tube; however, with the frequency of opening and closing of the tube and the use of stainless steel connectors to the tubing system the silica tube was too fragile to handle the wear and tear of its daily use. Because of this a stainless steel tube was put in its place, the alloy of stainless steel that was used is a 310S stainless steel. This is to allow us to use the furnace over its entire operating range. The maximum usage temperature is the same as the maximum temperature of the furnace (1100 ºC).

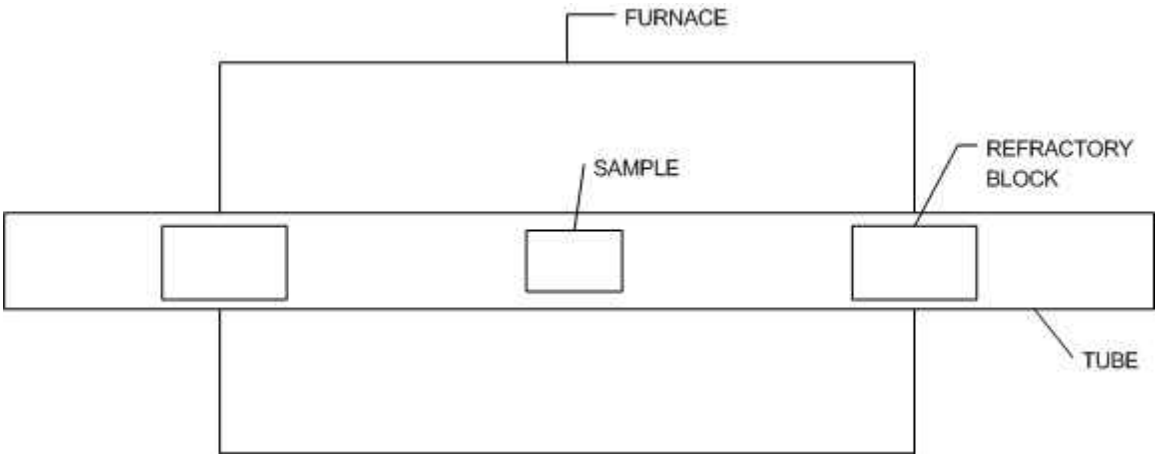

Figure 2. 7: Cutaway schematic of furnace

A cylinder of argon is used to help to reduce the amount of oxygen in the tube furnace. Argon can be used to help prevent oxidation. To help prevent any oxygen mixed with the argon gas an oxygen trap is used upstream of the furnace to help remove as much oxygen as possible from being put into the system. This cylinder and oxygen trap is used in combination with a vacuum pump that will remove as much of the oxygen from the system as possible. The vacuum pump that we are using is capable of reaching a vacuum level of 0.03 Torr. However, this level is not enough to prevent oxidation in most cases such as with Al and Mg systems

Microstructure Sample Preparation Procedure

Samples of Ni are cut from 1/4" rod stock using an IsoMet® Low Speed Saw, Figure 2.8a, from Buehler at a length of 0.35". Each microstructure sample requires two 0.35" pieces. To prepare the samples for bonding they need to be polished from their cut form. Utilizing Buehler Roll Grinders, Figure 2.8b, (320 grit, 400 grit, 550 grit, 600 grit) the samples are progressively polished. To polish to 800 grit we will use the Allied MetPrep™ polisher, Figure 2.8c, using a rotating platen.

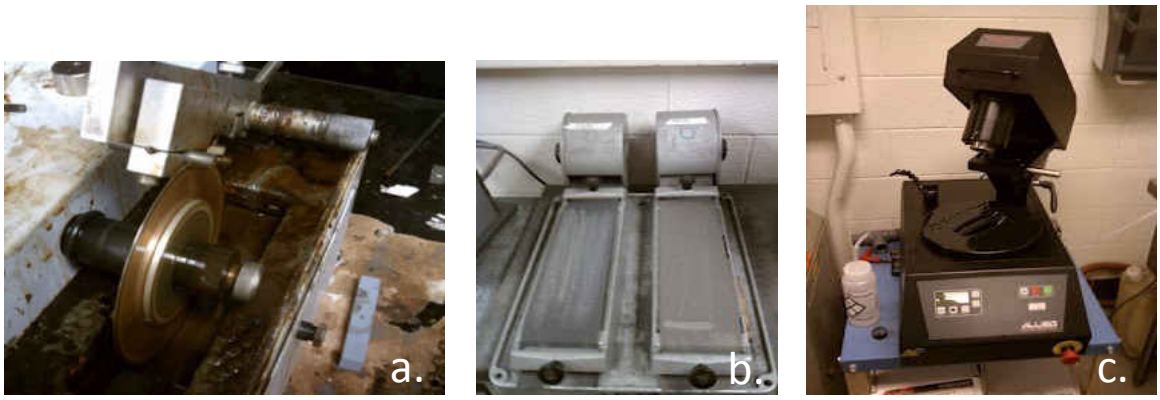

Figure 2.8: a. IsoMet® Low Speed Saw, b. Buehler Roll Grinders, c. Allied MetPrep™

After the samples have been polished to the desired finish they will be mounted in a jig Figure 2.9 and 2.10. To mount the sample in the jig two ceramic hemispheres are used to maintain force alignment. The sample is placed into the center of the jig and the holder. Anti-seize is placed on the screws and a torque of 10N*m is applied as a bonding force.

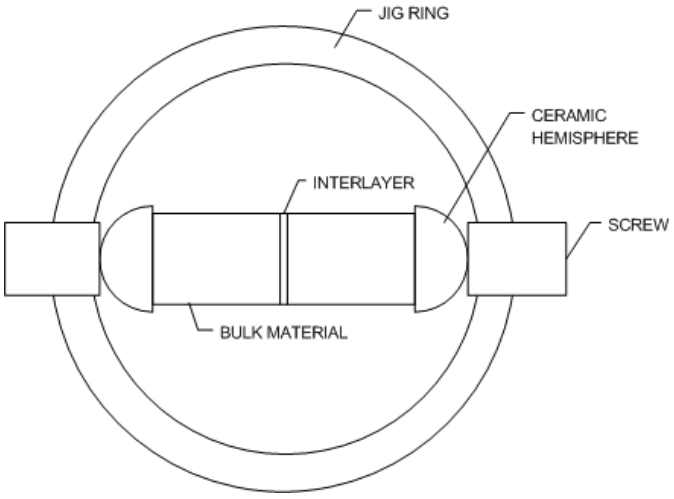

Figure 2.9: Schematic of microstructure sample in jig.

Figure 2.10: Actual image of specimen in the jig with anti-seize on the screws.

Once the sample is mounted in the bonding jig the furnace needs to be prepared. To prepare the calibrated furnace (calibration instructions in Appendix A) the sample is placed on a ceramic tray and placed in the constant heat zone of the furnace similar to Figure 2.7. Once the sample is placed in the furnace ceramic refractory blocks are placed in the ends of the furnace to help maintain heating and a constant temperature. The furnace is sealed and prepped for vacuum using the provided end caps.

Once the furnace is sealed, the furnace is vacuumed down. Once a vacuum level of ≤ 0.04 Torr is achieved according to the thermocouple vacuum gage, the purging cycle begins. Argon is used to purge the system to help in the removal of oxygen. The purge cycle procedure is to fill the tube with argon until the thermocouple gage reads ≥ 4.00 Torr. Once this is reached, close the argon valve and vacuum back down to ≤ 0.04 Torr. Repeat this process until ten purge cycles have been completed. This is to ensure as much oxygen as possible is removed from the system in a reasonable amount of time.

The furnace is set to the desired temperature and time following the procedure provided by MTI. An example of a furnace program is provided in Appendix A. The furnace is calibrated based on the intended temperature program. The offset temperature value for calibration is 86. This offset means that the furnace will be at the correct temp, without this offset the furnace would be approximately 86 ºC too high. Once the furnace has executed the program it will begin to air cool. We will allow the furnace to cool until the temperature of the furnace is less than 100 ºC. Then the furnace can be opened and the sample can be removed.

The next step to preparing a sample for the SEM is that it needs to be mounted in EpoxiCure Resin (Buhler, USA). To mount the sample in resin, a glass plate is used on a level surface. Buehler Release Agent (Buehler, USA) is applied to the glass and allowed to dry. The mixing ratio for air curing the resin is 5:1 by weight. For our sample rings a mass of 10 g of resin and 2 g of hardener will be used. After the resin has been thoroughly mixed it will be poured into a plastic sample ring with the sample in the center. Weights are placed on top of the ring to help keep resin from flowing out from under the ring. The sample is allowed to cure for approximately 12 hrs.

The samples are then polished so that we can analyze them under the SEM. This is accomplished by sanding the sample to approximately the midline of the sample. This is to allow us to see the whole picture of the bonding process. To remove this material a 3M 80 grit belt sander is used. Attention is paid to not overheat the sample during this removal process to help ensure that we are not introducing sources of error into the analysis. The sample after this process will look similar to Figure 2.10.

Figure 2.11: Samples after preliminary material removal and polishing, each plastic ring is approximately 25.4 mm wide.

The sample is then polished progressively from 320 grit to 600 grit. This process is done following a similar procedure to the surface prep for bonding the sample by rotating the sample by 90º and removing any traces of the previous polishing process. Once the sample has been polished to 600 grit, it can then be prepared using the 6 um diamond paste and MetaDi fluid, Buehler USA. To do this process a small amount of diamond paste will be placed on a Beuhler revolving platen, with a Microcloth pad, and then wetted with MetaDi fluid. The sample is held to the platen and polished until no change can be seen in the surface. Rinse the sample and begin the next stage of polishing. Using 1μm alumina powder mixed with water we will complete the polishing. To polish with

the alumina, first wet the pad with the mixture and then place the sample on the pad. This step takes approximately five minutes to complete, wetting the pad as needed.

The final step is to clean the surface of the sample after all polishing is done. To clean the sample the sample is cleaned with acetone and then wiped clean with a cloth that will not scratch the surface or leave any residue on the surface. Then a cap is placed over the sample and it is then taken to the SEM. The sample is labeled to identify it for its future analysis.

SEM and EDS Procedure

Once the sample is prepared and cleaned, it is ready to analyze using the SEM Figure 2.12. Carbon tape is applied to the sample so that the SEM can read the surface of the sample. The sample is placed on a pedestal and inserted into the SEM. The sample is analyzed by taking images of the bond at different magnifications 100x, 200x, 500x at a minimum. Certain samples are analyzed with other magnifications due to the size of the foil, points of interest in the sample, and in an effort to obtain high quality pictures for EDS analysis. From this imaging we will decide on a magnification that will allow us to perform EDS analysis. The necessary image for EDS analysis needs to have the entire diffusion area inside of it. This is estimated in the image by selecting an image that has the foil in the center of the image and has three times the foil thickness of area on each side of the bond. If this distance is not sufficient then the area is widened and the analysis is rerun.

To do the EDS analysis we will capture an image at a magnification that contains the area that we will need to scan. Then we will begin a line scan where we will select the

elements that we are interested in investigating. The elements we are looking for are those of interest contained in our materials, and those that are contained in the polishing media. The elements that we searched for were: Ni, Cu, Zn, Al, O, Si, and C. Then we chose a path that was perpendicular to the bond centerline, and analyzed the specimen for the elements contained in it. This information was extracted and analyzed in the next chapter along with the images of the joints.

Figure 2.12: Image of the SEM that was used for this analysis.

The EDS analysis is processed across the original foil thickness. This is done to smooth out any noise that the EDS analysis might have, while not affecting the other variables being researched. The EDS data output is in the form of an excel file with concentration values associated with a position in the scan. Utilizing the image we estimate the center of the bond area, and determine the area to average based on the foil thickness represented by that information. This information is then used as the Yield for the response surface design. The concentration measured for yield is Ni and Cu. Both will be compared in the results section of this paper to determine if there are any

discrepancies in the data. An example of a discrepancy would be, if in the Ni analysis a factor was significant, but in the Cu analysis that factor was insignificant.

Tensile Sample Preparation

Samples of Ni are machined from 1/2" rod stock to the specifications of ASTM E8. Then using an IsoMet® Low Speed Saw from Buehler at a length of 2.125" the sample is cut in half. Speed on the saw is set between 6 and 7 according to product information. To prepare the samples for bonding they need to be polished from their cut form. We will use the Allied MetPrep™ polisher using a spinning platen to manually polish the tensile samples by progressively increasing the grit of the abrasive disk (180, 320,600, 800). The samples that require 400 grit, are done manually on a Buhler roll grinder.

After the samples have been polished to the desired finish they are mounted in a jig. To mount the sample in the jig two ceramic hemispheres are used to maintain force alignment. The sample is placed into the center of the jig and the holder. Anti-seize is placed on the screws and a torque of 40N*m will be applied as a bonding force Figure 2.13. Once the sample is mounted in the bonding jig it is bonded using the same furnace procedure as was used for the microstructure samples.

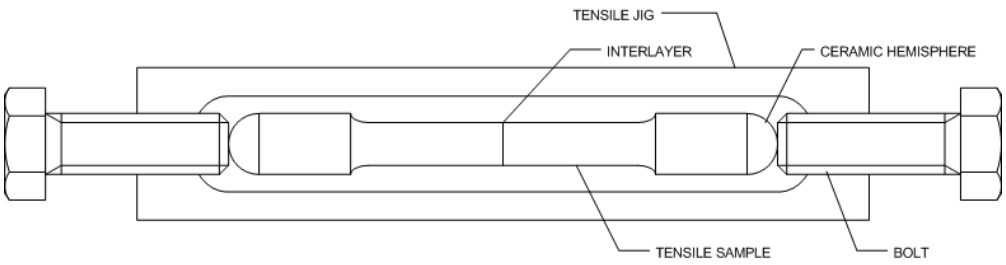

Figure 2. 13: Schematic of tensile specimen in bonding jig

To prepare the sample for tensile testing it is removed from the jig. It is then placed in the fixture in the Shimadzu AG-IS Universal Testing Machine as seen in Figure 2.15. Then the sample will be tested following ASTM E8. The rate for the test is 1 mm/min. The samples stroke vs. force curve is exported and analyzed in the results section of this thesis.

Figure 2. 14: Image of the actual tensile sample mounted in the Inconel jig.

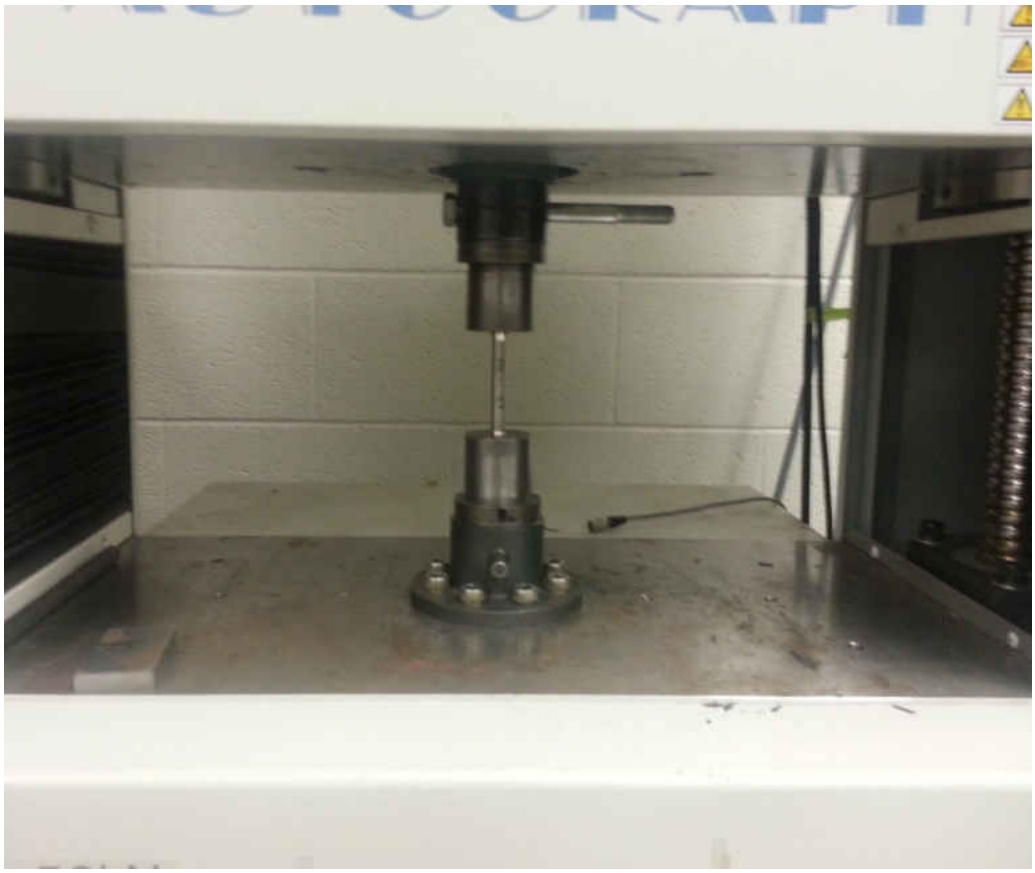

Figure 2.15: Shimadzu AG-IS Universal Testing Machine with round specimen tensile grips

Response Surface Methodology (RSM)

To analyze the information needed in the most efficient way, a response surface methodology (RSM) is used to provide us with a model of our system. A response surface methodology is a design of experiments method to analyze data utilizing as few runs as possible but gaining the most statistically significant data. The use of these methods eliminates the "hit or miss" experiments. In utilizing these methods each experiment has significance on the overall results of the work, not just that single experiment. Response surface methodology is generally used for three main steps. The design and collection of experimental data that will allow fitting a general quadratic

equation for smoothing and prediction. We will use regression analysis to select the best equation for description of the data. Finally, examine the fitted surface via contour plots and other graphical and numerical tools [27].

The generalized purpose of RSM is to determine a set of experiments that yield adequate and reliable results. The next phase is to determine a mathematical model to fit the response data utilizing the variables for the system. The final step of RSM is to determine the optimal settings of the experimental factors to gain the desired yield value.

A good RSM analysis method will be rotatable; this means that the accuracy of predictions from the quadratic equation only depends on how far from the origin the point is not the direction it is in. There are several methods for doing a RSM. A central composite design is the most common RSM analysis method. It builds on a 2^k design by adding center points and star points ($\pm\alpha$). This model is a rotatable design and fits all criterions for a good experimental design [27]. The next commonly used RSM is the Box-Behnken design. They are similar to a central composite and are explained in more detail in the next section.

Box-Behnken Design

The specific method of RSM analysis that will be used to process the data for these experiments is known as a Box-Behnken Design (BBD). BBDs have been used to optimize many systems including other joining processes such as welding and mechanical clinching [4, 24]. A BBD is made by combining two-level factorial designs with balanced incomplete block designs in a specific manner [28]. The end result is a second order rotatable design. The BBD has several advantages over other RSM

methods primarily it has fewer runs for 3 variable and 4 variable designs. The central composite design has 20 runs for 3 factors and the BBD has 15. For the four factor designs the central composite design has 30 runs while the BBD has 27.

The second major advantage of the BBD is that there are only three levels for each factor, the -1, 0, and 1 level. This is advantageous because a similar central composite design for the same number of factors requires 5 settings, the $-\alpha$,-1, 0, 1, α levels. When using commercially available products, it makes it much easier to fit three levels to commercial products as opposed to five. The BBD design runs all 2^2 designs, with the factor not being manipulated at the zero level. Center points are added to the design and replicated [27].

The downside to a BBD is that it is not a method that builds on a 2^k factorial design. This means that for four factors all 27 runs must be completed where in a central composite type design 16 runs are completed and evaluated to check to see if the additional runs are needed. For this work the assumption was made that the model would require a full response and there were significant advantages to only needing three levels of each factor. Otherwise, a central composite design would have been selected [27]. Table 2.2 shows the BBD table of experiments in their un-coded form. The analysis needs to be coded so that the importance of any one variable is not outweighed by the range of another variable so they are all scaled down to between -1 and 1.

Table 2.2: Box-Behnken Design for Ni-260 Brass diffusion bonding

run	Time (h)	Temp (ºC)	Grit (ANSI)	Foil (mm)
1	1	950	600	0.13
2	19	950	600	0.13
3	1	1050	600	0.13
4	19	1050	600	0.13
5	10	1000	400	0.025
6	10	1000	800	0.025
7	10	1000	400	0.25
8	10	1000	800	0.25
9	10	1000	600	0.13
10	1	1000	400	0.13
11	19	1000	400	0.13
12	1	1000	800	0.13
13	19	1000	800	0.13
14	10	950	600	0.025
15	10	1050	600	0.025
16	10	950	600	0.25
17	10	1050	600	0.25
18	10	1000	600	0.13
19	1	1000	600	0.025
20	19	1000	600	0.025
21	1	1000	600	0.25
22	19	1000	600	0.25
23	10	950	400	0.13
24	10	1050	400	0.13
25	10	950	800	0.13
26	10	1050	800	0.13
27	10	1000	600	0.13

Box-Behnken Analysis Methods

The Box-Behnken design (BBD) for this research will be analyzed in Minitab a computer program that has embedded statistical analysis software. The variables that will be utilized to fill the DOE table will be time, temperature, surface finish (Grit), and interlayer thickness (Foil). For a BBD there are three levels that will be used for each of

the variables we are testing. A -1, 0, and 1 coded setting is used. Due to commercial availability of specific foil thicknesses the 0 value for foil is actually -.0667. This is calculated using equation 2.1 and 2.2. This can also be seen in Table 2.3 that displays the experimental set up and the randomized run order for the experiments. The BBD was chosen for this research because only three levels were required for experimentation. This was favorable because of the use of commercially available products for Foil and Grit, and matching specific values to fit the design is a challenge.

$$Center = \frac{High\ Factor\ Value + Low\ Factor\ Value}{2} \qquad \text{Eq. 2.1}$$

$$X = \frac{Factor\ Value - Center}{High\ Factor\ Value - Center} \qquad \text{Eq. 2.2}$$

Once the analysis is run the results must be analyzed to ensure that they are as accurate as possible. First we will fit the full quadratic model. This model will utilize all of the variable terms in it and will be based on the minimization of the residual sum of squares. The next step is to check the data for outliers. This is done by calculating the residuals and constructing a normal residual plot. If the residuals appear to fall on a straight line then the data appears to have no outliers. The next step is to trim the model down to the smallest function that still models the system. This is done by deleting higher order terms that are not significant to the model. This is done one term at a time starting with the term that has the smallest t-value. If a linear term is not significant but a higher order term using that linear term is significant then we would not drop the linear term. Then we will check the residuals for trends. This is accomplished by plotting the residuals against run order if there are any trends then it indicates something should be

added to model. The final step is to display the current model in the form of contour plots.

Table 2.3: Run orders and coded values for BBD

Microstructure run order	Strength run order	standard run order	time	temp	grit	foil
2	15	1	-1	-1	0	-0.06667
25	4	2	1	-1	0	-0.06667
21	3	3	-1	1	0	-0.06667
7	11	4	1	1	0	-0.06667
22	7	5	0	0	-1	-1
8	14	6	0	0	1	-1
16	22	7	0	0	-1	1
19	24	8	0	0	1	1
11	1	9	0	0	0	-0.06667
17	18	10	-1	0	-1	-0.06667
3	5	11	1	0	-1	-0.06667
12	6	12	-1	0	1	-0.06667
27	27	13	1	0	1	-0.06667
24	26	14	0	-1	0	-1
9	12	15	0	1	0	-1
4	9	16	0	-1	0	1
23	10	17	0	1	0	1
20	25	18	0	0	0	-0.06667
6	19	19	-1	0	0	-1
15	17	20	1	0	0	-1
14	21	21	-1	0	0	1
18	2	22	1	0	0	1
13	23	23	0	-1	-1	-0.06667
10	8	24	0	1	-1	-0.06667
1	16	25	0	-1	1	-0.06667
26	20	26	0	1	1	-0.06667
5	13	27	0	0	0	-0.06667

Area Analysis of Tensile Specimen

From initial results of tensile strength testing of the diffusion based bonding joints, further analysis of the tensile specimen needed to be conducted. The initial results will be discussed in the results section in the next chapter. One potential source of these problems was incomplete bonding of the entire surface area of the bonding specimen. This was noticed after testing was completed and the analysis was beginning. To define the area that was bonded is a difficult task. One method to acquire the bonded area is to use a program designed to determine the area of parts of an image. This process is done by using thresholding of a greyscale image. Thresholding is done by using specific greyscale values to determine upper and lower control limits and selecting the material remaining in those boundaries.

Image Acquisition and Processing

To capture the images for analysis a systematic approach needed to be taken. From visual inspection, it was seen that each sample has different characteristics that define the bonded region. Each sample will start with a calibration image that is taken from the same distance, with the same manual camera settings. A manual camera was used for this process to allow for better consistency with each picture so that the process can be streamlined in the future steps. The camera is on a tripod, the lighting is the same, and the other conditions are nominally the same. The images are saved as JPEGs to the cameras hard drive for downloading and processing later.

An image is composed of pixels. Pixels are small rectangles that will display the color of that location of the image. The pixels of the image are arranged in a rectangular

array across the picture. These pixels are data points on the image. Once the image is captured, it is saved as a series of data points in the form of a JPEG or Joint Photographic Experts Group image format. This file contains information from three filters in the camera a red filter, a blue filter, and a green filter. These three colors red, green, and blue, give name to the color model that comprises the image and is known as the RGB color model or Red, Green, Blue color model. The three filters each store information on their respective colors in the form of an 8 bit code. This means that there are a possible 256 levels of intensity of each of the filter colors detected by the camera. The values of intensity stored in the image range from 0-255. The values of 255 would be a pure value for that color while 0 would mean none of that color was in that pixel. The combination of the three filters makes up the color we see with our eyes. Using this three channel 8 bit color system we are able to generate a possible 16,777,216 colors [29].

Using a tool such as Photoshop (ADOBE) it is possible to manipulate the image in terms of HSV (hue, saturation, intensity) this will not change the color characteristics, but it will change the way that we perceive the image. Contrast can also be manipulated to try and increase the difference between certain areas of an image. The images for this project will be processed to allow for the highest potential accuracy during the area analysis. The images will be cropped to only include the outside surface area of the rod (forms a circular image) saved and opened using the program ImageJ. An example of the pre-threshold image is found in Figure 2.13.

Figure 2. 16: Example of the Image before image analysis has begun.

Area Analysis

To process the area of the image the image is converted to grayscale taking the image from a 24 bit image down to an 8 bit image. This process is necessary to allow for thresholding which is a method that will allow us to capture pixels that fall within a certain limit. Essentially, thresholding is going to set upper control limits and lower control limits that allow for the bonded area to be analyzed and measured. The image will be analyzed to determine the total rod area this is done by first converting the image to a greyscale image and then adjusting the threshold settings to encompass the total area of

the rod. After this analysis is done and the value is recorded we will crop the image to only include the bonded region. The upper and lower control limits will be modified to attempt to capture the bonded area of the image. This area is measured and the value is recorded. This process will be done for each of the samples. Since this method is based on the intensity of the grey scale color it is still an estimate, but it is far more accurate than attempting to measure by hand.

Figure 2.17: Example of a fracture surface converted to a grayscale image.

CHAPTER III

RESULTS & DISCUSSION

Concentration Model

Minitab was used for all statistical analysis. A Box-Behnken response surface analysis was calculated based on the average wt. % Ni that diffuses into the brass interlayer. The experiment is set up in Minitab as a 4 factor Box-Behnken response surface design. Due to commercial availability, the Box-Behnken design had to be modified so that the zero point for foil thickness was set to -1/15. The Minitab design table can be seen in Table 3.1 this table includes the yield of wt. % Ni through the thickness of the foil used for bonding.

To calculate the yield of the concentration model, SEM and EDS analysis were done for each of the experimental runs. The EDS analysis that was performed was a fast linescan perpendicular to the bond line. The analysis distance is from an area of pure Ni through the diffusion area to another region of pure Ni. An example of the EDS analysis can be found in Figure 3.1a and b. In Figure 3.1a, we can see the joint from the SEM image, and in Figure 3.1b we see the EDS analysis curve.

Each of the 27 experimental runs underwent EDS analysis and the yield calculation is used to determine the centerline of the bond. Symmetric diffusion about the bond line is assumed. Then, using the scale of the EDS composition curve, we can

calculate and scale the data output by the EDS analysis. Knowing the thickness of the foil we can analyze the output for yield by averaging the Ni wt. % across the foil thickness for that experiment. The reason for the averaging is to try to smooth out the data from the EDS output. This allows for a more accurate picture of what is happening in the bond as opposed to taking a single data point at the centerline which could be an outlier in the data.

a.

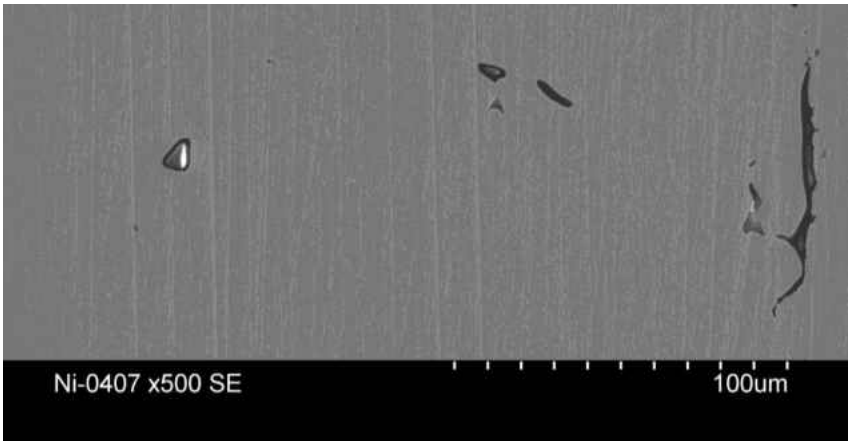

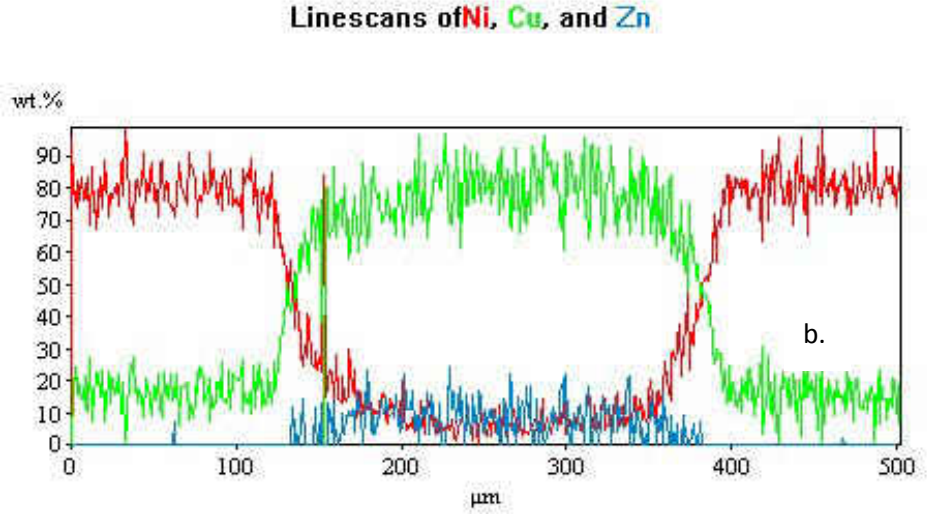

Figure 3.1 a.) SEM image of the joint, b.) EDS linescan of a bonded joint.

Table 3.1: Box-Behnken experiments table with coded values and the yield of wt. % Ni

Run	time	temp	grit	foil	wt.% Ni
1	-1	-1	0	-0.06667	20.8
2	1	-1	0	-0.06667	30.4
3	-1	1	0	-0.06667	32.1
4	1	1	0	-0.06667	42.3
5	0	0	-1	-1	50.8
6	0	0	1	-1	70.2
7	0	0	-1	1	13
8	0	0	1	1	24.1
9	0	0	0	-0.06667	9.3
10	-1	0	-1	-0.06667	17.2
11	1	0	-1	-0.06667	27.2
12	-1	0	1	-0.06667	20.4
13	1	0	1	-0.06667	50.7
14	0	-1	0	-1	49.4
15	0	1	0	-1	73.1
16	0	-1	0	1	26.3
17	0	1	0	1	22.6
18	0	0	0	-0.06667	18.2
19	-1	0	0	-1	45.1
20	1	0	0	-1	74.9
21	-1	0	0	1	15.6
22	1	0	0	1	4.5
23	0	-1	-1	-0.06667	26.9
24	0	1	-1	-0.06667	45.5
25	0	-1	1	-0.06667	41.2
26	0	1	1	-0.06667	38.4
27	0	0	0	-0.06667	24

Once the yield has been calculated Minitab is utilized to determine the model that will define the experimental windows of each of the variables analyzed if they are determined to be significant effects on the system. Once the response surface is known the model will be checked for outliers. This is done by constructing a normal residual plot, Figure 3.2, from the results data. Since the data falls inside the 95% confidence intervals we can assume that the residuals follow a normal distribution. The next analysis

step is trimming the model to its simplest significant function. From Figure 3.2, we can see that the residuals follow a normal distribution and that they fall within the 95% confidence interval and that the p-value (when the P-value for a particular factor is less than 0.05, there is a 95% confidence that one or more of the effects for that factor are nonzero) is greater than the alpha value of 0.05. This means that our data does not appear to have any shortcomings.

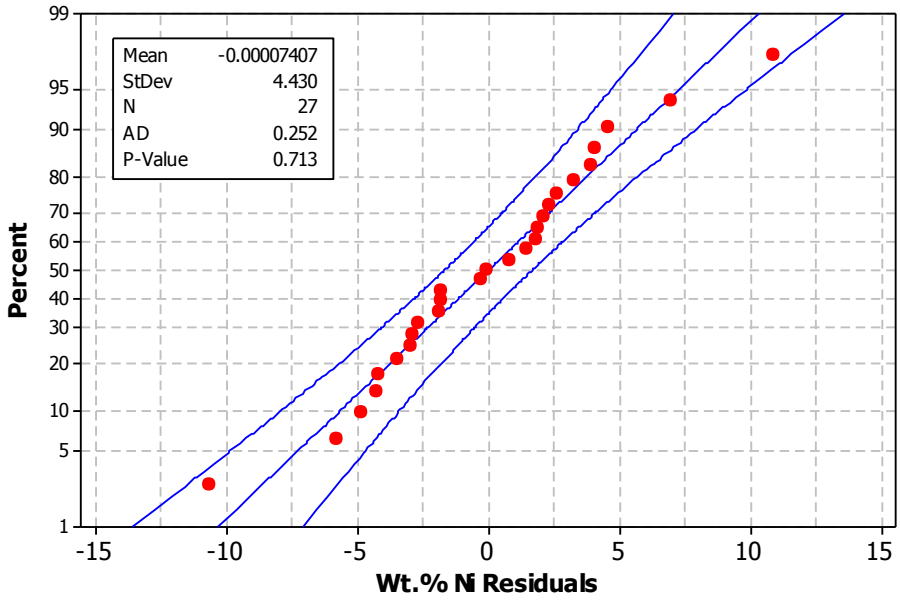

Figure 3. 2: Normal Probability Plot of the Wt.% Ni Residuals

Statistically insignificant terms are removed from the model one at a time. The analysis is then run to determine if there are additional insignificant variables to be removed. This starts with the term that has the smallest t-value [27]. Linear terms will not be dropped if there is a second order term that is significant. Second order terms are terms that combine two of the main factors such as time * temperature.

Table 3.2: Table of coefficients and their corresponding p-values

Term	Coef	t-value	p-value
Constant	15.667	4.974	0
time	6.108	3.878	0.002
temp	4.6134	2.929	0.013
grit	5.2814	3.353	0.006
foil	-21.45	-13.658	0
time*time	3.1208	1.325	0.21
temp*temp	11.5958	4.922	0
grit*grit	8.6708	3.681	0.003
foil*foil	15.6705	6.616	0
time*temp	0.15	0.055	0.957
time*grit	5.075	1.866	0.087
time*foil	-10.3205	-3.8	0.003
temp*grit	-5.35	-1.967	0.073
temp*foil	-6.8242	-2.512	0.027
grit*foil	-1.9188	-0.706	0.493

The next step in the analysis is to determine if the model is adequate. This is done by analyzing if there is a lack-of-fit, and to check the residuals for trend. Lack of fit is analyzed by Minitab and is larger than the confidence p-value of 0.05 which indicates that our model has an insignificant lack of fit, and that indicates that our model is adequate. To check the residuals for trends we will plot the residuals against run order,

Figure 3.3, to see if there are any trends that indicate that there should be something added to the model [27]. From Figure 3.3 it can be seen that there appears to be no trend in the residuals which indicates that the process did not have an impact on the experiments.

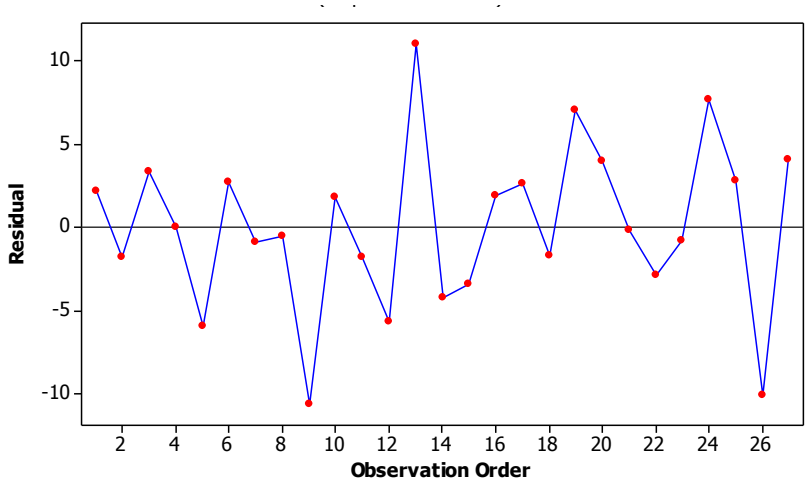

Figure 3.3: Plot of Residual Versus Observation Order

The RSM analysis that results after the model is trimmed and the residuals are checked for trends, is the model that defines the wt. % Ni at the joint midline as a function of the significant factors. The resulting model is a quadratic equation (Equation 3.1). Temperature is abbreviated as T, time is abbreviated as t, grit is abbreviated as g, foil is abbreviated as f. Figure 3.4 shows the contour plots of the model. These contour plots are a visual representation of the effects that each variable has on the yield of the system, and how they interact with other variables. Equation 3.1 and Figure 3.4 tell us that as time, temperature, surface finish increase, and foil thickness decrease, wt.% Ni increases. This fits with the theory of Fick's laws, and existing research. This tells us that the yield that we selected is one that reflects the theory behind the thermodynamics,

and that we should have confidence in using it to predict the composition of the wt.% Ni across the bond area.

$$10.556T^2 + 7.6311g^2 + 14.626f^2 + 10.32tf - 6.824Tf + 6.108T + 4.613t + 5.367g - 21.45f + 18.446 = wt.\%Ni \qquad \text{Equation 3.1}$$

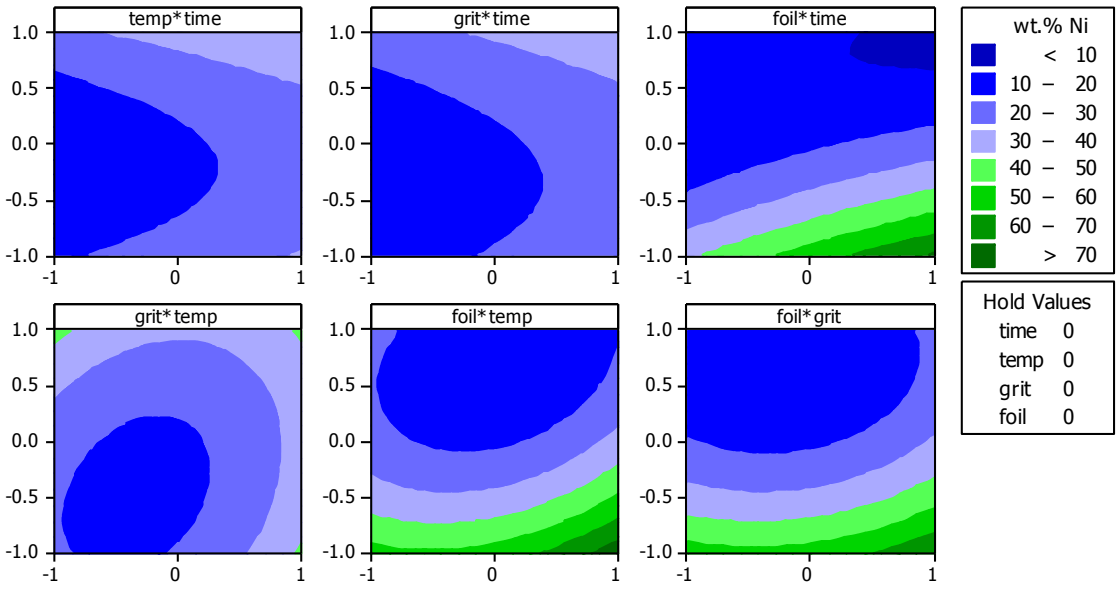

Figure 3.4: Contour plots of wt.% Ni. The green values show the settings for the model that will yield the greatest wt. % Ni.

Strength Model

The strength model will be based on the strength of diffusion bonded tensile specimens. Each specimen is tested based on ASTM E8 test standard. The yield of the strength model will be the maximum stress for each sample. This is obtained by the load cell on the universal testing machine. Then the force data is entered into Equation 3.3 where P is the load from the universal testing machine and A is the cross sectional area of the tensile specimen in the gage section. The initial analysis was done on the strength data using the cross sectional area of the tensile specimen and can be found in Appendix

D. From the initial analysis only a few factors were significant. The variance and errors were higher than those of the concentration samples, and the sign of the coefficients were the opposite of what was expected. After these results, the joints were investigated to see if there was a reason for this deviation from the expected values based on theory. One reason that was recognized was that the bonded area was not the same in each joint and that it did not span the entire cross section of the tensile sample. In an effort to better characterize strength through the maximum stress an investigation into ways to analyze the actual bond area was done. Several ideas from image analysis to EDS composition analysis were looked into. In the end Image analysis was selected due to its simplicity, and speed. The increased variance and errors meant that either the model that was fit was not suitable for this system, or that there is too much process variation in our manufacturing methods that cause this amount of noise. It is possible that the methods used to make strength joints has enough noise present in it, that the analysis simply is measuring noise.

By utilizing an image analysis program called ImageJ, it is possible to analyze an area of an image to get an estimate of area from the specimen. Information on the settings used for area analysis is contained in Appendix D. It also contains information on the new area stress (S). Equation 3.2 is applied to the initial stress calculations (σ) using the area ratio (AR). The new stress is input into Minitab as the yield for the strength model to see if there is an improvement in the results. The process remains the same as the previous RSM analysis methods. The initial model for S, Table 3.3, is checked to see if the data is adequate through the use of a normal residual plot, a residual versus observation order, and a lack of fit analysis. The model is then systematically

trimmed to its lowest significant form in an effort to have the simplest model that describes the system.

Table 3. 3: Initial RSM analysis of the Strength model

Term	Coef	SE Coef	t-value	p-value
Constant	67.8519	24.31	2.791	0.016
time	-0.4591	12.16	-0.038	0.97
temp	26.6976	12.16	2.196	0.049
grit	-5.2315	12.16	-0.43	0.675
foil	27.4594	12.12	2.265	0.043
time*time	22.4542	18.18	1.235	0.241
temp*temp	9.0253	18.18	0.496	0.629
grit*grit	-16.5373	18.18	-0.909	0.381
foil*foil	-3.8569	18.28	-0.211	0.836
time*temp	17.5501	21	0.836	0.42
time*grit	26.1935	21	1.247	0.236
time*foil	-18.7164	20.97	-0.893	0.39
temp*grit	6.3145	21	0.301	0.769
temp*foil	30.0473	20.97	1.433	0.177
grit*foil	8.1713	20.97	0.39	0.704

$$S = \sigma/AR \qquad 3.2$$

The model that results from the area analysis is shown in Equation 3.3. This model is built on the yield of the stress divided by the area ratio. The model was trimmed to three terms, the constant, plus a term for temperature and foil thickness. This made sense after the initial samples were investigated because it appears that the thicker the foil the more discernible the fracture surface was. It appeared that the thicker the foil the more bonding had occurred and a higher strength was measured. Appendix D contains images of all of the fracture surfaces and their bonding settings. For this model, the

variance and standard error of the samples increased. The procedure for the analysis is again the same. Figure 3.9 is the normal probability plot, and Figure 3.10 is the residuals versus run order plot. The final model for the new strength (S) samples is shown in Figure 3.11 in the form of surface contours.

$$25.36T + 27.21f + 72.76 = S \qquad \text{Eq 3.3}$$

The increase in standard error and residuals is a cause for concern. Ideally the area analysis would have reduced the residuals and the standard error. The larger the standard error and residuals, the harder it is for a variable to prove to be significant. The fact that the residuals and standard errors increased means that there may be something else going on with the samples that image analysis could not capture. This could be something qualitative such as the quality of the bond area. Some of the samples have a very distinguished bond area where the fracture surface is easily identified. However, other samples have a very hard to distinguish bond area, which makes image analysis more difficult, but also alludes to some form of qualitative analysis being required, or that there may be a significant variable missing to help to control the bonding. Figure 3.5 shows an example of a thick foil fracture surface and a thin foil fracture surface to show the difference.

Figure 3. 5: left image is of a 25µm foil sample and the image on the right is of a 250µm sample. These images display the differences in fracture surface of the samples.

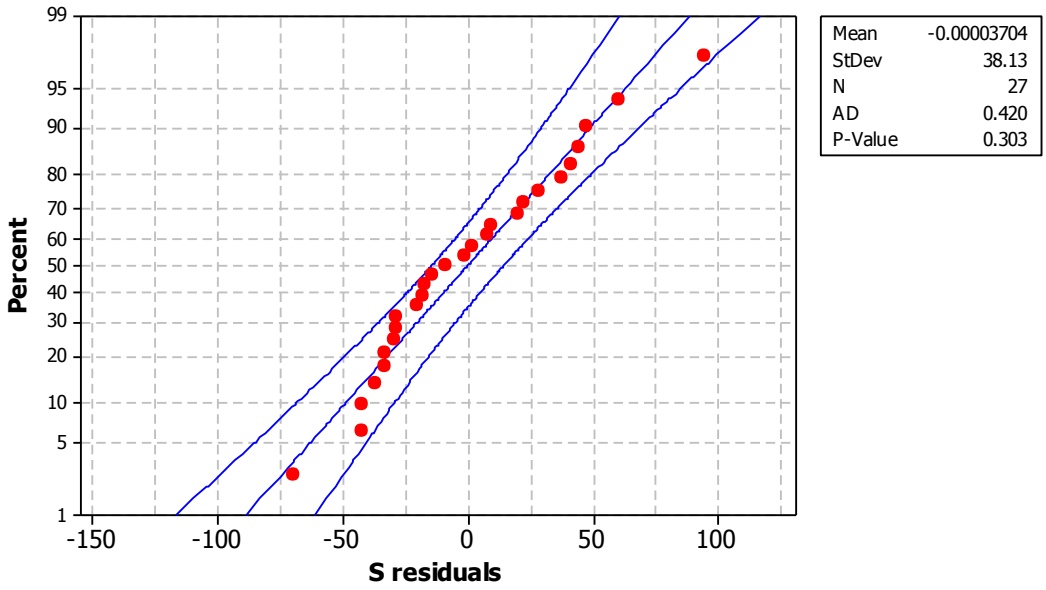

Figure 3.6: Normal residual plot for S residuals with 95% confidence intervals.

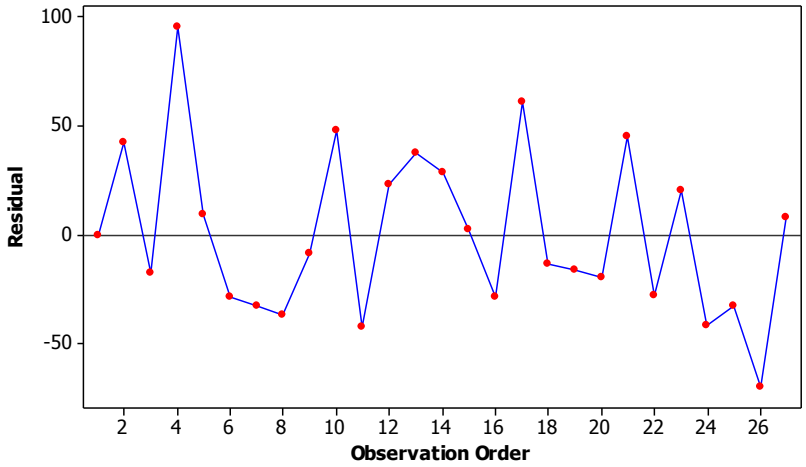

Figure 3.7: S residuals versus run order plot

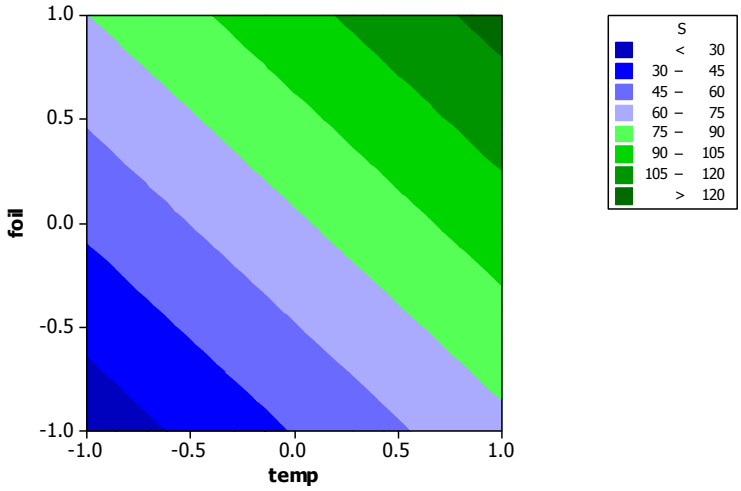

Figure 3.8: Contour plot of the S system. Areas of dark green show the highest strength. This model trimmed down to a linear model as its significant form.

Combining Concentration with Strength and RSM Optimization

The ultimate purpose of these experiments is to come up with a method for utilizing composition information of a system and being able to understand the strength that will result. By knowing how to manipulate the inputs of Time, Temperature, Surface finish, and Foil Thickness to optimize the strength of the bond that would be created. By doing this it could potentially allow an engineer to design for their system and have

confidence in the resultant strength. It would also allow for utilizing a system to develop concentration profiles and then determine the ultimate strength of the joint that would be made.

There are several models that have potential to model the system. Some of them come from composites industries, and others will come from metallurgy. These models will be examined and analyzed to see if we can utilize their theory to model our system from composition to strength. Metals are made up of an organized crystal structure based on the main element in the system. For example in steel, Fe is the main element. To give steel its properties carbon is added to it in small percentages. This increases the strength and hardness of the material by causing a disruption in the crystal structure of the material. When a stress is applied to the material that causes dislocation flow, these foreign atoms will get stuck on the dislocations and will need extra force to continue to move that dislocation. For our experiments we were using a commercially pure Ni. When diffusion bonding is done, other elements are added to the Ni in the form of Cu and Zn. It is known that Cu can be used to solid solution strengthen Ni. The combination of Cu-Ni-Zn is also known as nickel silver. Because of this we will look into solid solution strengthening models as a potential combining theory.

To determine what model should be used to fit our experimental data we will plot the experimental data obtained from the strength and concentration models. This will give us 27 data points to try and fit the model to. From the shape of this curve we will be able to determine if there is a model that we can easily fit to the data. From what we know about the Ni-Cu system it is hoped that a solid solution strengthening model will be adequately fit to the experimental data by the use of a few constants. If this model does

not fit the data then there are others that will be attempted. The variation in the strength data proved too much to allow a model to fit the data. The spread of strength for a given value of composition was too high with this number of data points to draw a conclusion. Significantly more data points would be needed to generate this model.

The rule of mixtures from composites is one of the other models that will be looked at if solid solution strengthening does not fit the data. The rule of mixtures is a method of combining the properties of two materials and getting the resulting properties of their mixture. This method is fairly simple when utilizing isotropic materials because their isotropic qualities make them more easily combined.

There are some potential reasons for deviations for the models that come from theory. Most of these will be analyzed in the next section but a few phenomenological effects that are diffusion based will be discussed in this section. The Kirkendall effect is the diffusion based effect that occurs when two or more elements are combined and they have significantly different diffusivities. This is a well-documented effect involving the elements (Ni, Cu, and Zn) that we are utilizing in this study [30]. Essentially this effect causes voids to form in the microstructure because the speed at which atoms are diffusing from one interface to the next is different. For example voids can form in the brass because the Zn is diffusing in the copper at a rapid rate [30]. Voids have also been shown to form when diffusing Cu into Ni which is the primary concentrations measured in this study. What this phenomenon will cause will be a reduction in strength because the bond area is porous, effectively reducing the cross sectional area more than can be measured in our area analysis program. The presence of voids will cause a reduction in strength. This will be reflected in the concentration strength data. Because of the way

the experiments were set up, there are 27 pairings of concentration and strength. When these samples are plotted there is too much spread in the data to see any significant trends in the data. This leads us to a very difficult time in applying any of the concentration profile because there is no discernible fit to the data. This leads me to the conclusion that work must be done to eliminate process variation from the joining process. This is the focus of the future work section of Chapter IV.

Model Verification

From the results of combining concentration and strength to one model, it was decided that each model (strength and concentration) needed to be validated through the making of additional samples. These samples were made using randomized factor values across the design window. For time, the potential values that could result were, 1 hr, 5 hr, 10 hr, 15 hr, and 19 hr. For temperature, the potential values were, 950 ºC, 975 ºC, 1000 ºC, 1025 ºC, and 1050 ºC, this was to make sure that each temperature was isolated. It is noticed that the oven may fluctuate approximately 1% of its operating temperature with an average of the programmed temperature, so temperatures were selected that would allow them have no overlap with other potential temperature settings. Foil thickness and surface finish were limited to the design variables because these are commercial products that cannot be modified easily. The settings allowed for surface finish are, 400, 600, 800 grit, and the foil thickness allowed were 25 μm, 130 μm, and 250 μm.

Table 3.6 contains the randomized settings for the three verification samples. The coded values for the samples were calculated using Equations 2.1 and 2.2. These samples were made using the same procedures as discussed in Chapter 2 and the analysis

techniques remained the same as well. To use these three points to verify the models generated for Wt. % Ni in the bond center and the model for strength, they will be compared to the value predicted by their respective models.

Table 3.4: Experimental settings and coded settings for verification specimen.

Sample	Input	Time (hr)	Temp (ºC)	Grit (ANSI)	Foil (μm)
VX1	Actual	1	950	600	25
	Coded	-1	-1	0	-1
VX2	Actual	5	1025	400	250
	Coded	- 5/9	1/2	-1	1
VX3	Actual	19	1050	800	25
	Coded	1	1	1	-1

Using a feature in Minitab to generate prediction values for experimental settings, the inputs for the variables were generated, with confidence and prediction intervals. The confidence intervals of the prediction represent a range that the mean response is most likely to fall under for those experimental settings. The prediction interval represents a range that a single observation is likely to fall given the experimental settings. The prediction interval is large because of the added variability of a single response. Table 3.4 contains the settings for the verification samples.

To determine if the model is capable of accurately predicting the experimental results we compared the experimental yields to those of the model. In this comparison we calculate the % Error and the residual of the predicted versus the experimental. This analysis was done for each set of samples (composition and strength). The results of this analysis can be seen in Table 3.5.

Table 3.5: Results of verification testing.

Sample	Input	Experiment	Predicted	Residual	% Error	Prediction Interval	
						Lower	Upper
VX1	wt. % Ni	33.2	37.2	4.0	10.80	19.6	54.9
	Strength (MPa)	30	20	-9.7	48.04	-70	110
VX2	wt. % Ni	30.7	17.8	-12.9	72.88	1.81	33.7
	Strength (MPa)	205	113	-92.1	81.72	25	200
VX3	wt. % Ni	67.9	105.9	38.0	35.89	87	124.5
	Strength (MPa)	40	71	31.2	44.03	-19	161

From this analysis it can be seen that the composition model more closely and more accurately predicts the response of the model. This is true for all but VX3. However, this point is labeled as an outlier from the Minitab output so this point is not regarded as a statistically accurate prediction. VX1 and VX2 fall within the prediction interval for composition so this means that the composition model is capable of predicting future results. The strength model has a discrepancy for VX2 in that the strength measured is higher than the strength allowed by the prediction interval. For this discrepancy the point is not an outlier so this point is considered valid. This tells us that there may be an issue with the strength model predicting future points across the experimental window. Also if we look into the prediction intervals for the strength model we will see that the range of values encompasses almost the entire range of strength values recorded. This means that essentially any of the measured data points would satisfy any of the experimental positions. This is due to the high standard error. The range of values for the prediction interval is ± 3 Standard errors. This is clearly an

issue for the strength model. It has the potential to predict values for strength, but with high standard error almost any value for strength would satisfy the prediction interval.

Potential sources of error

Solid solution strengthening will typically follow a √C trend [34]. The rule of mixtures will be a linear trend based on the strength of the main alloying elements. Of the two models looked at to fit the data this has the best chance of success. However, it would be beneficial if there was very little variation when it came to the strength of a sample at a given concentration. This is not the case, so it becomes impossible to match concentration to strength using this experimental data. To generate a tensile specimen made of a diffusion bonded joint, there is no room for error. In the composition samples, there is room for error and that is accounted for by measuring concentration at the center of the bonded joint. For a tensile specimen, the entire joint needs to be perfectly mated to its partner, with no edge effects, or defects. Since all parts are made with some form of tolerances, there is always going to be variation in the samples that we make and test, however it appears that there is something occurring with the strength samples that allows for increased error during the bonding and testing of the tensile strength joints.

There are several potential reasons for variation in the strength data. The reason for the focus on the strength data being the issue is that there is more room for error in that data, and the model showed larger residuals and variance over a similar range of yields. This is due to several factors. The first is in how the joints are machined. We have already stated that the bond area varied for each of the samples, and that that had an impact on the strength of the samples. Time as a variable can have effects on the strength

by annealing the sample at heightened temperatures. The heightened temperature of the system can relax the microstructure of the rolled bars of Ni. The fracture surface is also different for most of the samples. This indicates that the quality of the bonding is different for each of the samples as well. This can have many potential reasons: surface oxidation, variation of bonding pressure, variation of manufacturing, motion of the sample during bonding, and human imposed process variation. I believe that for future work, significant time should be spent on understanding the process parameters and their effects. For example, understanding the variation of the pressure apply by a bolt torque would be good to know so that it can be determined if the noise of that part of manufacturing is significant enough to attempt to apply a clamping load in a different way.

We know that the ability to remove oxygen from the system is limited with the equipment at UND. By not removing all of the oxygen from the system, we allow the materials the opportunity to oxidize. This is true especially at high temperature where these materials become more susceptible to oxidation. On a few of the samples there are indications (discoloration) of the Ni rods (Figure D.20). We also saw oxidation occur on the aluminum and magnesium interlayer samples. This should have a minimal effect on bonding because this area is sealed by the bonding pressure, but could increase the presence and size of edge effects. Edge effects are defined by phenomenon that only affect the edges of samples, but do not seem to impact the areas away from the edges of samples.

This would not have the same effect on the microstructure data because of the manufacturing method of the joints and the location of our measurements for yield.

Because the composition samples are manually polished the bonding surface of the composition samples becomes domed forcing contact at the center of the material where we are taking our measurements. This method of measurement was initially done in an effort to remove any edge effects, but also allows for an accurate measurement at the center of the specimen. The reason that the composition samples are hand polished is due to their small size. It is very difficult to use the automated polishing equipment for a specimen that is as small as the composition samples. Several iterations of jigs have been attempted to hold the specimen in the sample, but all had drawbacks either with their ability to hold the sample steady, or with the ability to remove the sample after polishing. In the end the manual method for polishing was selected because it was less complex and required fewer materials and time. It has already been stated that the effects of manual polishing are eliminated during analysis of the composition samples, and this iterative process is part of why this operation continued after UND gained an automated option for polishing.

Manufacturing variations are variations caused by the methods for manufacturing the samples to prepare them for bonding. One of these variations is, angled surfaces due to cutting and polishing. In the concentration samples these variations are well known and accounted for in how we process the joint for measurements, as we discussed in the above section. In the strength samples we are attempting to generate perfectly flat surfaces. We know that the surfaces will never be perfectly flat, so it is expected that there will be some variation in the mating surface and the angles at which the bond will be made, and we make the assumption that this will not impact the overall ability of our samples to be bonded together. To compensate for this all of the media used for

polishing are analyzed before each use to determine if they are holding the specimen at an angle. If the sample is held at an angle that polishing jig is discarded and a new one is made that is straight.

Over time these have the potential to drift, and that is why they are measured before each sample. However, from the strength model we saw that the bonded area is different for each sample. This indicates that there is significant variation in how the samples are bonding. From the area analysis samples it is seen that there is something else going on with the samples. This could be due to improper alignment of the two pieces of the sample. Similar to generating perfectly flat surfaces, it is impossible to perfectly match up the ends of two rods without deviating from a position that leaves no overhang. This along with surfaces that are not normal to the bonding would cause a complex stress state during bonding and during testing. During manufacturing of the joint special care is given to the samples in an attempt to create the best bonding conditions for the sample, this includes alignment.

With the equipment at UND for diffusion bonding it is impossible to control the bonding pressure during the entire process. The jigs that are used for diffusion bonding are clamped by two bolts that are wrenched to the same torque each time. By utilizing bolt torque as our clamping mode, there is a good chance that the applied load (bonding pressure) is different for every sample. Future work will be discussed in chapter 4, but I believe that future work should include pressure as a variable. Whether it is used it added as a variable factor, or it is held constant as a known impact factor, its significance needs to be investigated, or it needs to be accurately controlled. However, in this study it is neglected based on the capabilities at UND and its furnace system. Bolt torque being

constant will apply a different load each time it is applied. This is because there are changes to the threads each time the bolts are used. These changes can be, but are not limited to; debris, thread mismatch due to creep of the bolt or jig, and damaged or broken threads. All of these factors can lead to a difference in load applied by the same level of torque.

The way that the samples are held in place during bonding leaves a driving force for the sample to move, especially at high temperatures for extended periods of time. The span of the strength samples is much larger than that of the microstructure samples. This means that gravity has a much larger effect on the specimen. To counter this, supports are used during bonding to keep the sample from sagging, so it is possible that this does not factor into the problems with the strength samples. Any sagging of the sample would change the stress state from pure tension to a more complex stress state.

Human error is present in almost any scientific experiments, and while precautions are taken to limit these, they are always present in the data. Usually they will be accounted for in the noise of the experiments. From our experiments it appears that most of the noise falls in a normal distribution which means that it should not be affecting the results, but it does have the potential to skew the results. Places in this research where human error could be important, loading samples into the tensile machine, placing samples into jigs, and preparing samples for polishing are some of the potential sources of errors.

All of these potential errors could lead to the increased variance of the strength samples. From the models for strength, in the sigma model, factors like time, grit and foil,

all had signs that are the opposite of what would be expected. The signs on the coefficients are part of the assumption that there were processing errors on the strength samples. From the S and sigma samples, the positive on the foils means that the larger the foil thickness the better the strength. This goes against what I initially thought would be true and what has shown to be true in previous research [3]. The severe reduction in strength from the CP Ni samples tells me that there must be voids in the bond, or something else going on at the interface that is reducing the strength of the system.

From the strength results I believe that there is an un-accounted variable in our data that is causing significant changes to the strength of the joint. From research it appears that that variable could be bonding pressure. I believe that the processing of the concentration samples and the method of analysis reduces the effect of the manufacturing of the joints. There is a chance that there are Kirkendall voids in the area of the joint where the foil was based on the materials we are using. It is also possible that the samples are losing strength due to recrystallization of the microstructure. It appears that there is too much variation in the strength data to draw any significant conclusions about combining strength and concentration. This is unfortunate, but provides us with valuable information for future work.

The composition model follows what we expect from theory in terms of what the effect of the variables on the wt.% Ni across the bond interface would be. This tells me that while there may be some issues with the range of the model, this model can predict wt.% Ni and is a valid model. The strength results proved to have significant variation, and this points me towards the manufacturing process to create these joints. A post experiment analysis of the bonding methods left a lot to be desired in terms of

repeatability. There need to be fewer places for discrepancies to form. Weather this comes in the form of new jigs, new methods for polishing, or applying the bonding pressure, that will be the decision of future work for this project.

CHAPTER IV

CONCLUSIONS & FUTURE WORK

Conclusions

In this research study, a statistical approach was taken to examine experimental windows of time, temperature, surface finish, and foil thickness and their impact on the concentration and strength of diffusion bonded joints composed of commercially pure Nickel as the base metal with a brass interlayer. These samples were bonded in a tube furnace at a temperature range of 950 °C to 1050 °C across a range of time of 1 hour to 19 hours. The samples were made with three different foil thicknesses, 25µm, 130µm, and 250µm, and different surface finishes, 400 Grit, 600 Grit, and 800 Grit. The reason that surface finish and foil thickness contain three set values has to do with the commercial availability of the products, and the capabilities of the equipment at UND. Upon conclusions of these experiments, the results were analyzed for several different yields.

The first model was, the concentration of Ni that is diffused through the bond interface (the area of the bond that is originally composed of the interlayer) was modeled using a Box-Behnken design. This design was statistically significant in modeling the system based on the four input factors and their combinations. The model that resulted from the experiments and analysis fit theory as expected, with the signs on the coefficients of the models following what is known in theory. These known theory are,

temperature increases the diffusivity of the atoms increases, the longer the time the more atoms will diffuse across the interface, the more initial contact there is (related to surface finish) the more material should be allowed to diffuse, and the thinner the foil, the more Ni can penetrate into the bond interface because it has less distance to diffuse and the less Cu and Zn that has to diffuse out of the center. The shapes of the concentration curves obtained during EDS analysis have the same shape as those of composition profiles generated by Fick's second law. This means that the concentration analysis follows theory as presented in Chapter 1 of this thesis. The residuals for this sample followed a normal distribution which means that the errors of the measurements in relation to the model are most likely from random process variation, and not the input of an unknown factor or stimulus. The R-sq of the model being fairly high (93.17) indicates that our model accounts for most of the variability of the data. The lack of fit was insignificant meaning that there is not a significant lack of fit in our model. The validation samples fell within the prediction intervals which confirm that our model is adequate for modeling the average concentration of Ni wt.% across the bond centerline at a distance equal to that of the foil thickness.

The second model generated for this study was for the tensile strength of the diffusion bonded joints. This model was also a four factor Box-Behnken design with 27 runs, of these 27 runs, three were center points. These center points allow the model to calculate the variance. The experiments for this model matched 1 to 1 the experiments of the wt.% Ni model, meaning that for each combination of variables for the Box-Behnken design, there is a wt.% Ni value and a Strength value. This was in an attempt for future combination of the two models. The model for strength had approximately three times

the standard error and large variance in the residuals. However, the residuals followed a normal distribution. Again this distribution of residuals indicates that the errors of the measurements are generated from random process variation. The R-sq of the model being only 30.55 Indicates that most of the variability in the results is not accounted for in my data. The model passes the tests for lack of fit being insignificant, and the validation samples fell within the range allowed by the prediction intervals for the model. However, the range of allowable values for strength for each data point almost encompasses the entire range of the experimental data 11-200 MPa. This means that there is something not being accounted for causing a large error in the data. This caused a need to evaluate the methods for the experiments for the strength model.

The method for manufacturing and analyzing the strength joints leaves more room for potential errors than the composition samples. This is because the specimen leaves no room for errors in the manufacturing and bonding of the joint. To get a reliable stress value the entire cross section of the tensile sample needs to bond. This study proved that that does not happen with the current manufacturing methods. The difference between the composition samples and the strength samples is, that in the composition samples we can remove some of these manufacturing errors by polish away some of the edge effects or miss-alignment, and measuring the information on a very small scale of the sample. To counter the variation of the bond area, Image analysis was done to the samples to try to increase the accuracy of the stress measurements. This step, as seen in Appendix D, increased the standard error of the samples. This can mean many things; one interpretation of this phenomenon is that there is something going on in the process that is generating random errors following a normal distribution (the strength model's

residuals still fell within the confidence intervals of the normal probability plot, which indicates that the residuals follow a normal distribution). During processing of the samples before bonding, there are many potential places where errors could occur. These are discussed in detail in Chapter 3. These manufacturing defects are potentially uncontrollable defects. However, new attempts and methods for cutting, holding the sample during polishing, jigs used for bonding the specimen, and applying the clamp load for bonding are needed. I believe that by modifying these areas of the experimental set up the variability of the strength model would decrease and provide a much clearer picture of what is happening in the system because as of right now that image is not clear. By controlling the manufacturing methods the joints will be made in a more consistent maner than they are today. Today the joints are essentially free floating under a compressive load, if we could constrain the geometry so that there is no desire for misalignment to have an effect by using a jig that conforms precisely to the specimen geometry not allowing it the potential to move like there is today, that this could reduce the variation in strength of the samples. By reducing the process variation we may end up with a completely different strength model. This is true because if the error is high enough we stop measuring the actual strength and we are just measuring noise from the process used to make the samples. By eliminating any areas in the process that have the potential to influence the joint, hopefully, the process noise will be reduced and a more clear picture will be shown of the effect of these factors (time, temperature, surface finish, and foil thickness) on strength.

From these results an attempt was made to combine strength and concentration data. This was an important aspect of the study because it would allow for

thermodynamic simulation software to generate a concentration profile and have that profile be applied to an equation to estimate the strength of diffusion bonded joints. Having a model capable of this was the ultimate goal of this research. However, due to the size of the variance in the strength model, a model could not be easily fit that would provide any significant confidence or accuracy. From these findings it was decided that validation samples needed to be made for the models to determine if the models are adequate.

As mentioned earlier, an attempt was made to validate the models through the use of three samples generated within the design window, but not existing in the experimental design. To help the coupling of strength and concentration, the three samples for each of the two models utilized the same settings. These samples were compared to the predicted value from their respective model and in the case of the microstructure model, the model was found to be able to predict the wt.% with a decent amount of accuracy. In the case of the strength model validation, the samples proved to be fit the model well, but the prediction intervals for the samples fell across a range of 0-200 MPa. This is not a detailed enough window to draw a confident solution from. Statistically the models proved to be adequate. However, the variance of the strength model does not provide enough detail to differentiate strength values that have an order of magnitude difference.

The final conclusion of this study is a model that can predict the concentration of Ni present in the bond area after diffusion bonding. This model was validated with samples and proven to be capable of predicting future outcomes that are a part of the experimental window. This study has proven that Ni-Brass can form a diffusion bonded joint with a microstructure that has few voids, and has a high amount of Ni diffused

through the bond centerline. An attempt was made to combine the concentration model to the strength model. However, the variation of the strength data made combining the models with any amount of significance impossible. The potential reasons for this are that the process variance is high enough that the strength values vary across a large range for given experimental parameters. This means that there is a large range of strength values for a given concentration. This means that either there is something else that contributes to determining the strength of the sample, or that the process variance is too high.

Future work

For this research a lot of information on the process capabilities at UND was discovered. There are multiple places where human error or manufacturing error can have an impact on the results. I believe that a new approach should be taken in terms of generating strength samples. There are special geometry samples that allow for the measuring of tensile strength, but do not rely on the precision of bonding two rods end to end in free space. In this study there is no room for error in the strength samples based on the specimen geometry. A new jig for bonding tensile specimen or a new geometry should be designed to allow for greater process control, and the removal of any potential manufacturing errors. There are multiple references to specimen geometry for shear strength and a few that reference tensile strength as well [4, 31-33]. A reason for future work is to attempt to reduce the variance of strength data gathered for diffusion bonded joints, to try and generate greater accuracy for the models being investigated in the future.

Another potential experimental change would be to determine a way to directly control the bonding pressure of the joints. I believe that this has the greatest potential to

have significant results on diffusion bonded joints, and reduce the experimental noise. An area of potential error in these experiments is that the bonding pressure is determined by a bolt torque. This has the potential to be significantly different for each sample. Most likely these differences would appear as random noise and not cause a drift in the samples. It is likely that this noise would follow the normal distribution as well. This is because the jigs are re-threaded occasionally throughout the experimental process (every 2-3 Samples), new bolts are used after current bolts do not screw easily into the jigs anymore, the bolts and jigs are cleaned before each sample is mounted, and the bolts and jig threaded surfaces are covered in an anti-seize compound. However, all of these potential sources of drift in bonding pressure could be avoided if we had a way to simply apply a set stress to the specimen and allow it to be held constant over the bonding of the joint. If this information could then be applied to the concentration data collected here in an effort to better define the combination of strength and concentration which was the ultimate goal of this study.

A method that may work with the existing equipment would be to design the specimen geometry so that after bonding is complete the tensile specimen would be machined down from the initial specimen. Some experimentation would need to be done to determine the length to diameter ratio required to make a joint that has a fully bonded area, but this seems to be a feasible concept if the joint is sufficiently strong.

Moving the windows for experimentation would be another potentially beneficial study to complete. This study would potentially identify maximums or areas where increased polishing, time, temperature and foil thickness no longer have a significant effect on the joint. Identifying these areas is beneficial from an engineering standpoint

because it allows engineers to optimize their system not only for strength or composition, but also for cost. Applying additional time, temperature, material costs, and manufacturing (surface finishing) increases the cost of those joints. The area would potentially to be to increased temperatures, better surface finishes (higher polishing grits), a wider range of foil thicknesses, and potentially to plot the window between 0 and 1 hour. I feel that these experiments would be very helpful, but first the process variance must be investigated for the success of future work, or a method for determining strength which leaves room to remove manufacturing error before measuring strength could be useful as well.

The last suggestion for future work would be to apply this interlayer material to an engineering alloy with a high Ni content. Alloys such as nickel-based super-alloys would be perfect for these studies. Their ability to withstand high operation temperatures make them perfect for diffusion bonding because they would have a high resistance to recrystallization that could make them weaker during bonding. These high strength alloys could also be tested beyond strength for corrosion characteristics, and creep testing. This could provide very useful information into the field of diffusion bonding. In this study we have proven that we can successfully bond commercially pure Ni to itself with the use of a brass interlayer and that those joints have low void contents and provided some strength (certain samples reaching over 40% strength of the Ni samples themselves). This set of testing could prove to be of use to multiple industries but especially the aerospace industry in terms of the information it could provide.

APPENDICES

Appendix A

Furnace Programming and Calibration

Table A. 1: Furnace Programming Table

Code	Input	Notes
CXX	Temp	Temperature in ºC
TXX	Time	Time in minutes
C01	0	start temp always 0
T01	50	1000/20 = time to stage 1 temp
C02	875	Stage 1 temp (prevents overshoot)
T02	10	stabalization time
C03	875	Stage 1 temp (prevents overshoot)
T03	10	Time to stage 2 temp
C04	925	Stage 2 Temp (prevents overshoot)
T04	10	stabalization time
C05	925	Stage 2 Temp (prevents overshoot)
T05	25	1 ºC/min to bond temp
C06	950	bond temp
T06	600	duration of bonding temp
C07	950	bond temp
T07	-121	code to end furnace program and cool

To calibrate the tube furnace, the furnace should be set up with ceramic refractory blocks in each end. A data acquisition unit should be used to record the data. A type K thermocouple is placed in the hole of the refractory block into the center of the constant heat zone of the furnace. Run the temperature program and record the data. The offset of the furnace is the difference between the recorded temperature and the programed temperature. For these experiments the offset was a constant between 950 ºC and 1050

ºC. That offset was 68 ºC. Detailed and step by step procedures can be found in the literature for this furnace provided by MTI [36].

Appendix B

SEM Image Analysis and EDS Results

Sample 1: 1hr, 950ºC, 600grit, 130µm

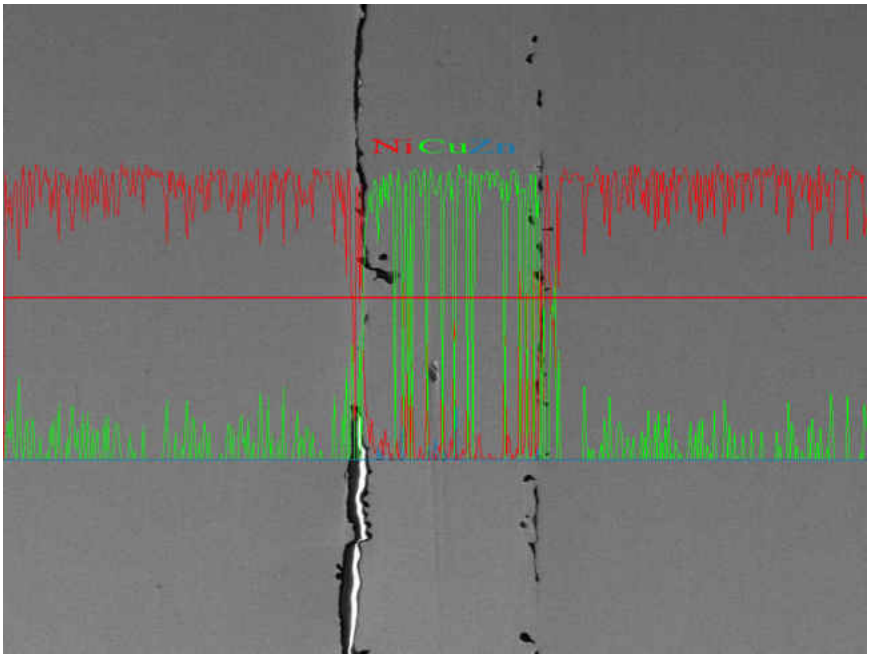

Figure B. 1: Linescan overlay on Image of Sample 1

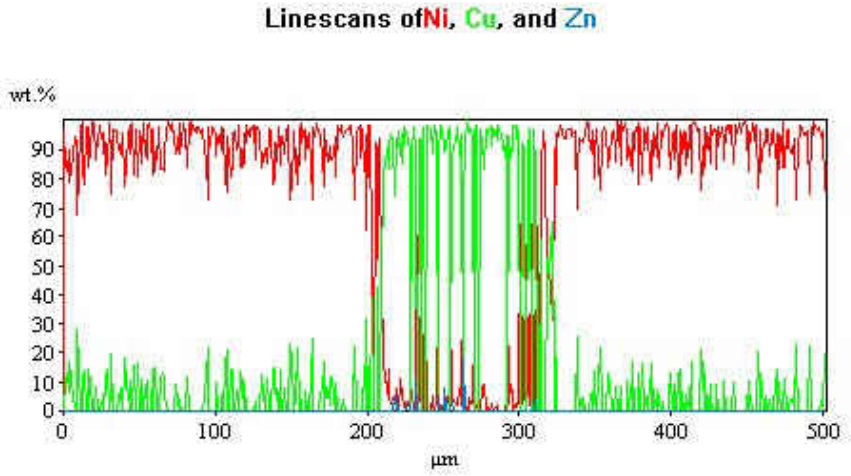

Figure B. 2: Scaled linescan showing concentration profiles of the joint of sample 1.

Sample 2: 19hr, 950ºC, 600grit, 130µm

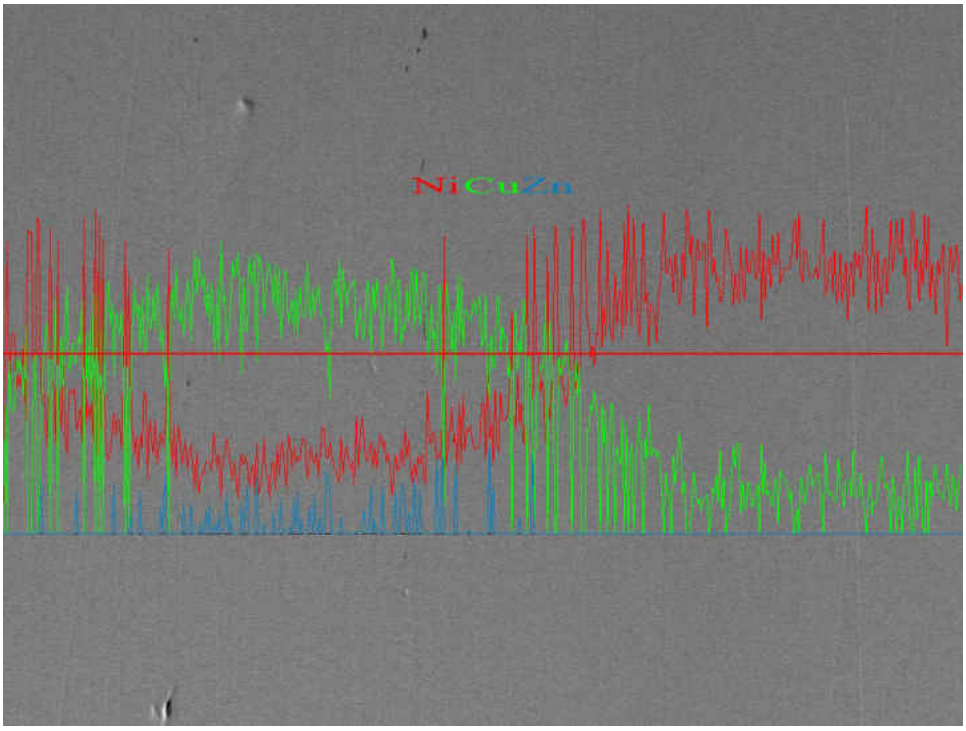

Figure B. 3: Linescan overlay on Image of Sample 2

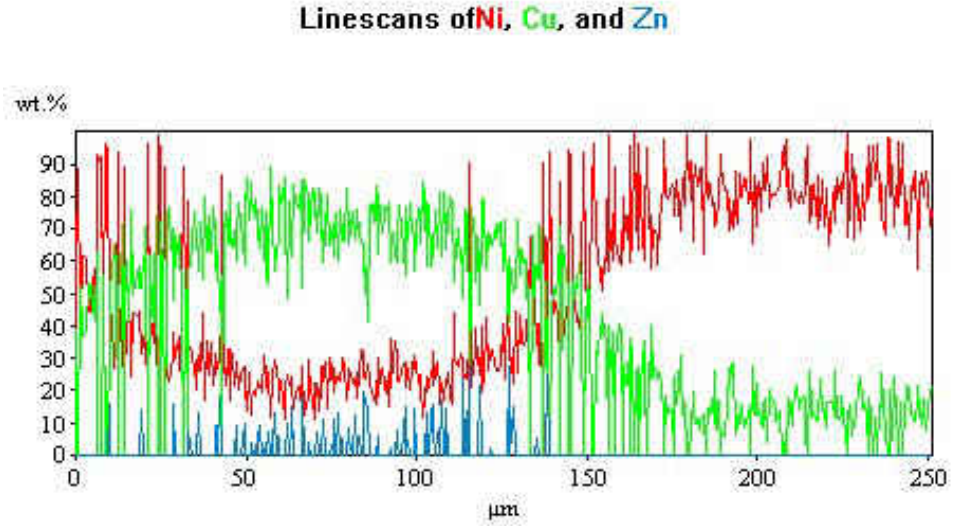

Figure B. 4: Scaled linescan showing concentration profiles of the joint of sample 2.

Sample 3: 1hr, 1050ºC, 600grit, 130µm

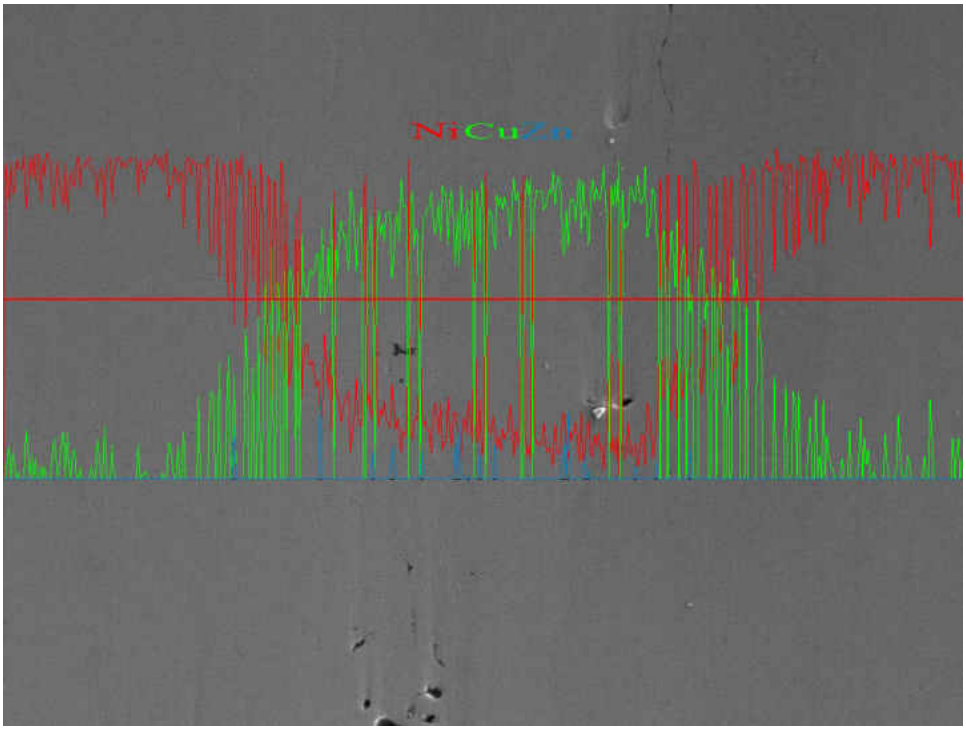

Figure B. 5: Linescan overlay on Image of Sample 3

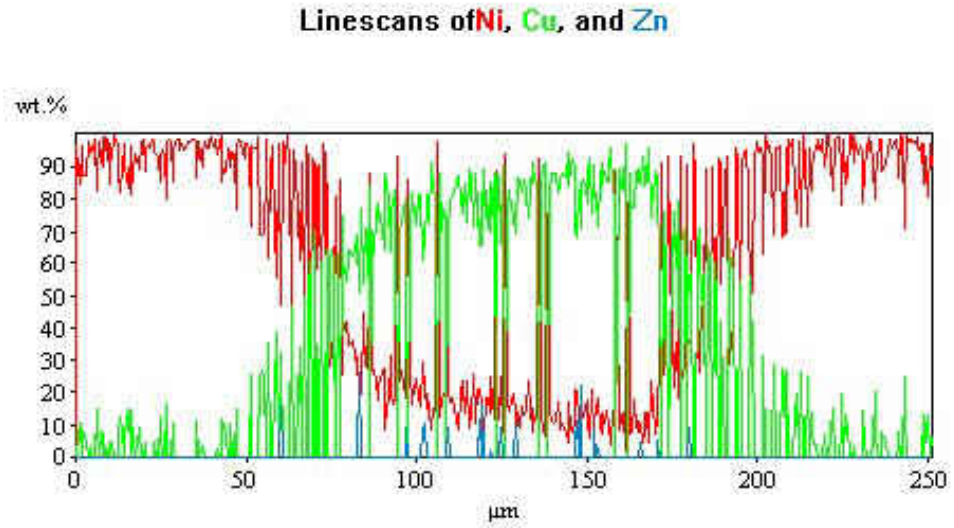

Figure B. 6: Scaled linescan showing concentration profiles of the joint of sample 3.

Sample 4: 19hr, 1050ºC, 600grit, 130µm

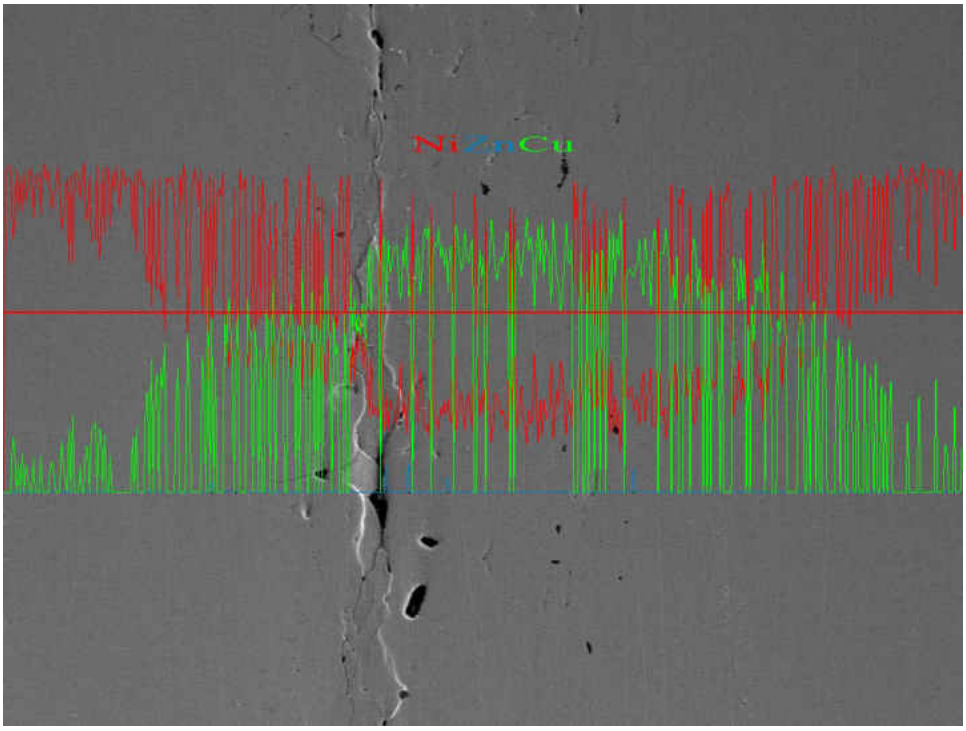

Figure B. 7: Linescan overlay on Image of Sample 4

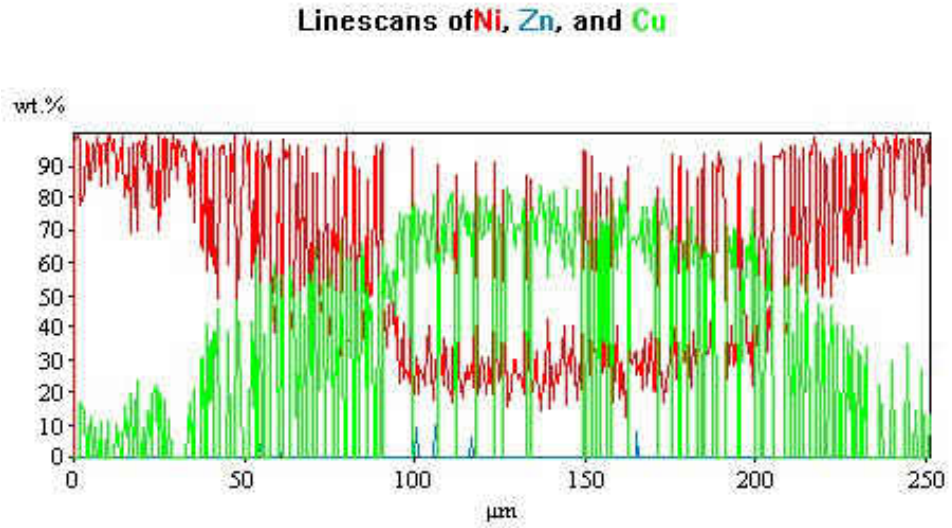

Figure B. 8: Scaled linescan showing concentration profiles of the joint of sample 4.

Sample 5: 10hr, 1000ºC, 400grit, 25µm

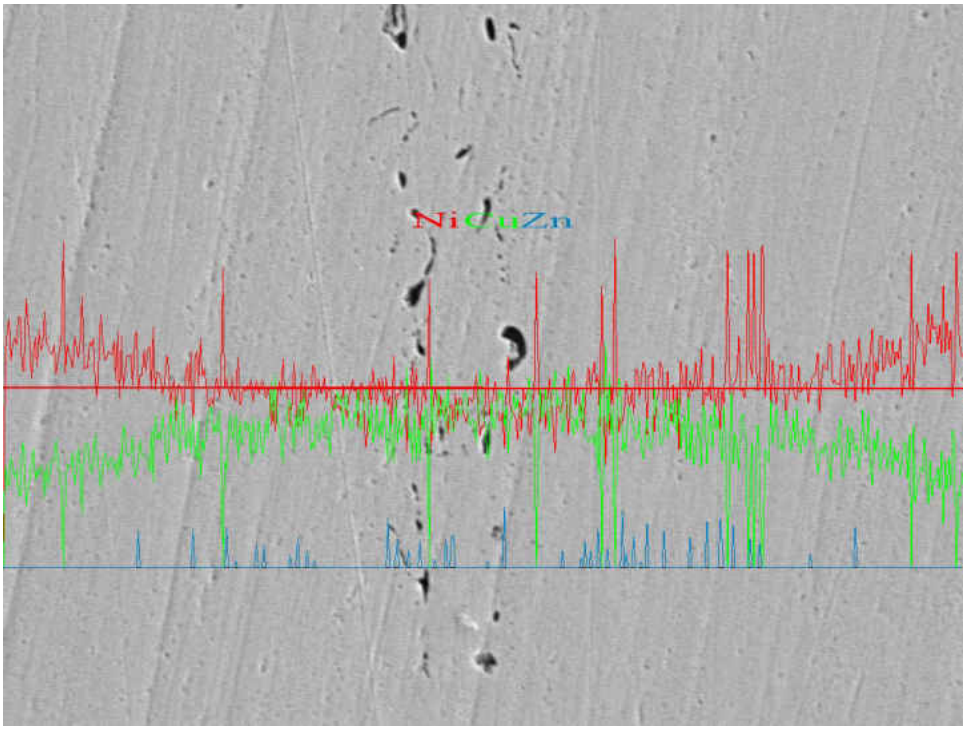

Figure B. 9: Linescan overlay on Image of Sample 5

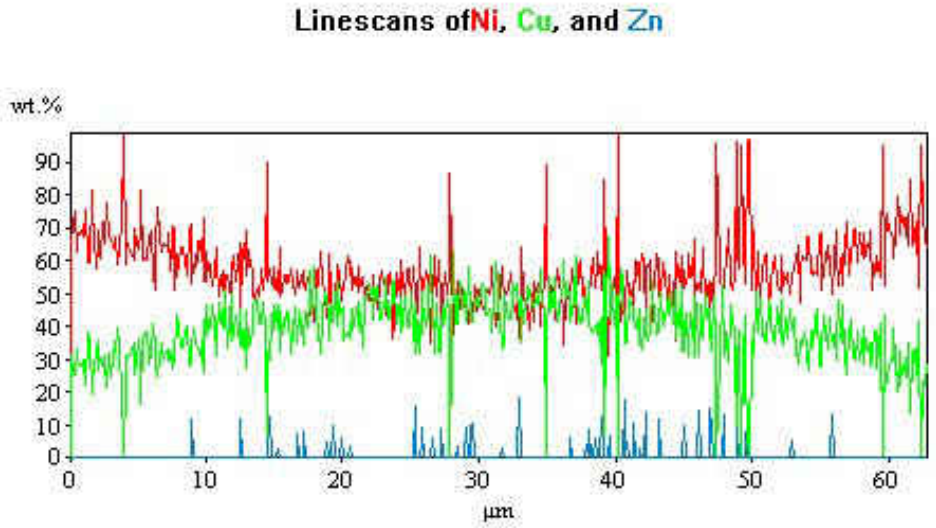

Figure B. 10: Scaled linescan showing concentration profiles of the joint of sample 5.

Sample 6: 10hr, 1000ºC, 800grit, 25µm

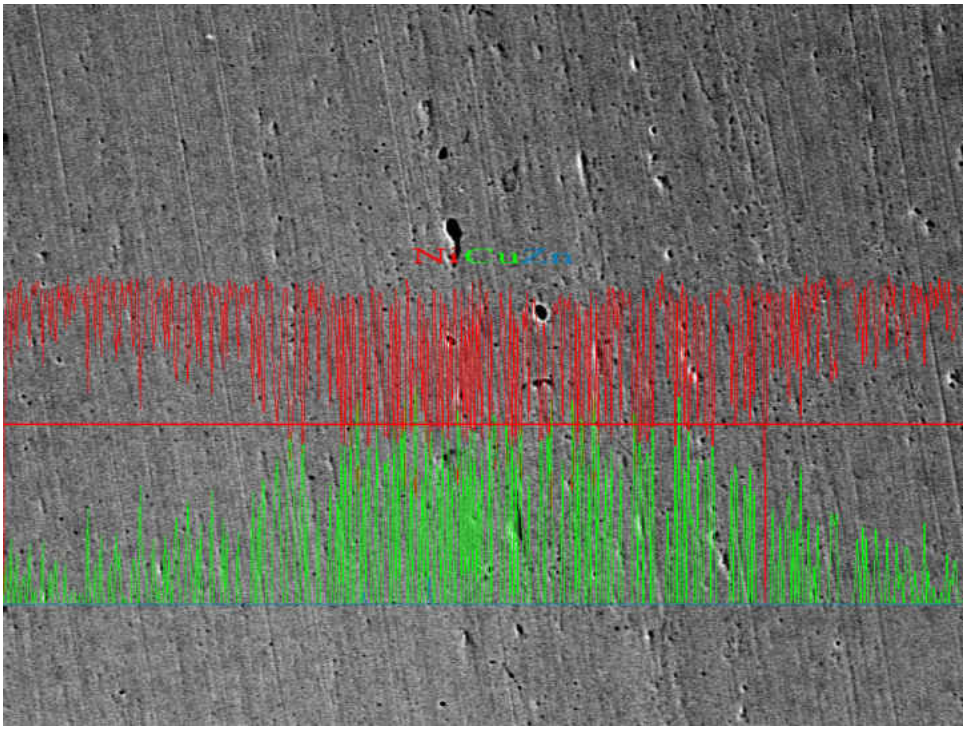

Figure B. 11: Linescan overlay on Image of Sample 6

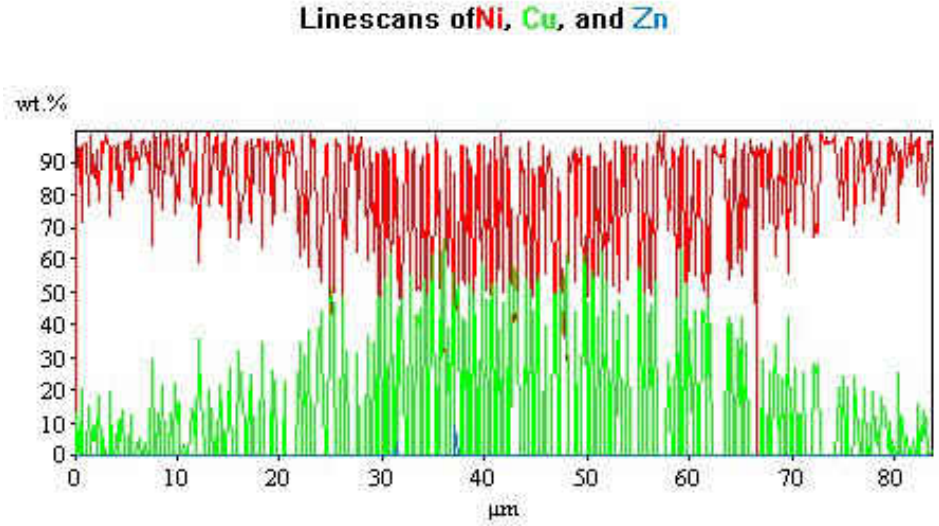

Figure B. 12: Scaled linescan showing concentration profiles of the joint of sample 6.

Sample 7: 10hr, 1000ºC, 400grit, 250µm

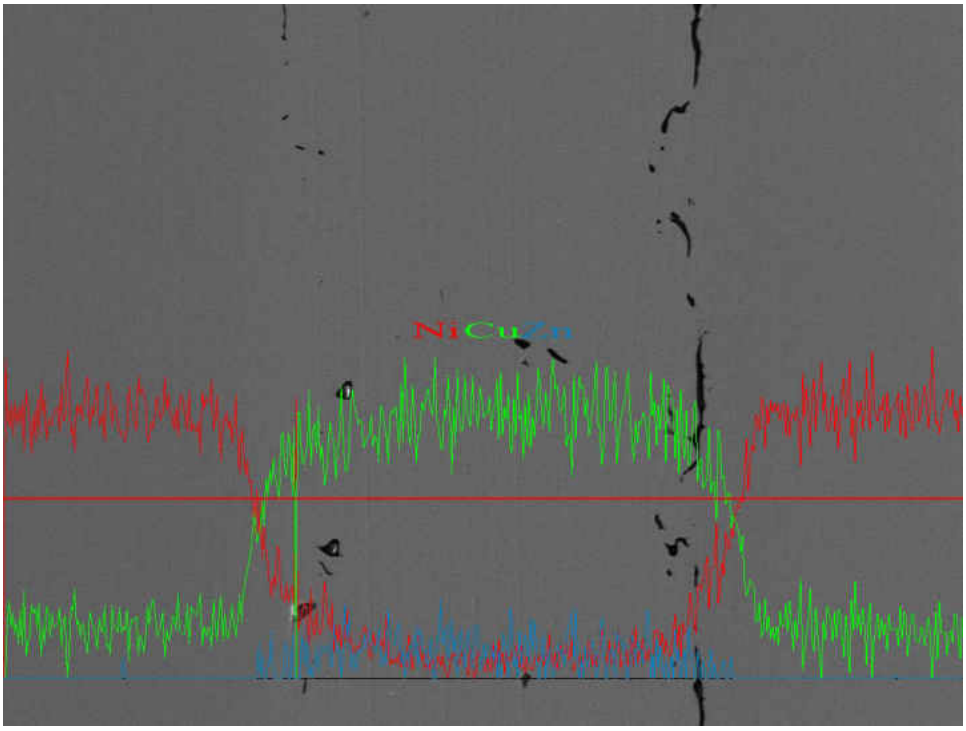

Figure B. 13: Linescan overlay on Image of Sample 7

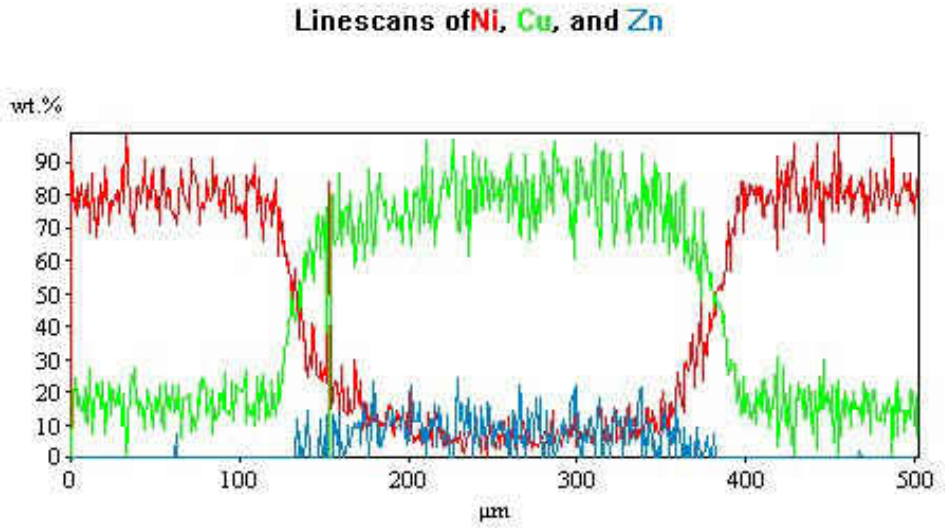

Figure B. 14: Scaled linescan showing concentration profiles of the joint of sample 7.

Sample 8: 10hr, 1000ºC, 800grit, 250µm

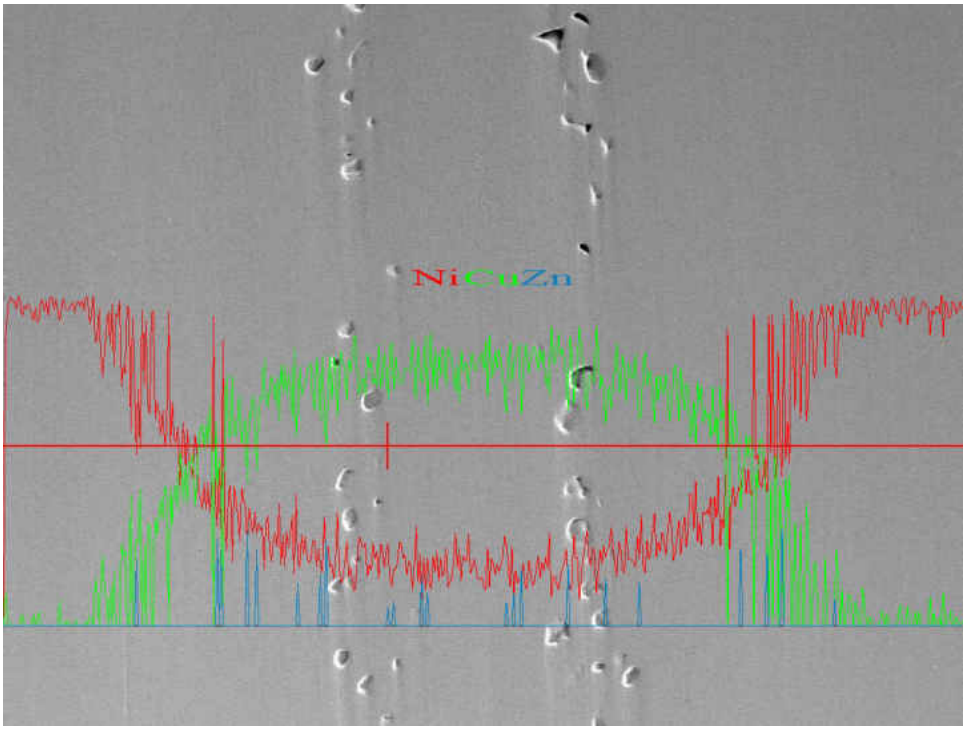

Figure B. 15: Linescan overlay on Image of Sample 8

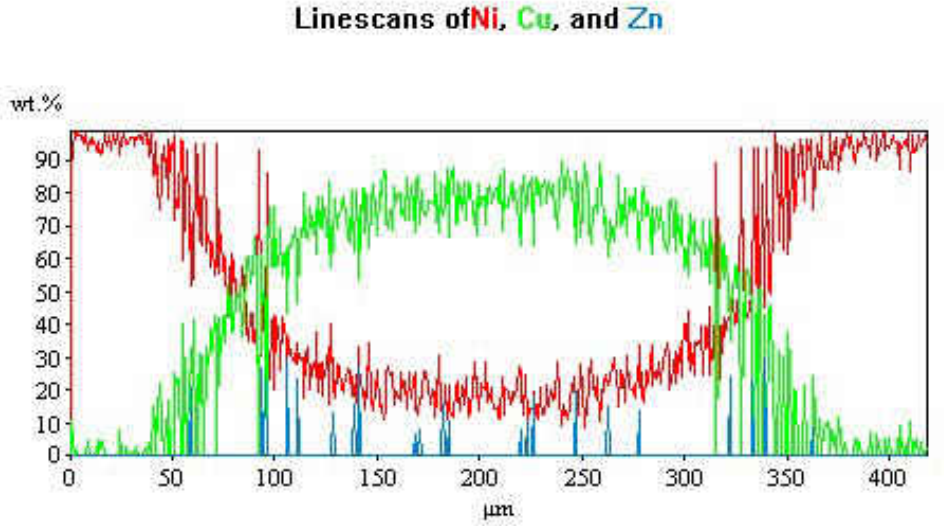

Figure B. 16: Scaled linescan showing concentration profiles of the joint of sample 8.

Sample 9: 10hr, 1000ºC, 600grit, 130µm

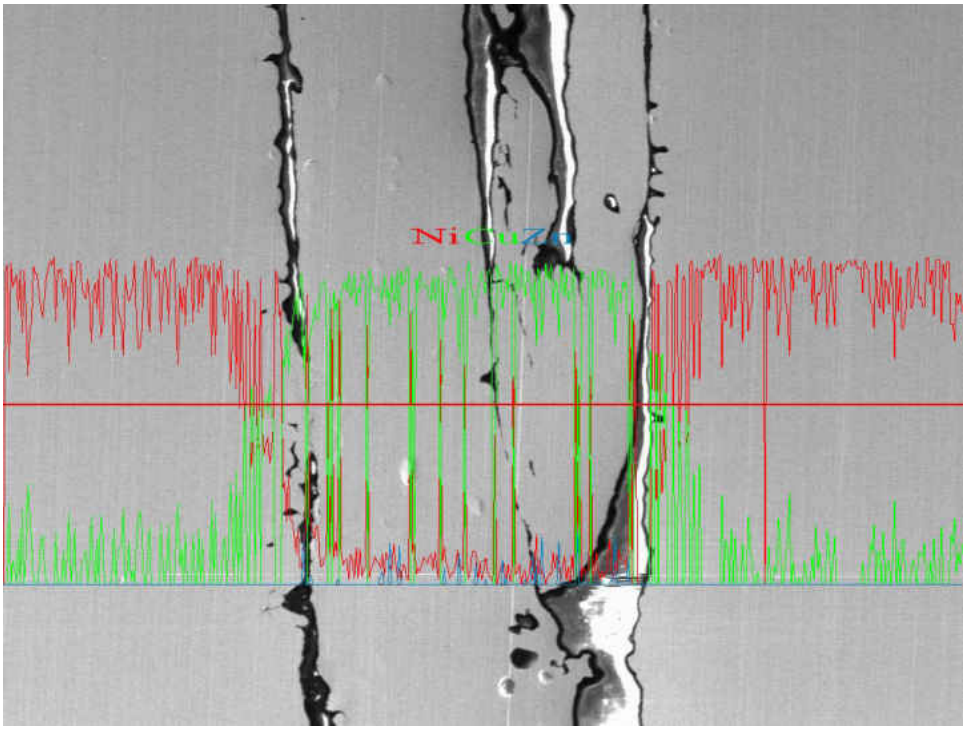

Figure B. 17: Linescan overlay on Image of Sample 9

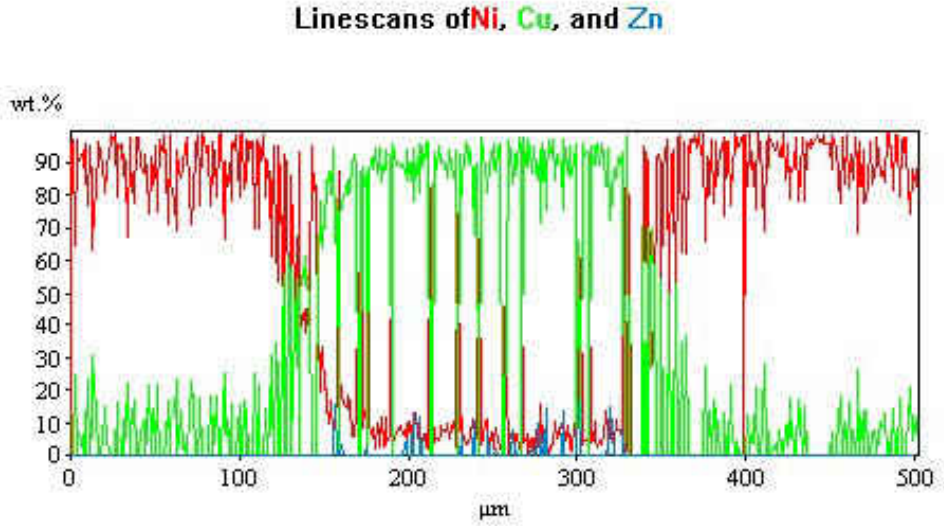

Figure B. 18: Scaled linescan showing concentration profiles of the joint of sample 9.

Sample 10: 1hr, 1000ºC, 400grit, 130µm

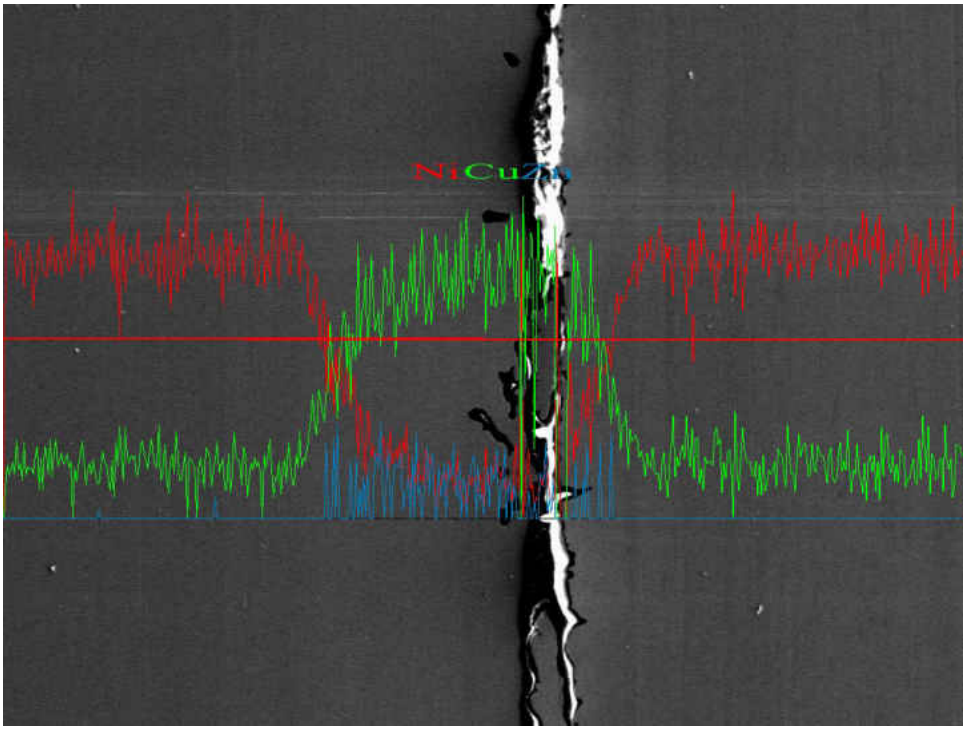

Figure B. 19: Linescan overlay on Image of Sample 10

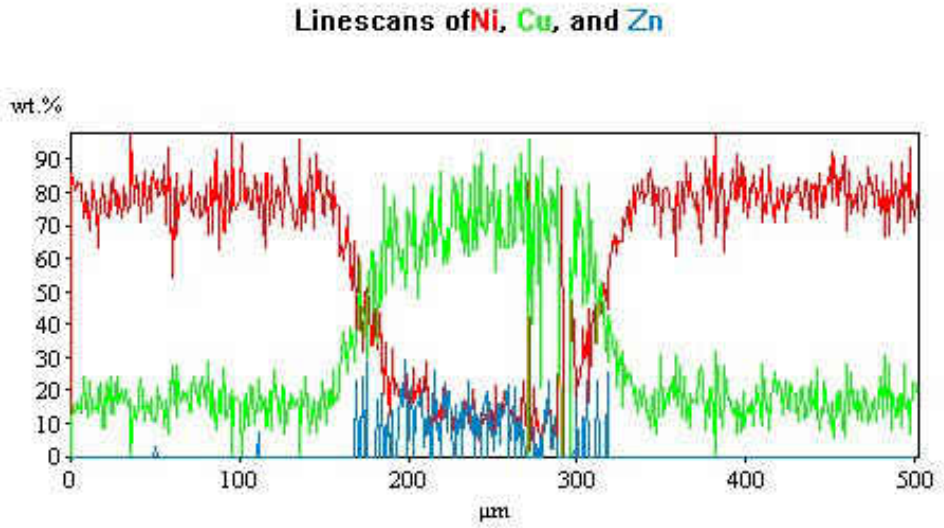

Figure B. 20: Scaled linescan showing concentration profiles of the joint of sample 10.

Sample 11: 19hr, 1000ºC, 400grit, 130µm

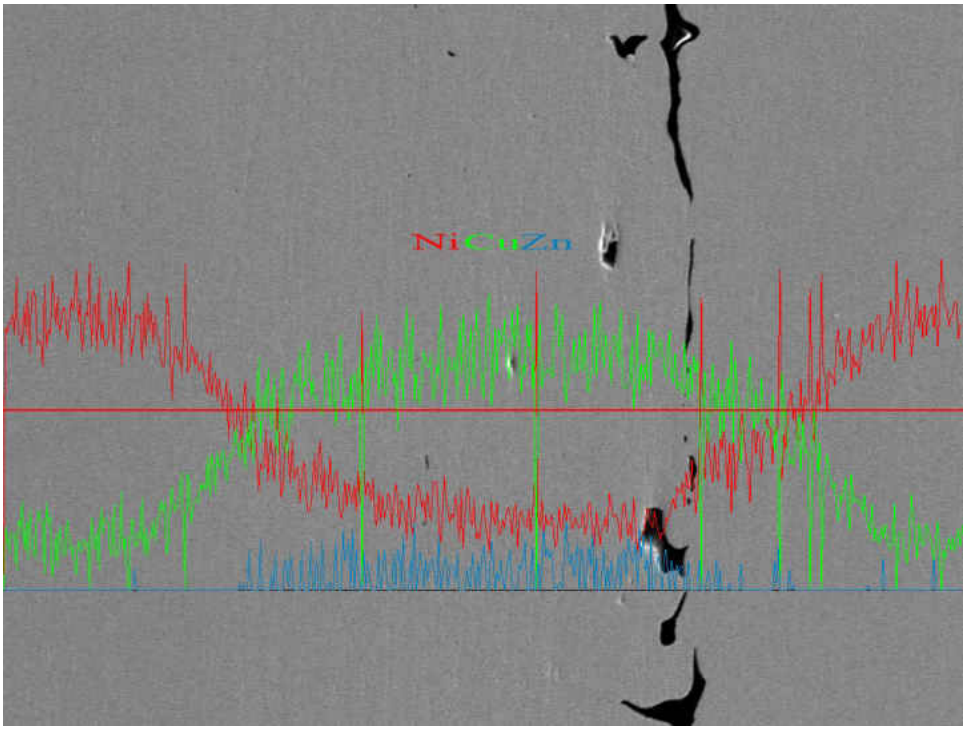

Figure B. 21: Linescan overlay on Image of Sample 11

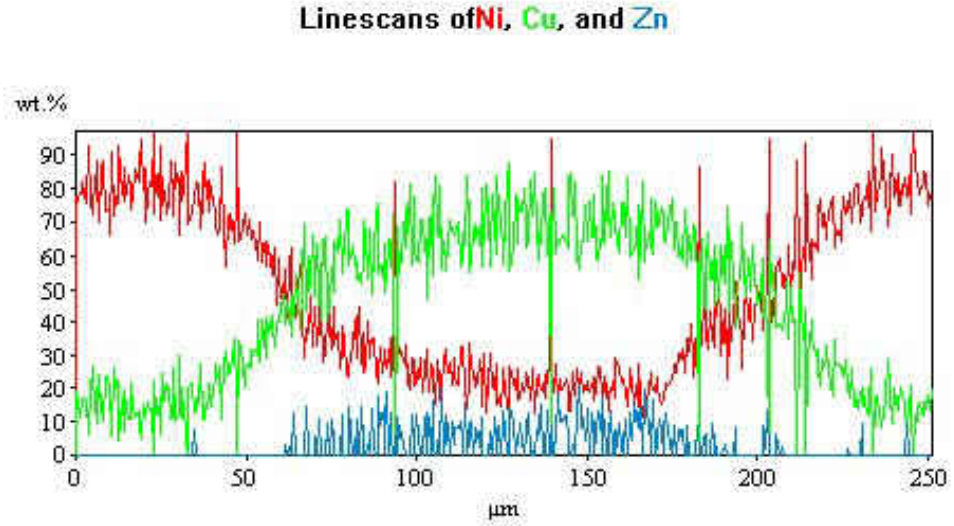

Figure B. 22: Scaled linescan showing concentration profiles of the joint of sample 11.

Sample 12: 1hr, 1000ºC, 800grit, 130µm

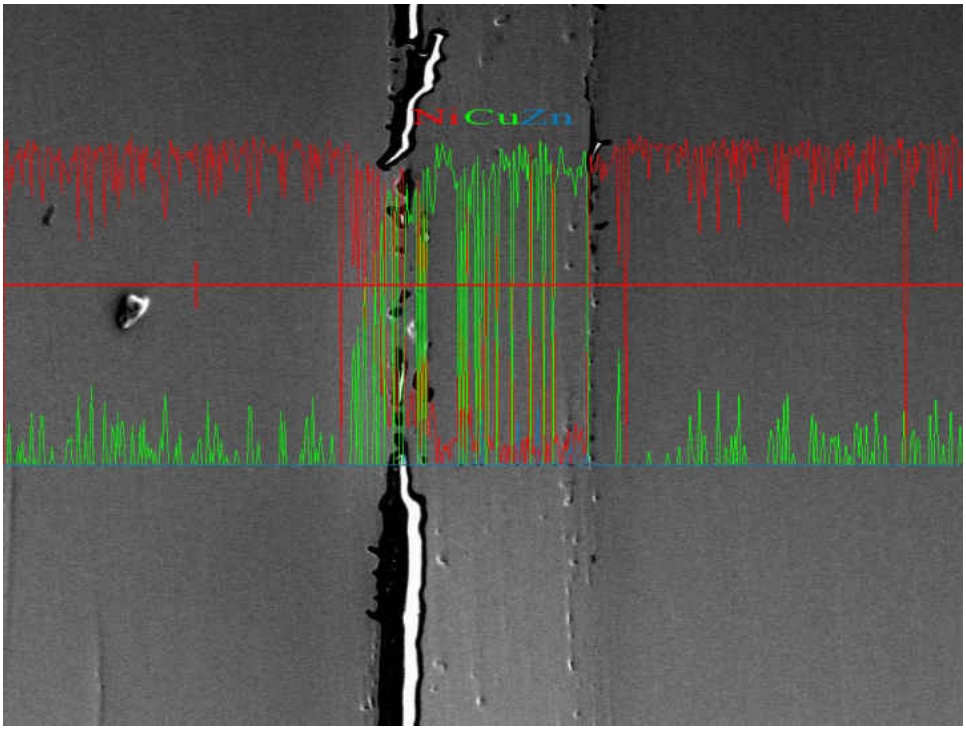

Figure B. 23: Linescan overlay on Image of Sample 12

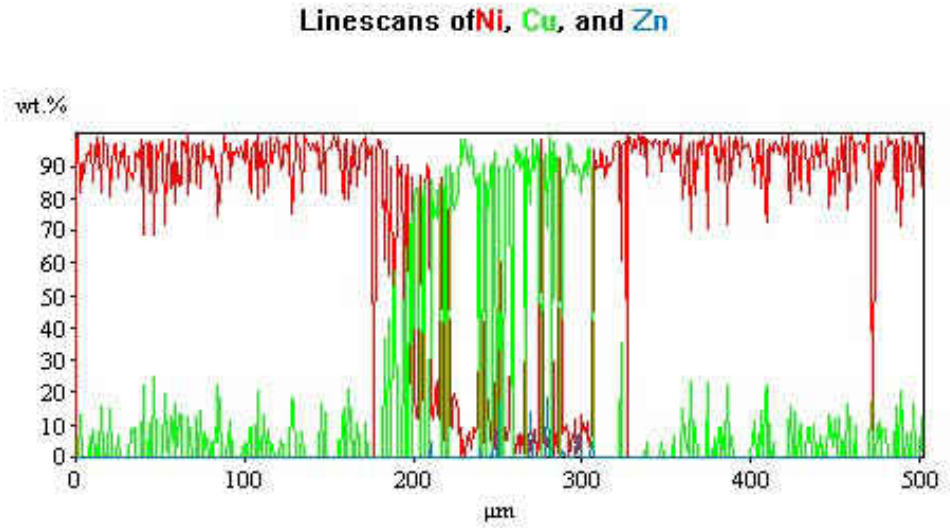

Figure B. 24: Scaled linescan showing concentration profiles of the joint of sample 12.

Sample 13: 19hr, 1000ºC, 800grit, 130µm

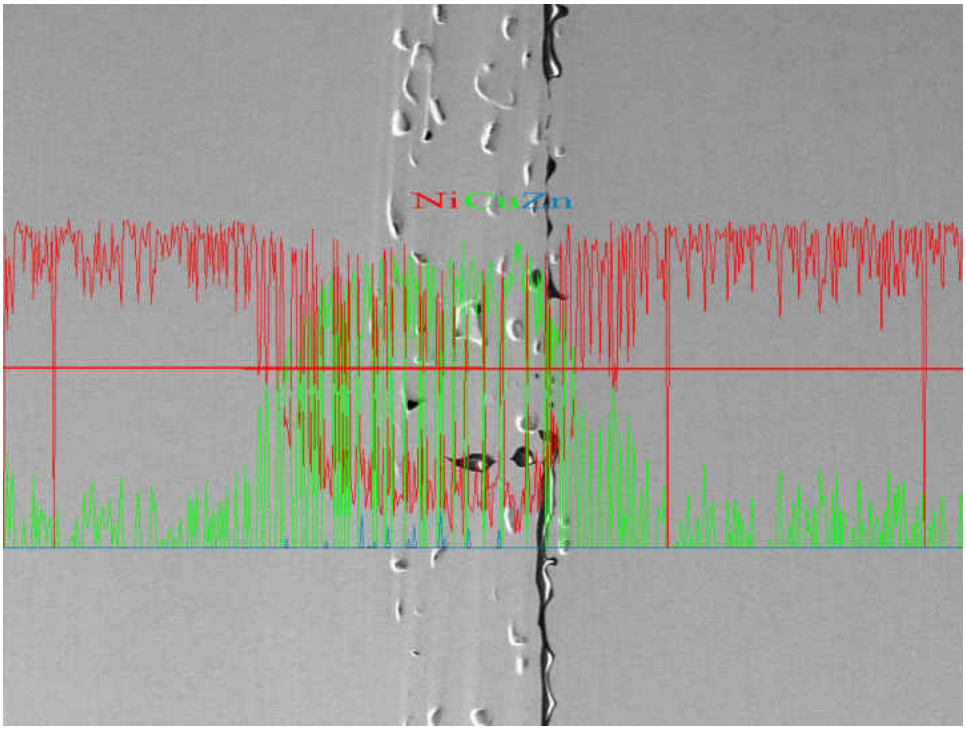

Figure B. 25: Linescan overlay on Image of Sample 13

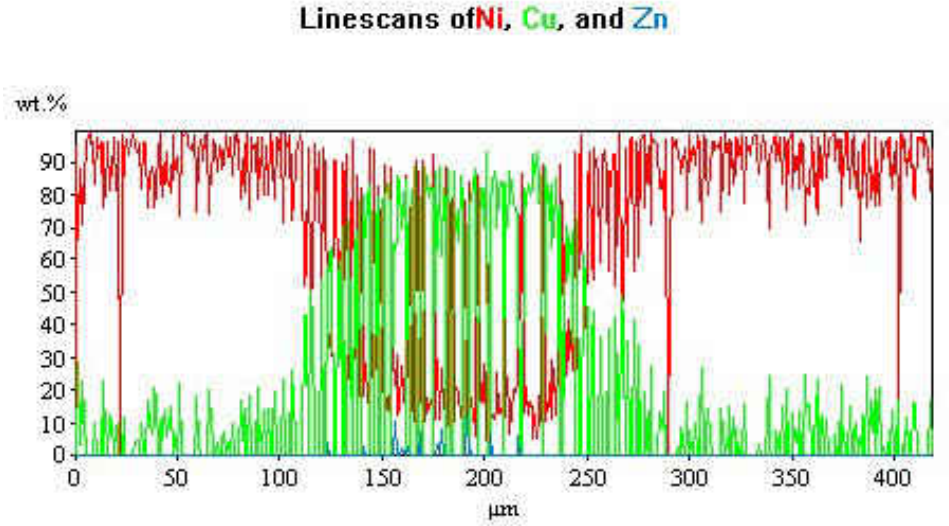

Figure B. 26: Scaled linescan showing concentration profiles of the joint of sample 13.

Sample 14: 10hr, 950ºC, 600grit, 25µm

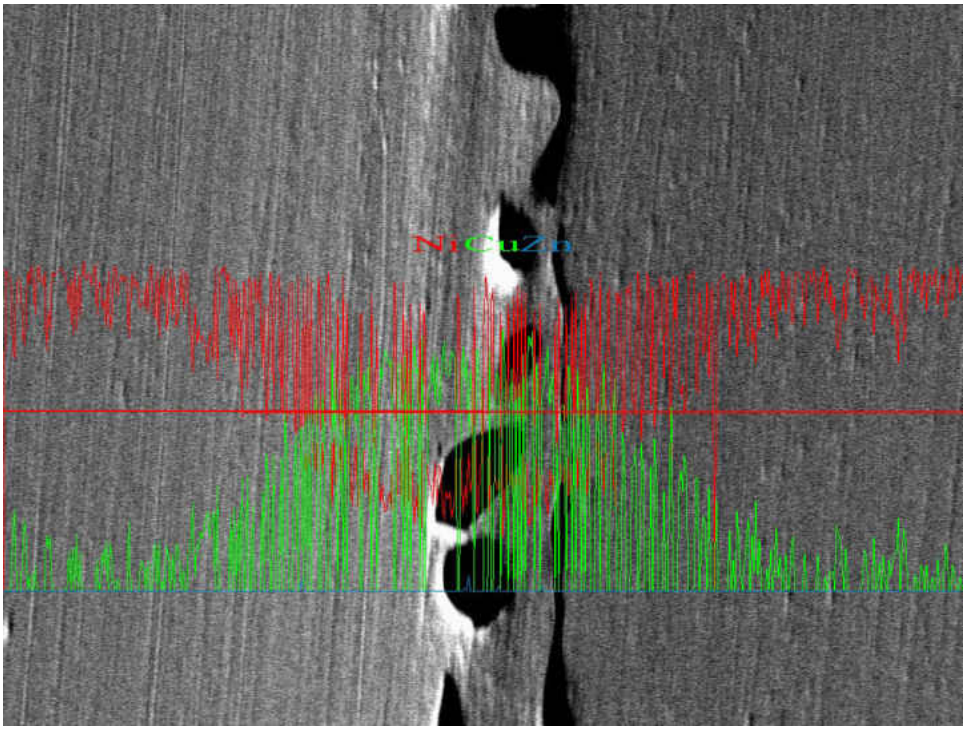

Figure B. 27: Linescan overlay on Image of Sample 14

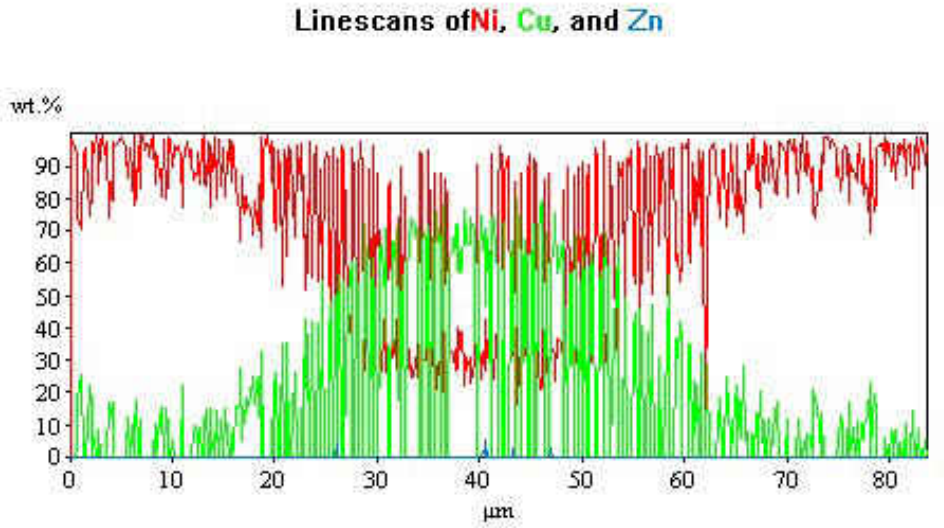

Figure B. 28: Scaled linescan showing concentration profiles of the joint of sample 14.

Sample 15: 10hr, 1050ºC, 600grit, 25µm

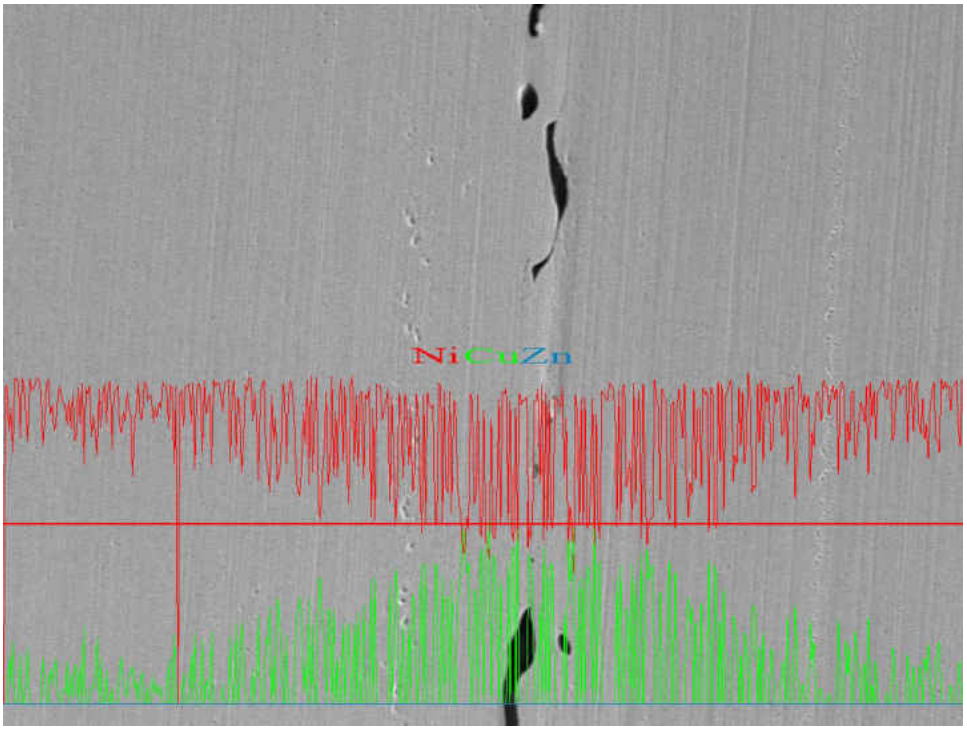

Figure B. 29: Linescan overlay on Image of Sample 15

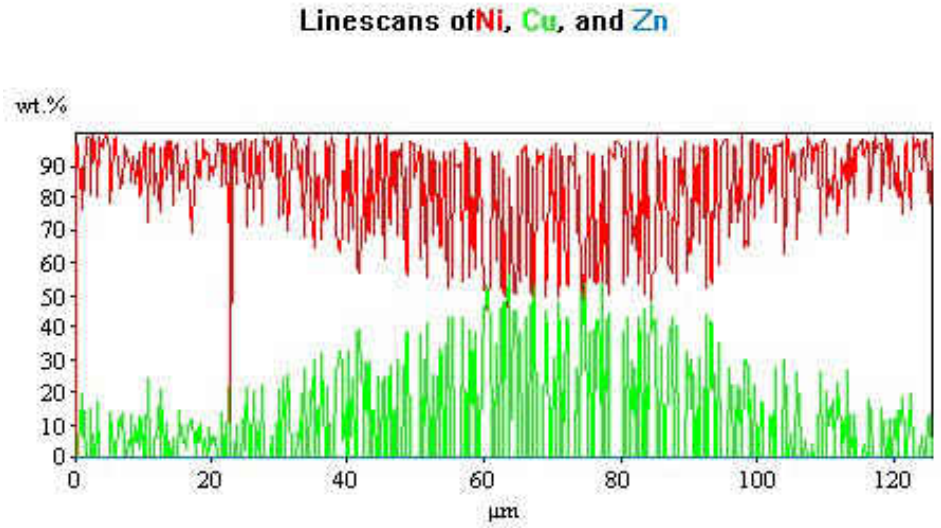

Figure B. 30: Scaled linescan showing concentration profiles of the joint of sample 15.

Sample 16: 10hr, 950ºC, 600grit, 250µm

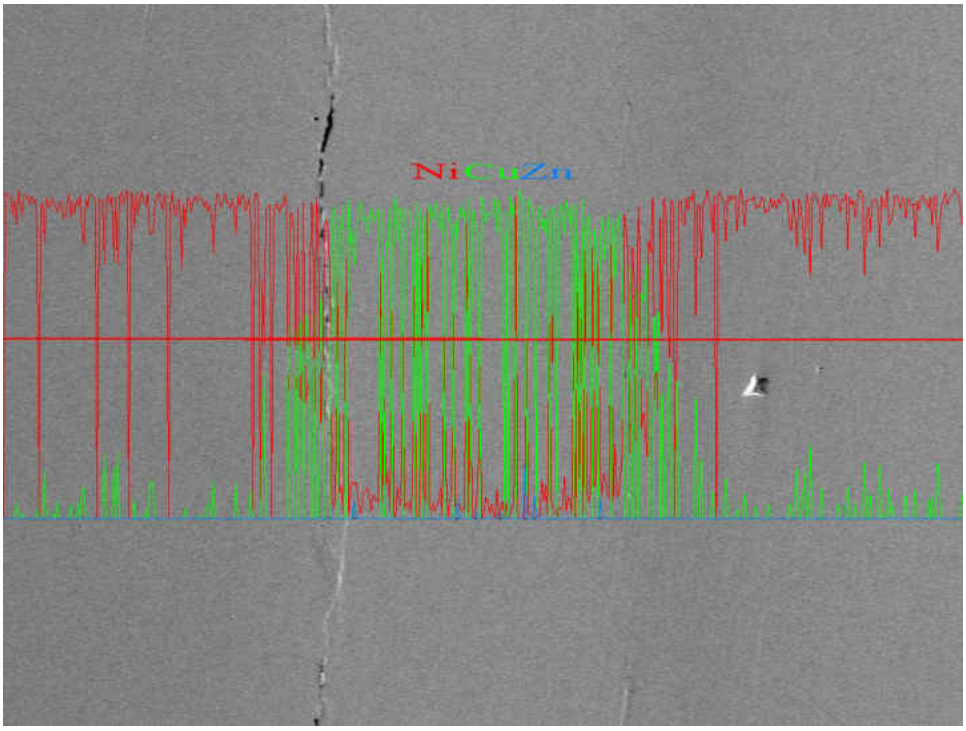

Figure B. 31: Linescan overlay on Image of Sample 16

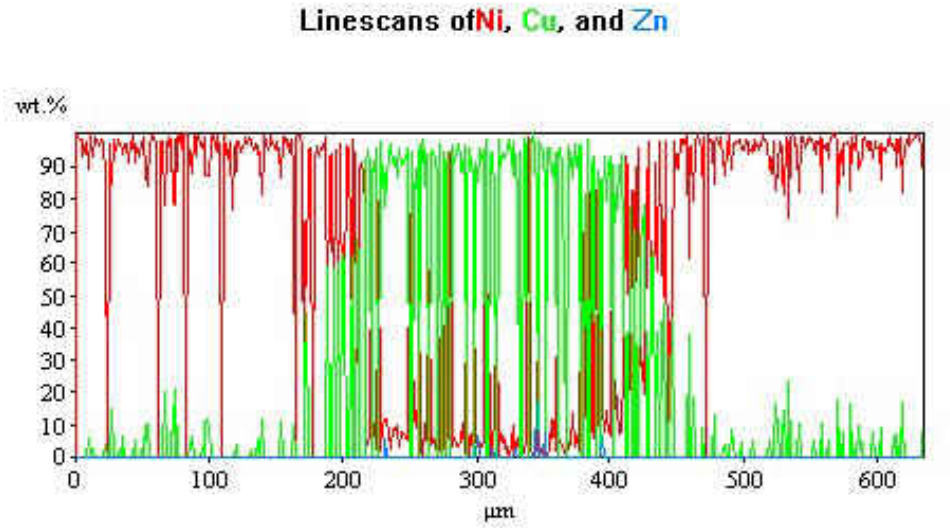

Figure B. 32: Scaled linescan showing concentration profiles of the joint of sample 16.

Sample 17: 10hr, 1050ºC, 600grit, 250µm

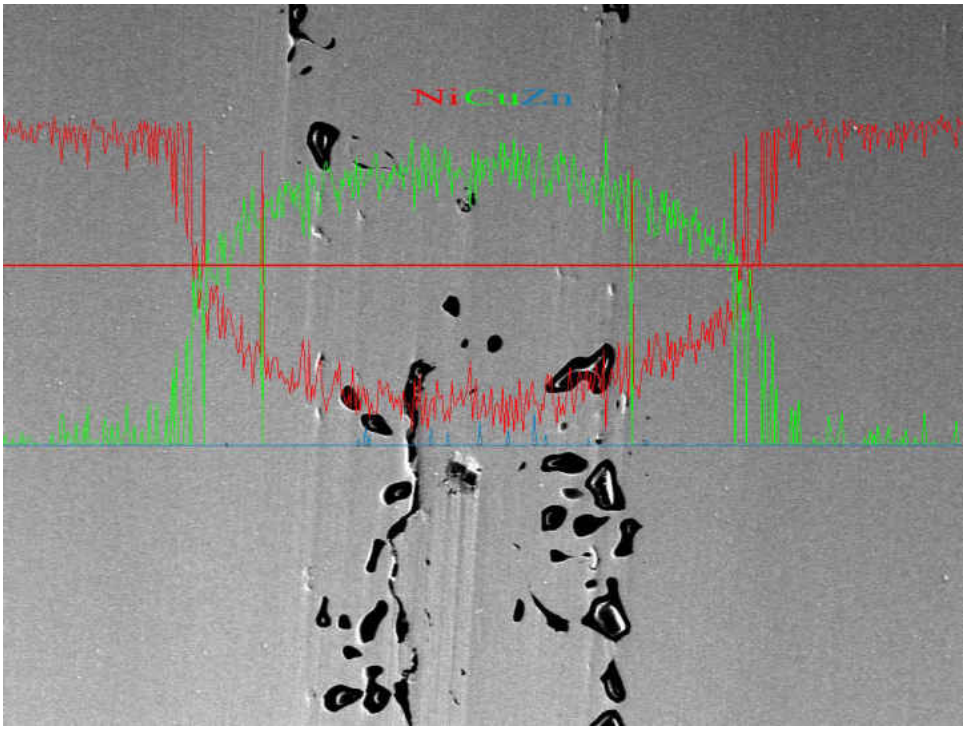

Figure B. 33: Linescan overlay on Image of Sample 17

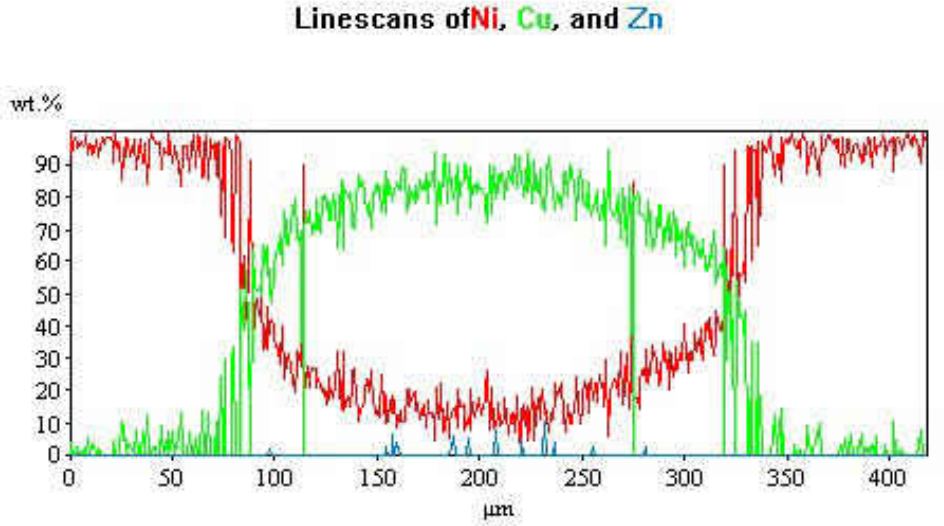

Figure B. 34: Scaled linescan showing concentration profiles of the joint of sample 17.

Sample 18: 10hr, 1000ºC, 600grit, 130µm

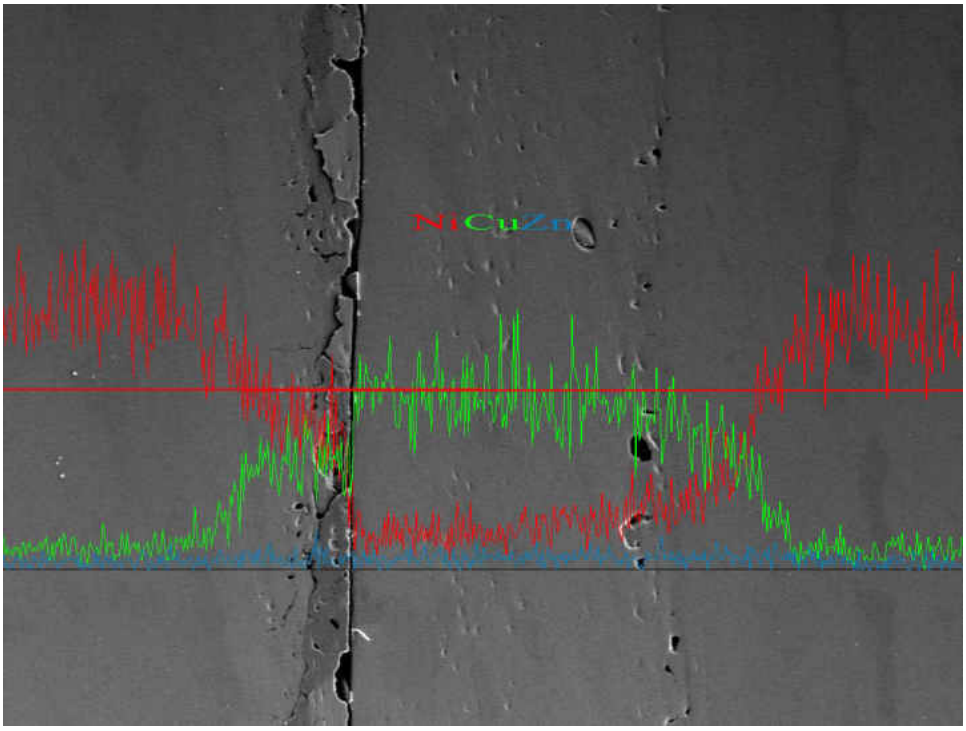

Figure B. 35: Linescan overlay on Image of Sample 18

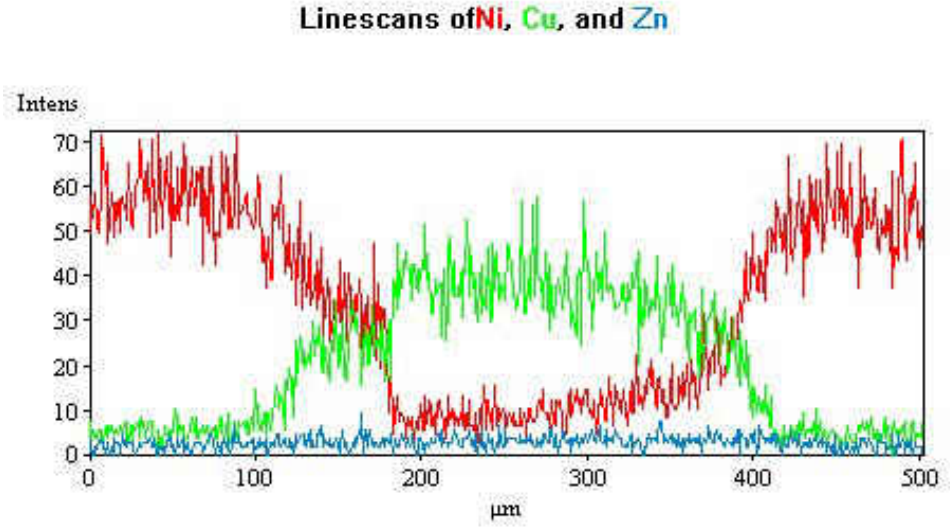

Figure B. 36: Scaled linescan showing concentration profiles of the joint of sample 18.

Sample 19: 1hr, 1000ºC, 600grit, 25µm

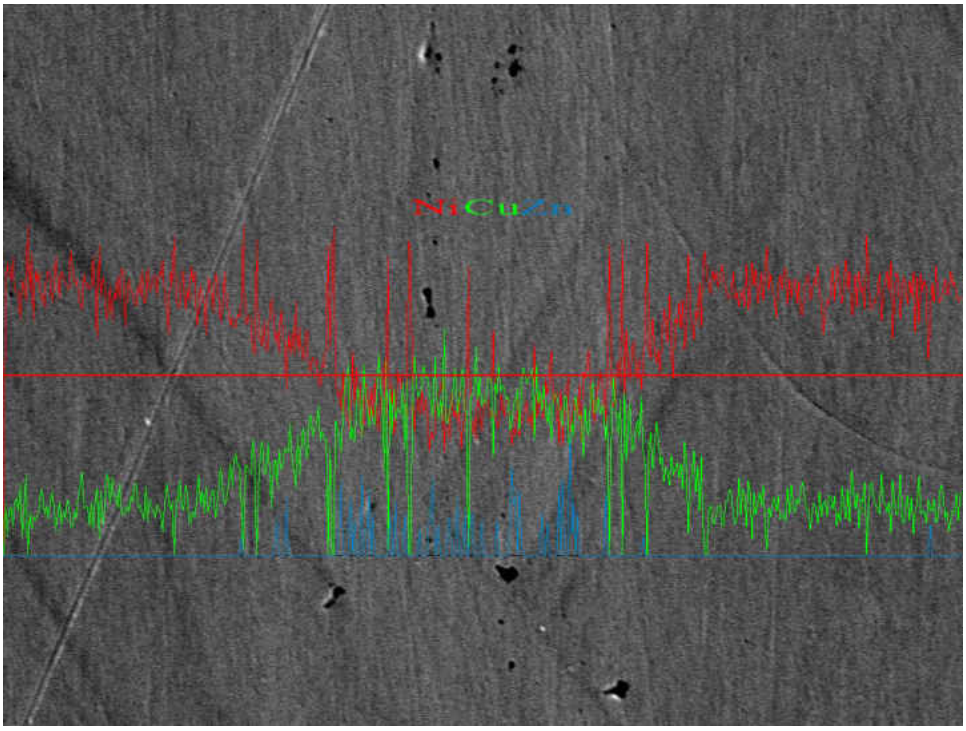

Figure B. 37: Linescan overlay on Image of Sample 19

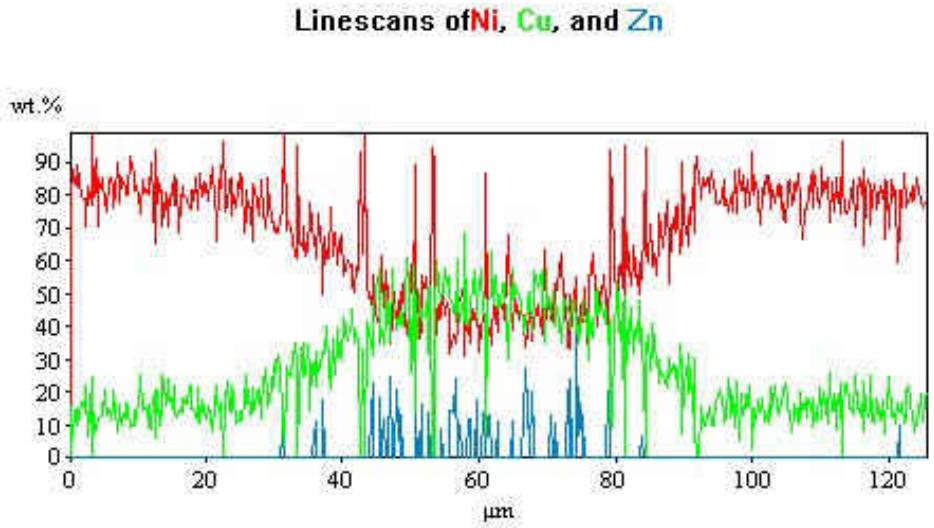

Figure B. 38: Scaled linescan showing concentration profiles of the joint of sample 19.

Sample 20: 19hr, 1000ºC, 600grit, 25µm

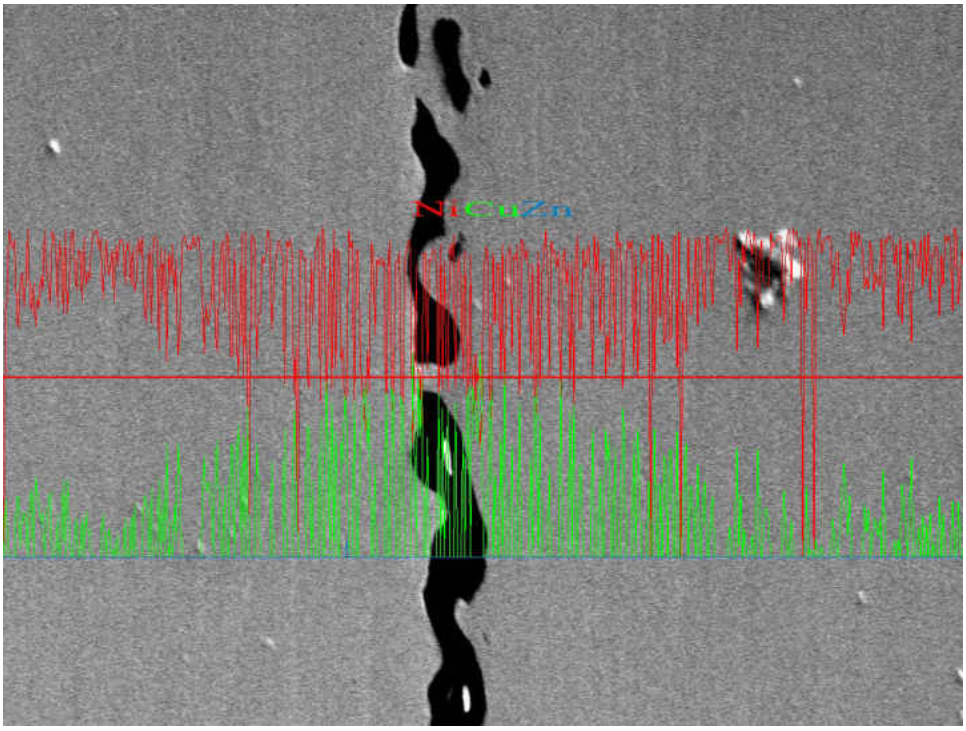

Figure B. 39: Linescan overlay on Image of Sample 20.

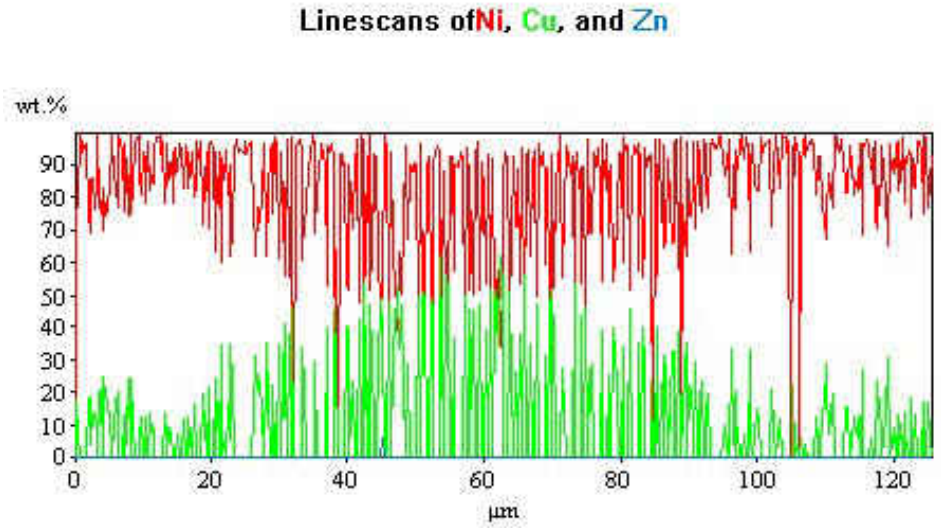

Figure B. 40: Scaled linescan showing concentration profiles of the joint of sample 20.

Sample 21: 1hr, 1000ºC, 600grit, 250µm

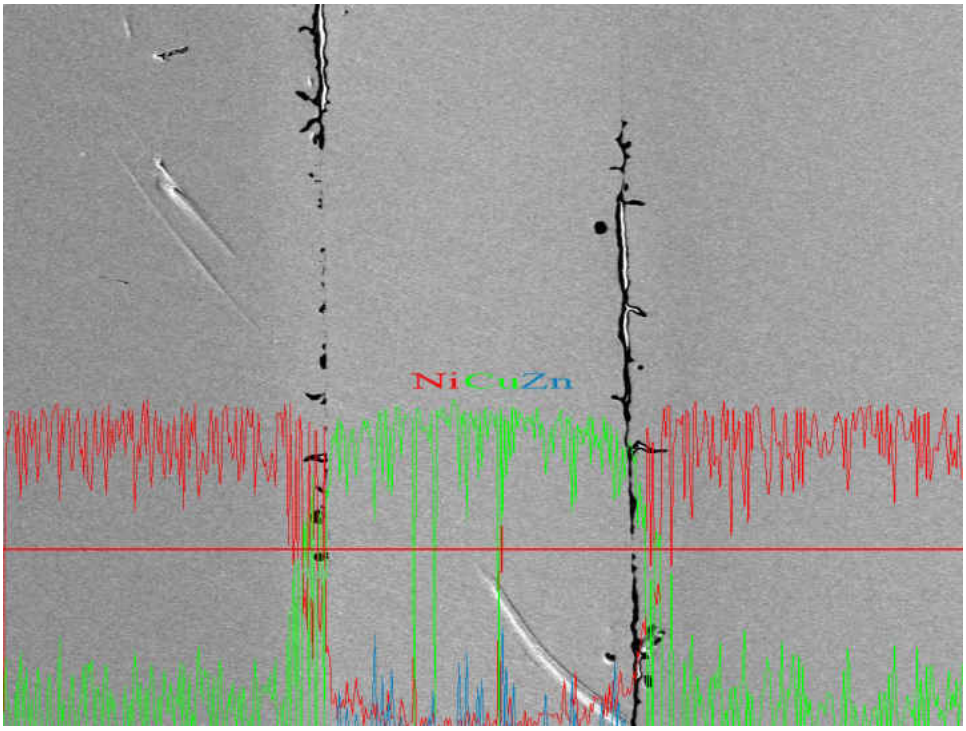

Figure B. 41: Linescan overlay on Image of Sample 21

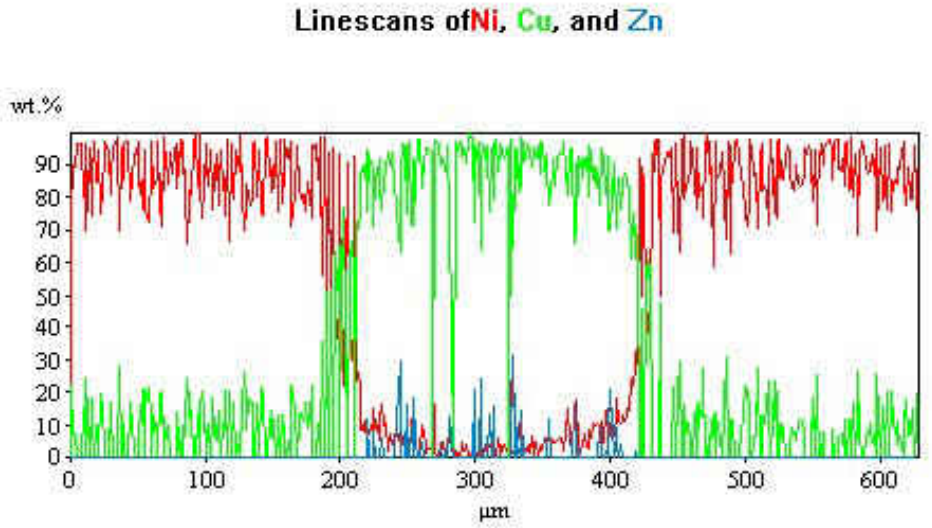

Figure B. 42: Scaled linescan showing concentration profiles of the joint of sample 21.

Sample 22: 19hr, 1000ºC, 600grit, 250µm

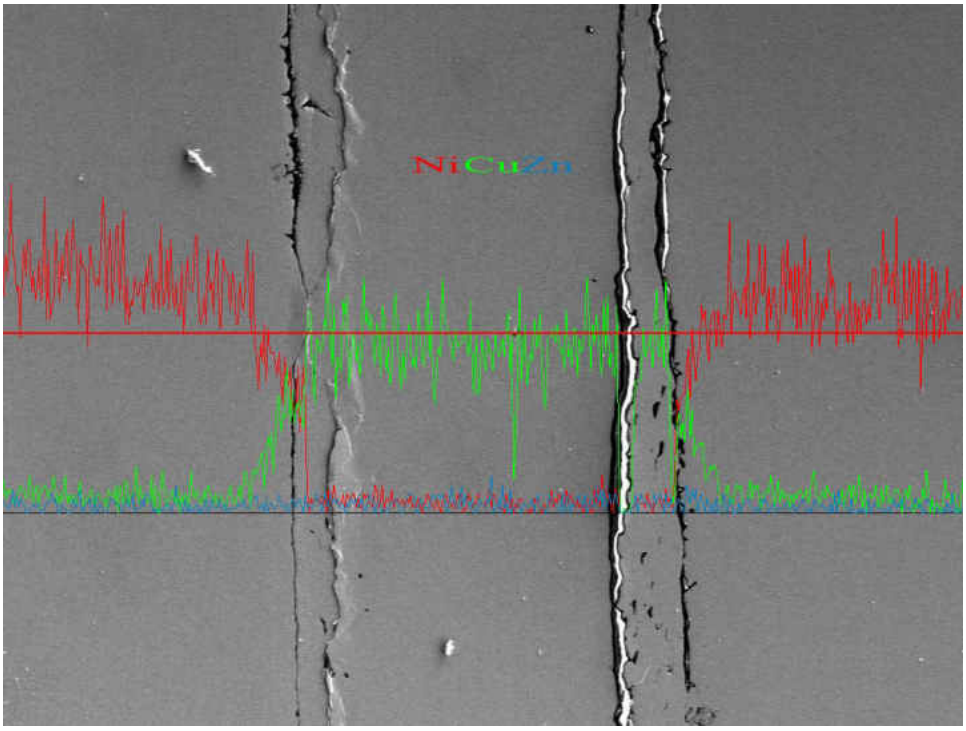

Figure B. 43: Linescan overlay on Image of Sample 22

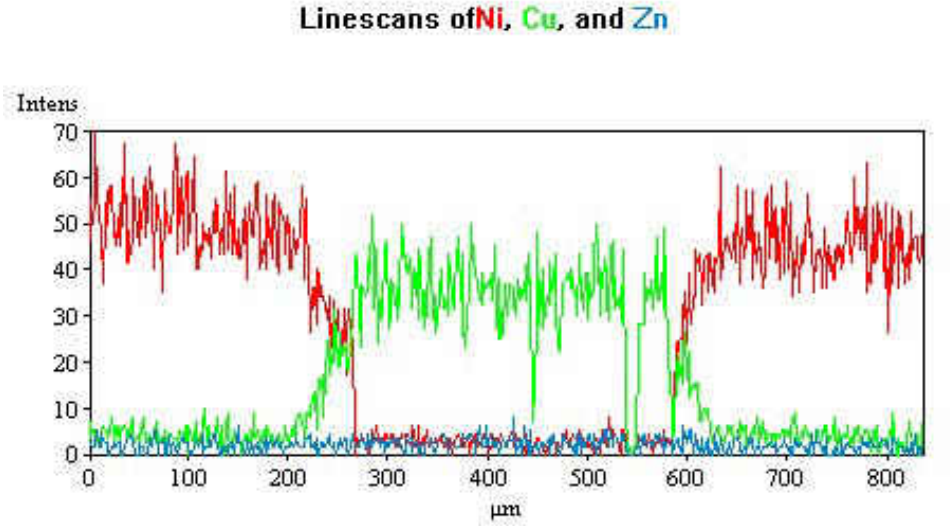

Figure B. 44: Scaled linescan showing concentration profiles of the joint of sample 22.

Sample 23: 10hr, 950ºC, 400grit, 130µm

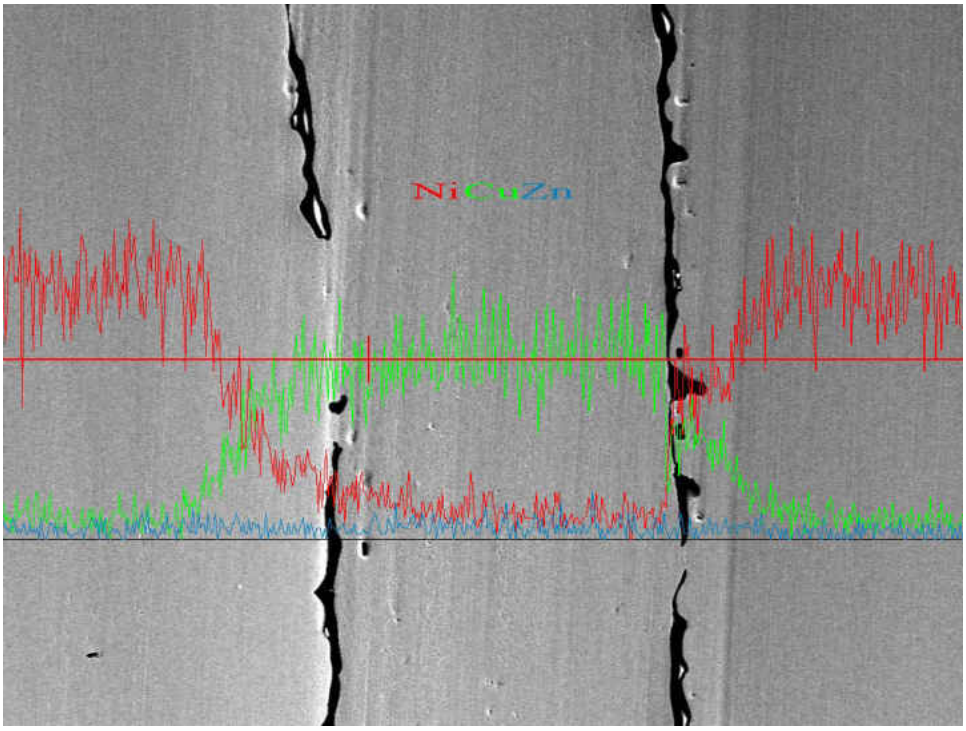

Figure B. 45: Linescan overlay on Image of Sample 23.

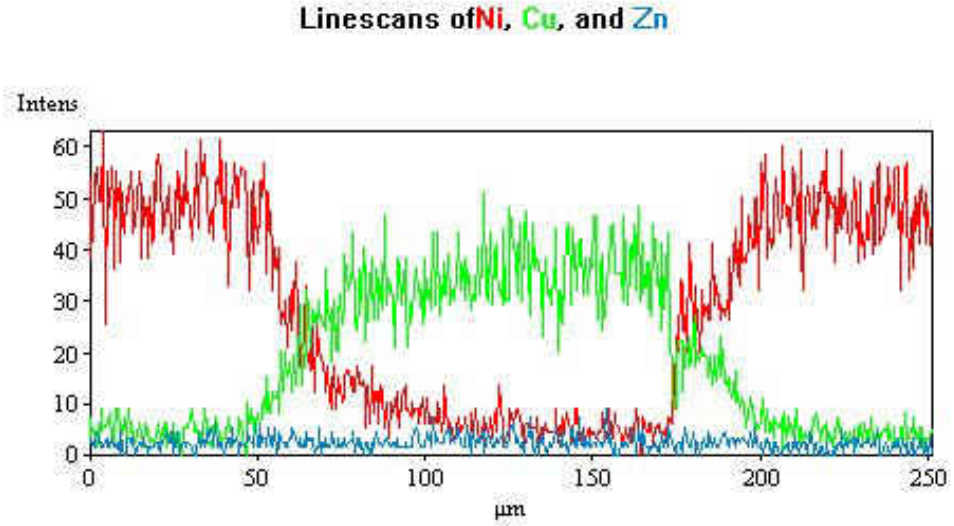

Figure B. 46: Scaled linescan showing concentration profiles of the joint of sample 23.

Sample 24: 10hr, 1050ºC, 400grit, 130µm

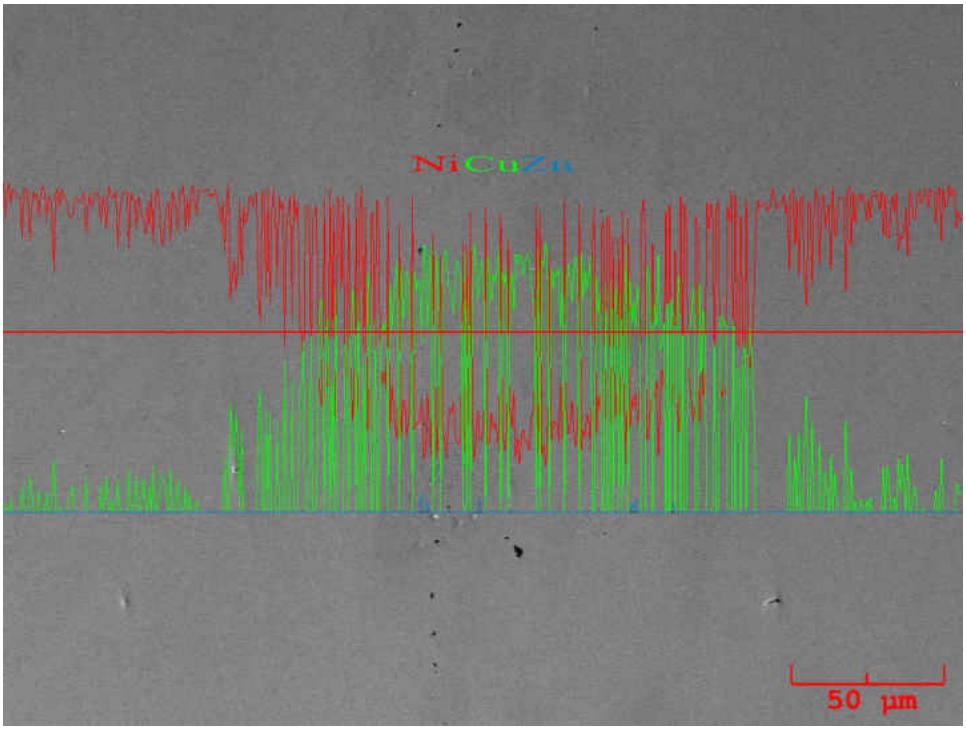

Figure B. 47: Linescan overlay on Image of Sample 24

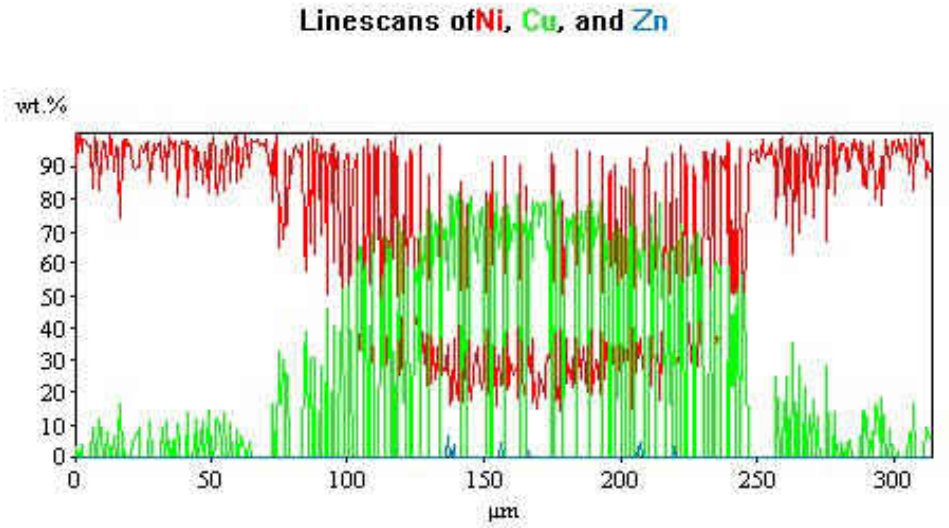

Figure B. 48: Scaled linescan showing concentration profiles of the joint of sample 24.

Sample 25: 10hr, 950ºC, 800grit, 130µm

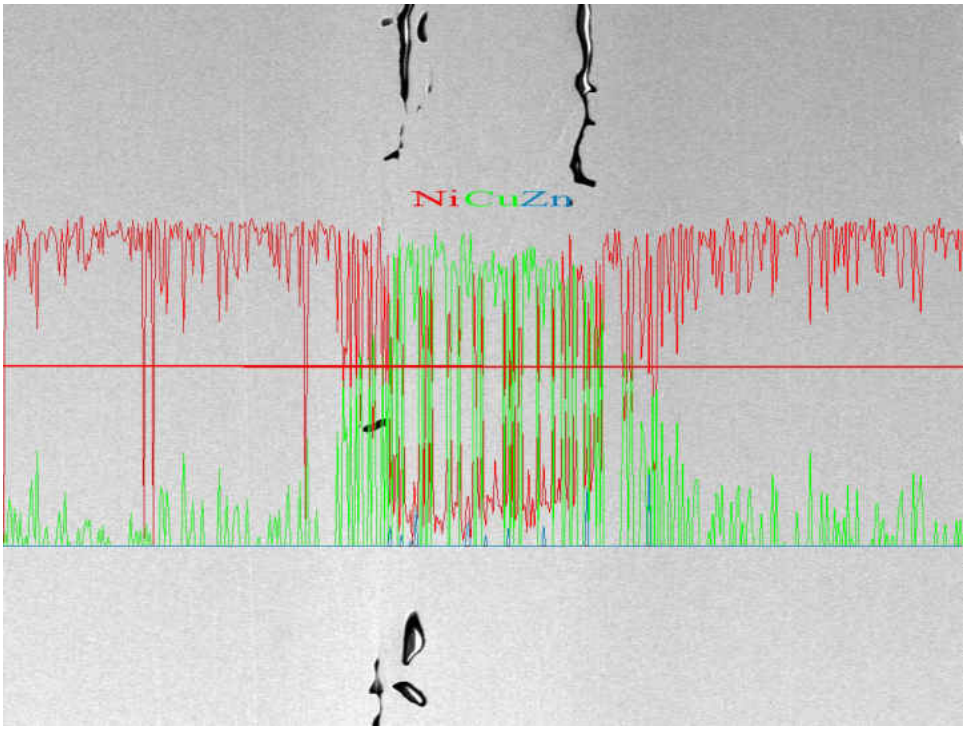

Figure B. 49: Linescan overlay on Image of Sample 25

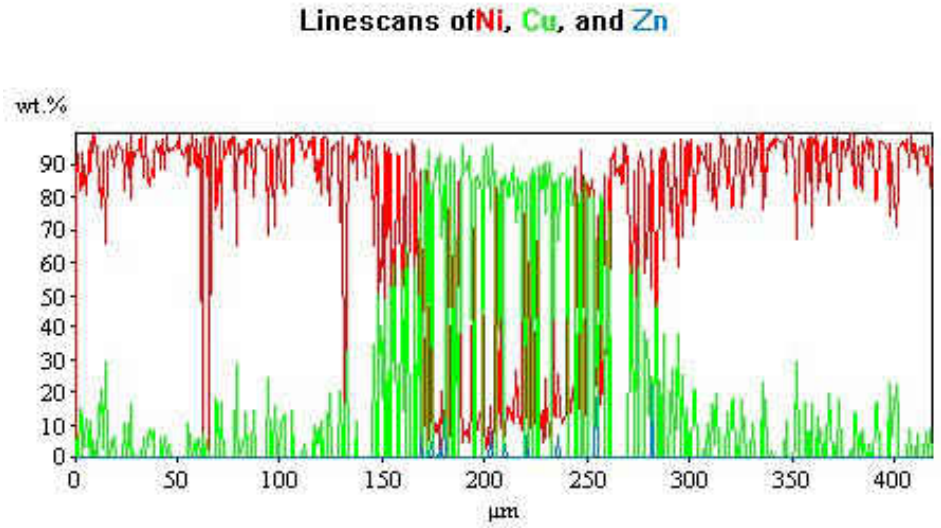

Figure B. 50: Scaled linescan showing concentration profiles of the joint of sample 25.

Sample 26: 10hr, 1050ºC, 800grit, 130µm

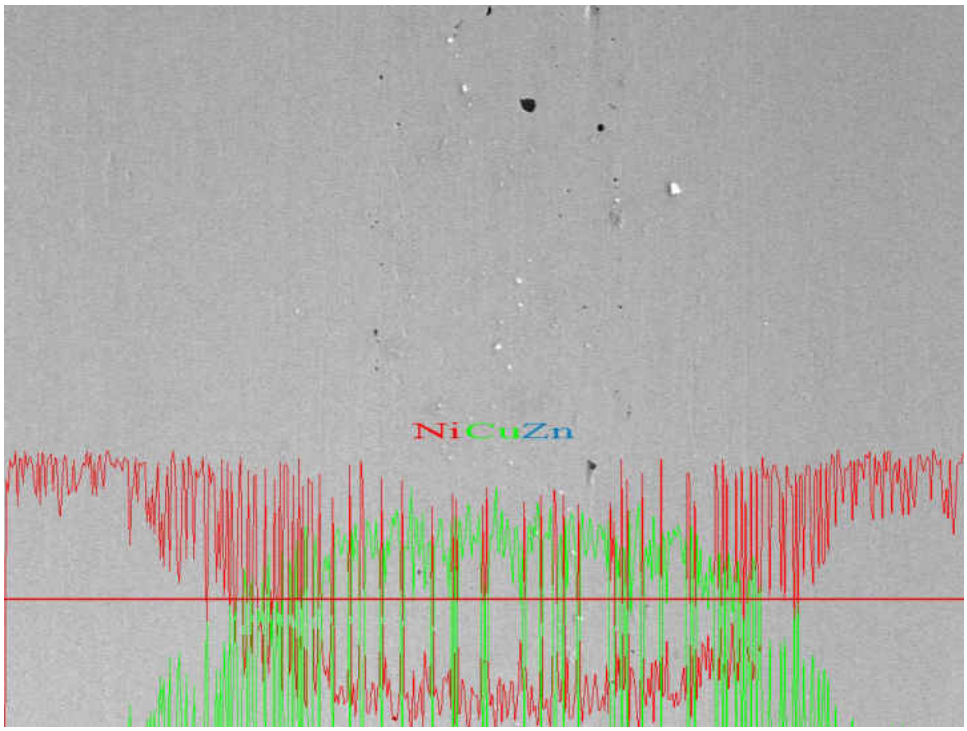

Figure B. 51: Linescan overlay on Image of Sample 26

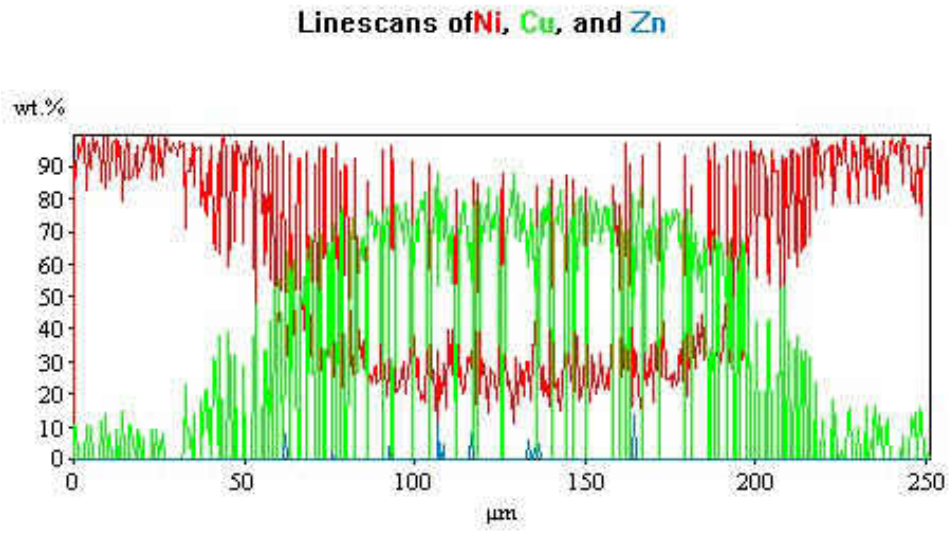

Figure B. 52: Scaled linescan showing concentration profiles of the joint of sample 26

Sample 27: 10hr, 1000ºC, 600grit, 130µm

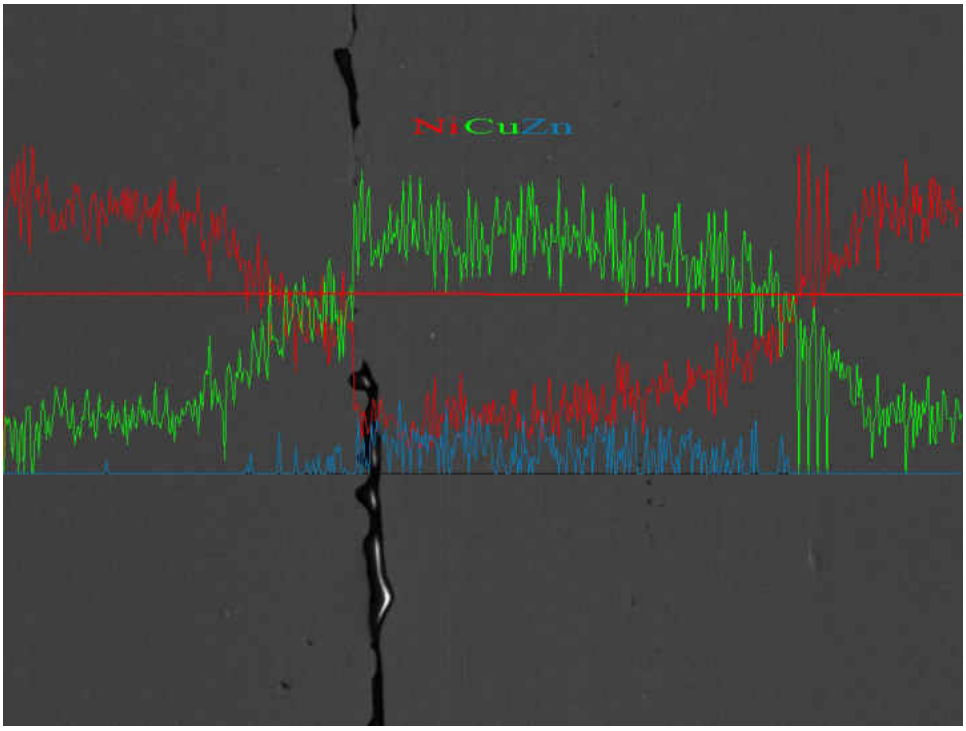

Figure B. 53: Linescan overlay on Image of Sample 27

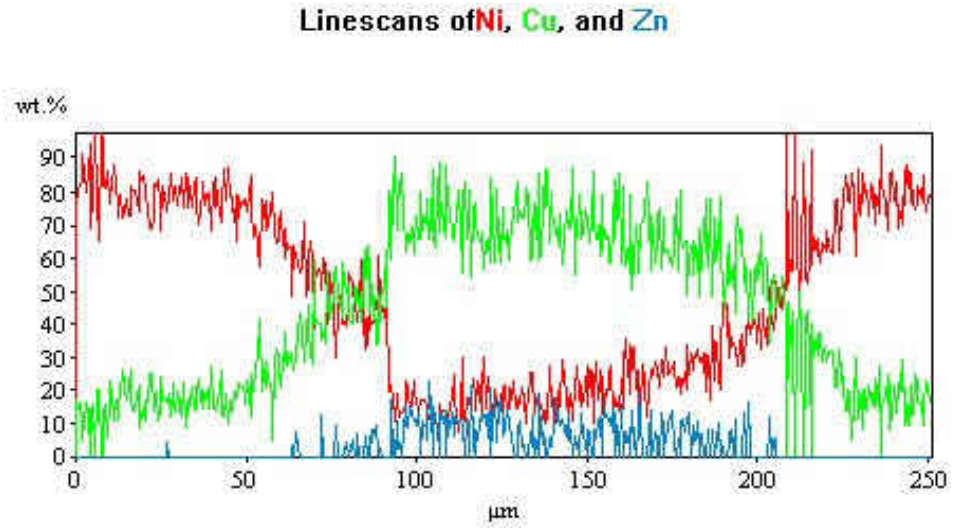

Figure B. 54: Scaled linescan showing concentration profiles of the joint of sample 27.

Appendix C

Wt.% Cu Analysis

In an effort to check the results of the wt. % Ni model, a second yield was calculated, wt. % Cu. This was done to check to see if the same factors were significant as for wt. % Ni, and to see if there are any discrepancies in the models. It is important to note that we expect the coefficients of the wt. % Cu to be opposite to those of the wt. % Ni. This is because for the wt. % Ni to be maximized the wt. % Cu will be at its lowest.

The same analysis for the wt.% Ni is done for the wt. % Cu. The procedure is the same. Table C.1 shows the values of wt. % Cu. The initial model is trimmed until only the significant terms remain from Table C.2. Then the model is analyzed to see if there are outliers using a normal residual plot (Figure C.1). From the normal residual plot it does appear that one of the points is a potential outlier in the data. The resulting model is checked for lack of fit and trends in the data by plotting the residuals versus the run order (Figure C.2). The model is trimmed to its simplest significant form. The resulting model defines the wt.% Cu across the experimental window for each parameter. The contour plots for this model can be seen in Figure C.3 and the model is defined in Equation C.1.

Table C. 1: Run order and coded values for wt.% Cu yield

time	temp	grit	foil	wt.% Cu
-1	-1	0	-0.06667	66.7
1	-1	0	-0.06667	62.2
-1	1	0	-0.06667	61.9
1	1	0	-0.06667	52.1
0	0	-1	-1	43.3
0	0	1	-1	21.9
0	0	-1	1	73.8
0	0	1	1	70.2
0	0	0	-0.06667	82.1
-1	0	-1	-0.06667	64.2
1	0	-1	-0.06667	62.9
-1	0	1	-0.06667	66.2
1	0	1	-0.06667	41
0	-1	0	-1	43.9
0	1	0	-1	20.4
0	-1	0	1	63
0	1	0	1	73.5
0	0	0	-0.06667	75
-1	0	0	-1	45.7
1	0	0	-1	16.9
-1	0	0	1	76.4
1	0	0	1	79.8
0	-1	-1	-0.06667	64.4
0	1	-1	-0.06667	48.4
0	-1	1	-0.06667	48.9
0	1	1	-0.06667	56.1
0	0	0	-0.06667	65.3

Table C. 2: Table of variables and their corresponding coefficients, t-values and p-values

Term	Coef	t-value	p-value
Constant	75.559	26.027	0
time	-5.162	-3.556	0.004
temp	-2.682	-1.848	0.089
grit	-4.2	-2.893	0.014
foil	20.383	14.082	0
time*time	-5.225	-2.406	0.033
temp*temp	-9.538	-4.393	0.001
grit*grit	-9.562	-4.404	0.001
foil*foil	-15.051	-6.894	0
time*temp	-1.325	-0.528	0.607
time*grit	-5.975	-2.383	0.035
time*foil	7.971	3.184	0.008
temp*grit	5.8	2.313	0.039
temp*foil	8.462	3.38	0.005
grit*foil	4.313	1.723	0.111

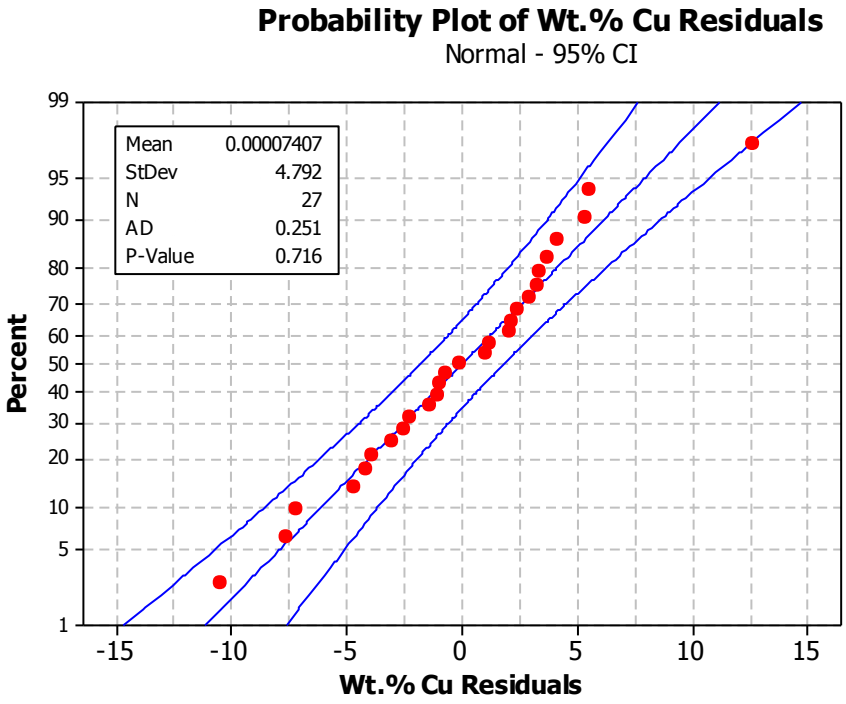

Figure C. 1: Normal Probability Plot of the residuals for wt. % Cu analysis with 95% confidence intervals.

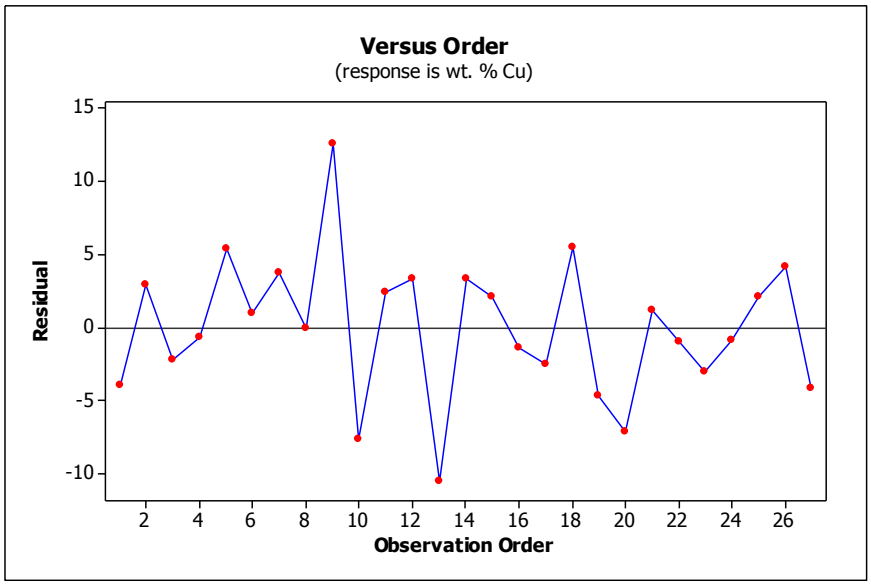

Figure C. 2: Residuals for wt.% Cu plotted versus run order

$$-5.225t^2 - 9.5375T^2 - 9.5625g^2 - 15.0508f^2 - 5.975tg + 7.97tf +$$

$$5.8Tg + 8.46215Tf - 5.16241t - 2.68224T - 4.39167g + 20.3833f + 75.5591 =$$

$wt.\%\ Cu$ Equation C.1

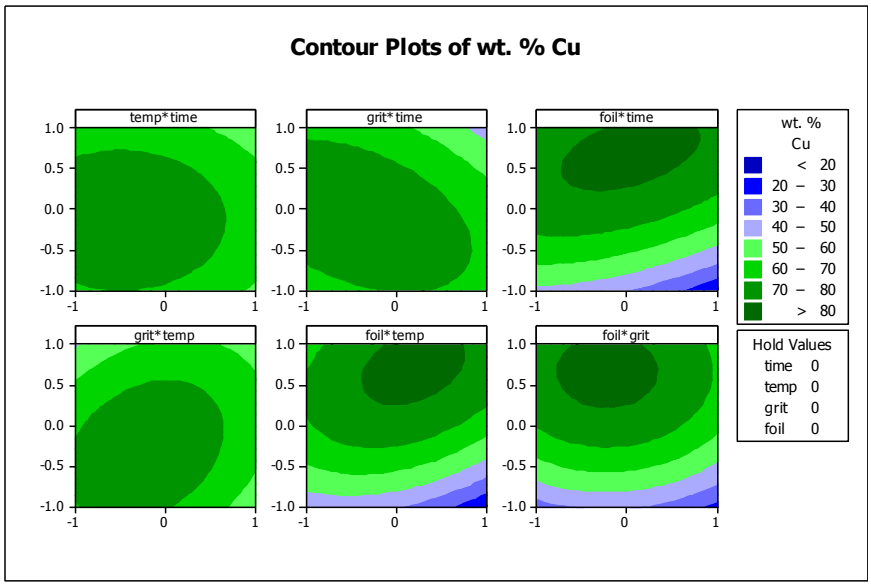

Figure C. 3: Contour plots of wt.% Cu model

This model will have coefficients that are the opposite of the wt.% Ni model because they are mutually exclusive for the Ni wt% to be high the Cu Wt. % has to go down. The results for the wt. % Cu indicate that the model we have for Ni is a good model that accurately describes the experimental system. For the future analysis we will utilize the wt.% Ni model because it best matches with the expected signs on the coefficients for strength analysis based on what we know from theory. Discrepancies from the model for wt.% Cu and wt.% Ni can be explained by overlapping peak energies. EDS is not a purely quantitative tool, but a semi-quantitative tool with some qualitative analysis incorporated.

A second method for yield was attempted to determine if the method used in this research was artificially impacting the results of the study. This method was not used for the final models because of how it was analyzed. For this analysis, a point 25μm away from the bond interface (the area of the joint that originally was the interlayer) was used as the yield component for the composition model. The following analysis follows the same steps as all other response surface analysis in this paper.

Response Surface Regression: Wt. % Cu at 25μm versus time, temp, grit, foil

```
The analysis was done using coded units.

Estimated Regression Coefficients for Cu@25

Term          Coef  SE Coef       T      P
Constant    35.627    5.685   6.267  0.000
time         4.444    6.371   0.698  0.494
temp         2.865    6.352   0.451  0.657
grit         2.237    6.352   0.352  0.729
foil        10.225    6.345   1.612  0.124
temp*temp  -20.685    8.523  -2.427  0.025
time*grit  -25.268   11.002  -2.297  0.033
time*foil   23.465   10.986   2.136  0.046


S = 22.0042    PRESS = 20622.0
R-Sq = 50.02%  R-Sq(pred) = 0.00%  R-Sq(adj) = 31.61%


Analysis of Variance for Cu@25

Source          DF  Seq SS  Adj SS  Adj MS     F      P
Regression       7    9208    9208  1315.4  2.72  0.039
  Linear         4    1593    1652   412.9  0.85  0.510
  Square         1    2852    2852  2852.3  5.89  0.025
  Interaction    2    4763    4763  2381.4  4.92  0.019
Residual Error  19    9199    9199   484.2
  Lack-of-Fit   17    7215    7215   424.4  0.43  0.873
  Pure Error     2    1984    1984   992.1
Total           26   18407


Obs  StdOrder   Cu@25     Fit  SE Fit  Residual  St Resid
  1         1   3.600   8.515  11.006    -4.915     -0.26
  2         2  20.729  14.276  11.006     6.453      0.34
  3         3  13.184  14.245  11.006    -1.061     -0.06
  4         4  30.505  20.005  11.006    10.500      0.55
  5         5  24.303  23.166  10.508     1.137      0.06
  6         6   3.835  27.639  10.508   -23.804     -1.23
  7         7  22.327  43.615  10.744   -21.288     -1.11
```

8	8	26.897	48.088	10.744	-21.191	-1.10
9	9	70.150	34.945	5.686	35.205	1.66
10	10	17.279	4.561	15.301	12.718	0.80
11	11	32.852	60.857	15.301	-28.005	-1.77
12	12	88.158	59.570	15.301	28.588	1.81
13	13	2.659	14.794	15.301	-12.135	-0.77
14	14	9.573	1.852	10.838	7.721	0.40
15	15	2.990	7.582	10.838	-4.592	-0.24
16	16	18.025	22.302	11.163	-4.277	-0.23
17	17	11.569	28.031	11.163	-16.462	-0.87
18	18	81.710	34.945	5.686	46.765	2.20 R
19	19	15.094	44.423	14.853	-29.329	-1.81
20	20	8.262	6.382	14.853	1.880	0.12
21	21	15.341	17.943	15.719	-2.602	-0.17
22	22	98.467	73.761	15.719	24.706	1.60
23	23	3.082	9.159	11.003	-6.077	-0.32
24	24	27.729	14.888	11.003	12.841	0.67
25	25	14.727	13.632	11.003	1.095	0.06
26	26	18.135	19.361	11.003	-1.226	-0.06
27	27	22.301	34.945	5.686	-12.644	-0.59

R denotes an observation with a large standardized residual.

Estimated Regression Coefficients for Cu@25 using data in uncoded units

Term	Coef
Constant	35.6271
time	4.44438
temp	2.86467
grit	2.23658
foil	10.2246
temp*temp	-20.6853
time*grit	-25.2680
time*foil	23.4648

This model says to minimize wt. % Cu we want to increase the temperature. And that we would lower the time, increase the surface finish, and increase the foil thickness. I feel that from doing this analysis, it is impossible to use a single data point from the EDS analysis as there exists too much variation in that information (plus, minus 10 wt.% from one point to the next in some cases with some points to register a value of 0, most likely from a peak overlap.) In Appendix B you can see the EDS plots for each of the samples and see the variation in the EDS analysis. Because of this variation, averaging across the foil thickness provided a better value, and does not impact the significance of the factors. While the EDS linescan does not represent an exact value for composition as it is a semi-

quantitative analysis, it is useful as it was use consistently across all samples for this research. It is a more accurate method than analyzing point by point only searching for a few select elements. The linescan will detect all elements, and not only the ones you are scanning for.

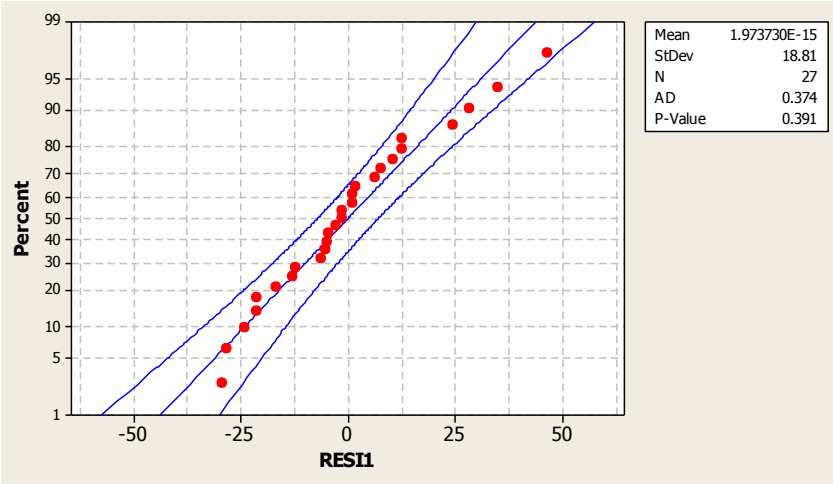

Figure C. 4: Normal Probability plot of the residuals for wt.% Cu 25µm from the bond interface.

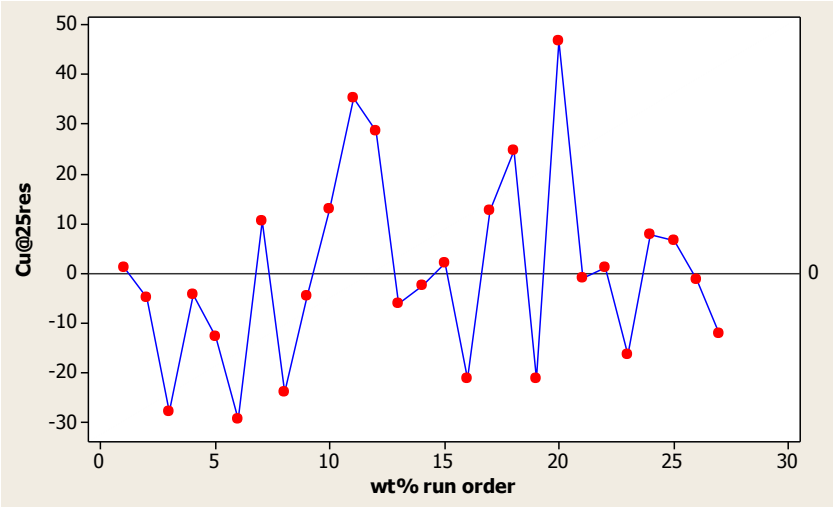

Figure C. 5: Residuals of wt. % Cu 25µm from the bond interface versus the run order for wt.% samples.

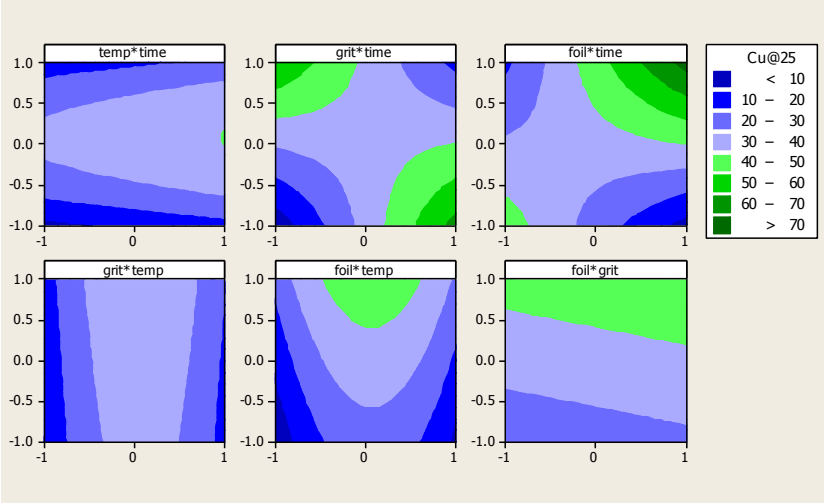

Figure C. 6: Contour plots of the wt.% Cu 25 μm from the bond interface.

Appendix D

Strength Analysis

Initial Strength

Table D.1 shows the strength values that are used for the analysis. Table D.2 shows the values of the initial analysis for strength.

$$\sigma = \frac{P}{A} \qquad \text{Equation D.1}$$

Table D. 1: Strength Values for RSM analysis

time	temp	grit	foil	Strength
-1	-1	0	-0.06667	41.57
1	-1	0	-0.06667	38.98
-1	1	0	-0.06667	39.81
1	1	0	-0.06667	8.19
0	0	-1	-1	25.54
0	0	1	-1	20.09
0	0	-1	1	40.86
0	0	1	1	25.19
0	0	0	-0.06667	17.68
-1	0	-1	-0.06667	22.23
1	0	-1	-0.06667	36.74
-1	0	1	-0.06667	12.08
1	0	1	-0.06667	18.94
0	-1	0	-1	18.46
0	1	0	-1	19.82
0	-1	0	1	10.77
0	1	0	1	33.63
0	0	0	-0.06667	4.75
-1	0	0	-1	21.80
1	0	0	-1	64.67
-1	0	0	1	52.99
1	0	0	1	9.44
0	-1	-1	-0.06667	38.15
0	1	-1	-0.06667	38.60
0	-1	1	-0.06667	16.83
0	1	1	-0.06667	17.68
0	0	0	-0.06667	23.84

Figure D.1 shows the normal residual plot for the strength results and Figure D.2 shows the residuals versus the run order. Equation D.2 shows the model for just the strength analysis.

Table D.2: Shows the coefficients, t-values, and p-values for the initial analysis of the strength data.

Term	Coef.	t-value	p-value
Constant	15.4033	2.154	0.052
time	-2.0806	-0.582	0.571
temp	-0.3283	-0.092	0.928
grit	-7.7165	-2.158	0.052
foil	0.2093	0.059	0.954
time*time	10.1751	1.902	0.081
temp*temp	4.5554	0.852	0.411
grit*grit	3.3624	0.629	0.541
foil*foil	7.1728	1.334	0.207
time*temp	-7.2585	-1.175	0.263
time*grit	-1.9151	-0.31	0.762
time*foil	-21.4786	-3.483	0.005
temp*grit	0.1005	0.016	0.987
temp*foil	5.8002	0.941	0.365
grit*foil	-2.3932	-0.388	0.705

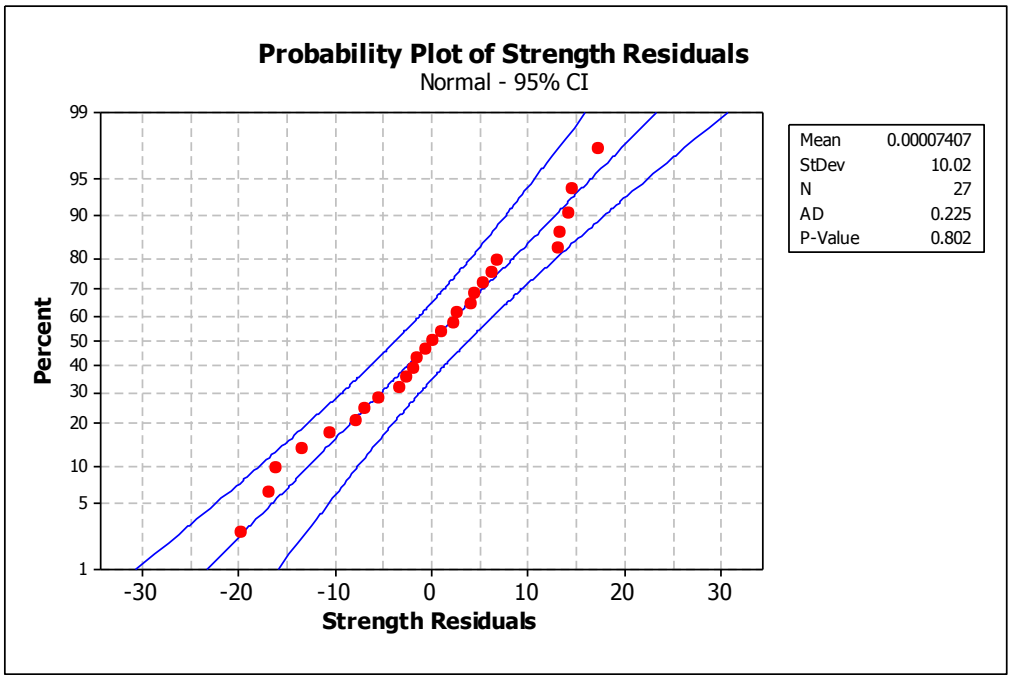

Figure D.1: Normal residual plot for Strength results

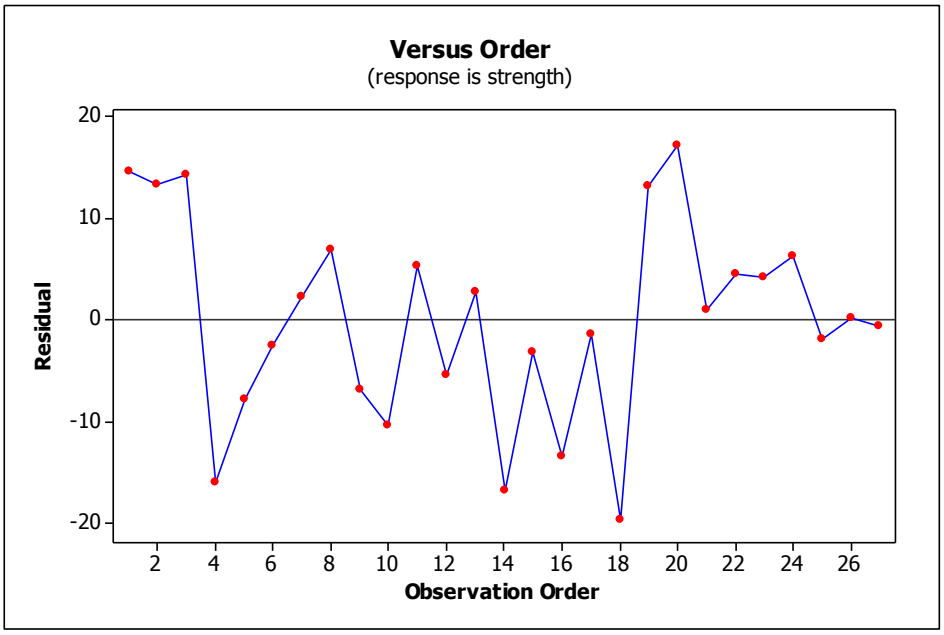

Figure D.2: Residuals versus run order

$$9.354f^2 + 7.387f + 9.378T + 22.43 = \sigma \qquad \text{D.2}$$

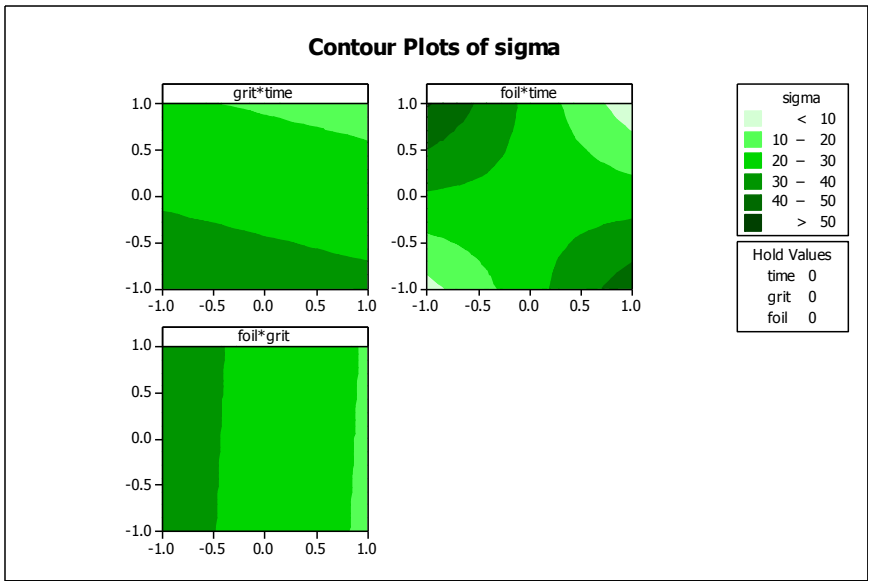

Figure D.3: Contour plot of the un-modified strength values (MPa). The areas of dark greed define the areas of greatest strength.

Area Analysis

This appendix holds the images used for area analysis. There are two images per sample and are labeled accordingly. The purpose of the area analysis is to determine the area of the joint that actually joined during bonding. The images were taken with a Nikon D-90 with an 18-55 mm lens. To make the images, Photoshop was used. The steps to make the images were to crop to a smaller area to capture the sample. Then use the circle selection tool to capture only the sample. The next step was to copy and paste the selected circle, hide the background and use a transparent background so that it is not included in the analysis.

Figure D. 1: Experiment 1 run 9 fracture surface 1

Figure D. 2: Experiment 1 run 9 fracture surface 2

Figure D. 3: Experiment 2 run 22 fracture surface 1.

Figure D. 4: Experiment 2 run 22 fracture surface 2.

Figure D. 5: Experiment 3 run 3 fracture surface 1.

Figure D. 6: Experiment 3 run 3 fracture surface 2.

Figure D. 7: Experiment 4 run 2 fracture surface 1

Figure D. 8: Experiment 4 run 2 fracture surface 2

Figure D. 9: Experiment 5 run 11 fracture surface 1

Figure D. 10: Experiment 5 run 11 fracture surface 2

Figure D. 11: Experiment 6 run 12 fracture surface 1.

Figure D. 12: Experiment 6 run 12 fracture surface 2.

Figure D. 13: Experiment 7 run 5 fracture surface 1.

Figure D. 14: Experiment 7 run 5 fracture surface 2.

Figure D. 15: Experiment 8 run 24 fracture surface 1.

Figure D. 16: Experiment 8 run 24 fracture surface 2.

Figure D. 17: Experiment 9 run 16 fracture surface 1.

Figure D. 18: Experiment 9 run 16 fracture surface 2.

Figure D. 19: Experiment 10 run 17 fracture surface 1.

Figure D. 20: Experiment 10 run 17 fracture surface 2.

Figure D. 21: Experiment 11 run 4 fracture surface 1.

Figure D. 22: Experiment 11 run 4 fracture surface 2.

Figure D. 23: Experiment 12 run 15 fracture surface 1.

Figure D. 24: Experiment 12 run 15 fracture surface 2.

Figure D. 25: Experiment 13 run 27 fracture surface 1.

Figure D. 26: Experiment 13 run 27 fracture surface 2.

Figure D. 27: Experiment 14 run 6 fracture surface 1.

Figure D. 28: Experiment 14 run 6 fracture surface 2.

Figure D. 29: Experiment 15 run 1 fracture surface 1.

Figure D. 30: Experiment 15 run 1 fracture surface 2.

Figure D. 31: Experiment 16 run 25 fracture surface 1.

Figure D. 32: Experiment 16 run 25 fracture surface 2.

Figure D. 33: Experiment 17 run 20 fracture surface 1.

Figure D. 34: Experiment 17 run 20 fracture surface 2.

Figure D. 35: Experiment 18 run 10 fracture surface 1.

Figure D. 36: Experiment 18 run 10 fracture surface 2.

Figure D. 37: Experiment 19 run 19 fracture surface 1.

Figure D. 38: Experiment 19 run 19 fracture surface 2.

Figure D. 39: Experiment 20 run 26 fracture surface 1.

Figure D. 40: Experiment 20 run 26 fracture surface 2.

Figure D. 41: Experiment 21 run 21 fracture surface 1.

Figure D. 42: Experiment 21 run 21 fracture surface 2.

Figure D. 43: Experiment 22 run 7 fracture surface 1.

Figure D. 44: Experiment 22 run 7 fracture surface 2.

Figure D. 45: Experiment 23 run 23 fracture surface 1.

Figure D. 46: Experiment 23 run 23 fracture surface 2.

Figure D. 47: Experiment 24 run 8 fracture surface 1.

Figure D. 48: Experiment 24 run 8 fracture surface 2.

Figure D. 49: Experiment 25 run 18 fracture surface 1.

Figure D. 50: Experiment 25 run 18 fracture surface 2.

Figure D. 51: Experiment 26 run 14 fracture surface 1.

Figure D. 52: Experiment 26 run 14 fracture surface 2.

Figure D. 53: Experiment 27 run 13 fracture surface 1.

Figure D. 54: Experiment 27 run 13 fracture surface 2.

Table D. 2: Table of initial areas.

D1	D2	D3	Avg. D	Area	run	experiment
0.355	0.355	0.355	0.355	63.858	9	1
0.355	0.355	0.355	0.355	63.858	22	2
0.353	0.355	0.354	0.354	63.499	3	3
0.353	0.355	0.353	0.3537	63.379	2	4
0.355	0.355	0.355	0.355	63.858	11	5
0.354	0.353	0.354	0.3537	63.379	12	6
0.354	0.354	0.353	0.3537	63.379	5	7
0.354	0.354	0.353	0.3537	63.379	24	8
0.353	0.353	0.355	0.3537	63.379	16	9
0.354	0.355	0.354	0.3543	63.618	17	10
0.354	0.353	0.354	0.3537	63.379	4	11
0.354	0.354	0.355	0.3543	63.618	15	12
0.353	0.354	0.354	0.3537	63.379	27	13
0.354	0.355	0.355	0.3547	63.738	6	14
0.355	0.355	0.355	0.355	63.858	1	15
0.353	0.353	0.354	0.3533	63.26	25	16
0.354	0.353	0.354	0.3537	63.379	20	17
0.355	0.354	0.354	0.3543	63.618	10	18
0.353	0.354	0.355	0.354	63.499	19	19
0.355	0.355	0.354	0.3547	63.738	26	20
0.354	0.355	0.353	0.354	63.499	21	21
0.354	0.353	0.354	0.3537	63.379	7	22
0.355	0.354	0.354	0.3543	63.618	23	23
0.355	0.355	0.353	0.3543	63.618	8	24
0.354	0.355	0.354	0.3543	63.618	18	25
0.354	0.355	0.355	0.3547	63.738	14	26
0.354	0.353	0.355	0.354	63.499	13	27

Table D. 3: Area ratio information in terms of pixels for fracture surface 1.

Fracture surface 1					
Run	area measurements		threshold		ratio
	total area	bonded area	min	max	
1	91455	49950	55	81	0.54617
2	96902	18231	68	149	0.188139
3	88276	43924	72	126	0.497576
4	86156	23908	58	85	0.277497
5	98557	36661	64	98	0.371978
6	88757	37030	58	106	0.417207
7	86680	48376	64	144	0.558099
8	82022	37110	60	76	0.45244
9	92508	46078	3	16	0.498097
10	79048	30138	63	110	0.381262
11	77044	50221	51	76	0.651848
12	68925	48200	64	74	0.699311
13	76541	18170	69	88	0.237389
14	77557	52802	60	88	0.680815
15	74132	15575	63	78	0.210098
16	76541	11592	60	67	0.151448
17	75076	21838	60	85	0.290879
18	75076	26994	55	92	0.359556
19	76080	56429	21	67	0.741706
20	76541	25561	61	133	0.333952
21	75565	26502	73	251	0.350718
22	73657	7736	57	81	0.105027
23	71681	40602	52	84	0.566426
24	70765	44350	64	116	0.626722
25	83549	30474	65	133	0.364744
26	76541	50035	57	78	0.653702
27	80560	16640	52	69	0.206554

Table D. 4: Area ratio information in terms of pixels for fracture surface 2.

Fracture surface 2					
Run	area measurements		threshold		ratio
	total area	bonded area	min	max	
1	86156	48109	55	70	0.558394
2	88276	18686	71	128	0.211677
3	88276	43880	76	126	0.497077
4	87728	24791	63	78	0.282589
5	87184	32863	78	130	0.376938
6	87729	33625	57	96	0.383283
7	85641	47994	64	134	0.560409
8	82023	37436	58	121	0.456409
9	82024	47169	55	122	0.575063
10	79528	30146	55	85	0.379061
11	77557	50585	58	73	0.65223
12	77044	53084	57	92	0.689009
13	82023	19170	72	89	0.233715
14	74625	50749	50	69	0.680054
15	75075	15217	69	81	0.202691
16	77043	14587	60	72	0.189336
17	90344	23782	60	97	0.263238
18	79048	28657	44	113	0.362527
19	76080	55913	13	62	0.734924
20	78048	27117	55	128	0.34744
21	77044	28266	69	110	0.366881
22	79048	8302	58	88	0.105025
23	71276	40397	55	84	0.566769
24	71656	41015	57	124	0.572388
25	72219	25968	39	72	0.359573
26	74617	50805	57	86	0.680877
27	71276	15970	58	74	0.224059

Table D. 5: Table of stress calculations, area ratio is an average of the ratio from fracture surface 1 and fracture surface 2.

Area	run	experiment	Force N	Stress MPa	Area ratio	actual stress MPa
63.858	9	1	1535.9	24.05187	0.54	45
63.858	22	2	587.5	9.200128	0.11	88
63.499	3	3	2476.563	39.00188	0.50	78
63.379	2	4	2425	38.26187	0.20	191
63.858	11	5	2285.938	35.79731	0.65	55
63.379	12	6	751.5625	11.85822	0.69	17
63.379	5	7	1589.062	25.07236	0.37	67
63.379	24	8	2401.562	37.89206	0.60	63
63.379	16	9	670.3125	10.57625	0.17	62
63.618	17	10	2092.187	32.88661	0.28	119
63.379	4	11	509.375	8.036965	0.28	29
63.618	15	12	1232.813	19.37831	0.21	94
63.379	27	13	1482.813	23.39596	0.22	109
63.738	6	14	1250	19.61155	0.40	49
63.858	1	15	2585.938	40.49525	0.55	73
63.26	25	16	1046.875	16.54887	0.36	46
63.379	20	17	4023.438	63.48217	0.34	186
63.618	10	18	1382.813	21.73612	0.38	57
63.499	19	19	1356.25	21.35875	0.74	29
63.738	26	20	1100	17.25817	0.67	26
63.499	21	21	3296.875	51.92047	0.36	145
63.379	7	22	2542.187	40.11086	0.56	72
63.618	23	23	2373.437	37.30752	0.57	66
63.618	8	24	1567.188	24.63427	0.45	54
63.618	18	25	295.3125	4.64195	0.36	13
63.738	14	26	1148.438	18.01812	0.68	26
63.499	13	27	1178.125	18.55357	0.24	79

Appendix E

Minitab Analysis

Wt.% Ni Minitab outputs

Response Surface Regression: wt.% Ni versus time, temp, grit, foil

```
The analysis was done using coded units.

Estimated Regression Coefficients for wt.% Ni

Term           Coef  SE Coef        T      P
Constant    15.6670    3.150    4.974  0.000
time         6.1080    1.575    3.878  0.002
temp         4.6134    1.575    2.929  0.013
grit         5.2814    1.575    3.353  0.006
foil       -21.4500    1.571  -13.658  0.000
time*time    3.1208    2.356    1.325  0.210
temp*temp   11.5958    2.356    4.922  0.000
grit*grit    8.6708    2.356    3.681  0.003
foil*foil   15.6705    2.369    6.616  0.000
time*temp    0.1500    2.720    0.055  0.957
time*grit    5.0750    2.720    1.866  0.087
time*foil  -10.3205    2.716   -3.800  0.003
temp*grit   -5.3500    2.720   -1.967  0.073
temp*foil   -6.8242    2.716   -2.512  0.027
grit*foil   -1.9188    2.716   -0.706  0.493


S = 5.44037    PRESS = 1652.15
R-Sq = 96.20%  R-Sq(pred) = 82.34%  R-Sq(adj) = 91.78%


Analysis of Variance for wt.% Ni

Source          DF  Seq SS  Adj SS   Adj MS      F      P
Regression      14  9001.7  9001.7   642.98  21.72  0.000
  Linear         4  6481.7  6552.9  1638.23  55.35  0.000
  Square         4  1673.4  1673.4   418.36  14.13  0.000
  Interaction    6   846.5   846.5   141.09   4.77  0.010
Residual Error  12   355.2   355.2    29.60
  Lack-of-Fit   10   245.5   245.5    24.55   0.45  0.842
  Pure Error     2   109.6   109.6    54.82
Total           26  9356.8


Obs  StdOrder  wt.% Ni     Fit  SE Fit  Residual  St Resid
  1         1   20.800  20.169   4.156     0.631      0.18
  2         2   30.400  33.461   4.156    -3.061     -0.87
  3         3   32.100  30.006   4.156     2.094      0.60
  4         4   42.300  43.898   4.156    -1.598     -0.46
  5         5   50.800  54.258   4.075    -3.458     -0.96
  6         6   70.200  68.658   4.075     1.542      0.43
  7         7   13.000  15.196   4.232    -2.196     -0.64
  8         8   24.100  21.921   4.232     2.179      0.64
```

9	9	9.300	17.167	3.141	-7.867	-1.77
10	10	17.200	21.828	4.156	-4.628	-1.32
11	11	27.200	25.270	4.156	1.930	0.55
12	12	20.400	22.497	4.156	-2.097	-0.60
13	13	50.700	46.239	4.156	4.461	1.27
14	14	49.400	52.946	4.075	-3.546	-0.98
15	15	73.100	75.821	4.075	-2.721	-0.75
16	16	26.300	23.694	4.232	2.606	0.76
17	17	22.600	19.272	4.232	3.328	0.97
18	18	18.200	17.167	3.141	1.033	0.23
19	19	45.100	39.480	4.075	5.620	1.56
20	20	74.900	72.337	4.075	2.563	0.71
21	21	15.600	17.221	4.232	-1.621	-0.47
22	22	4.500	8.796	4.232	-4.296	-1.26
23	23	26.900	21.606	4.156	5.294	1.51
24	24	45.500	42.442	4.156	3.058	0.87
25	25	41.200	43.124	4.156	-1.924	-0.55
26	26	38.400	42.561	4.156	-4.161	-1.19
27	27	24.000	17.167	3.141	6.833	1.54

Remove first term

Response Surface Regression: wt.% Ni versus time, temp, grit, foil

The analysis was done using coded units.

Estimated Regression Coefficients for wt.% Ni

Term	Coef	SE Coef	T	P
Constant	15.667	3.027	5.176	0.000
time	6.108	1.514	4.036	0.001
temp	4.613	1.514	3.048	0.009
grit	5.281	1.514	3.489	0.004
foil	-21.450	1.509	-14.214	0.000
time*time	3.121	2.264	1.379	0.191
temp*temp	11.596	2.264	5.123	0.000
grit*grit	8.671	2.264	3.831	0.002
foil*foil	15.670	2.276	6.885	0.000
time*grit	5.075	2.614	1.942	0.074
time*foil	-10.321	2.610	-3.954	0.002
temp*grit	-5.350	2.614	-2.047	0.061
temp*foil	-6.824	2.610	-2.615	0.021
grit*foil	-1.919	2.610	-0.735	0.475

S = 5.22760 PRESS = 1593.63
R-Sq = 96.20% R-Sq(pred) = 82.97% R-Sq(adj) = 92.41%

Analysis of Variance for wt.% Ni

Source	DF	Seq SS	Adj SS	Adj MS	F	P
Regression	13	9001.6	9001.6	692.43	25.34	0.000
Linear	4	6481.7	6552.9	1638.23	59.95	0.000
Square	4	1673.4	1673.4	418.36	15.31	0.000
Interaction	5	846.4	846.4	169.29	6.19	0.004
Residual Error	13	355.3	355.3	27.33		
Lack-of-Fit	11	245.6	245.6	22.33	0.41	0.869
Pure Error	2	109.6	109.6	54.82		
Total	26	9356.8				

Obs	StdOrder	wt.% Ni	Fit	SE Fit	Residual	St Resid

1	1	20.800	20.019	3.019	0.781	0.18
2	2	30.400	33.611	3.019	-3.211	-0.75
3	3	32.100	30.156	3.019	1.944	0.46
4	4	42.300	43.748	3.019	-1.448	-0.34
5	5	50.800	54.258	3.915	-3.458	-1.00
6	6	70.200	68.658	3.915	1.542	0.45
7	7	13.000	15.196	4.067	-2.196	-0.67
8	8	24.100	21.921	4.067	2.179	0.66
9	9	9.300	17.167	3.018	-7.867	-1.84
10	10	17.200	21.828	3.993	-4.628	-1.37
11	11	27.200	25.270	3.993	1.930	0.57
12	12	20.400	22.497	3.993	-2.097	-0.62
13	13	50.700	46.239	3.993	4.461	1.32
14	14	49.400	52.946	3.915	-3.546	-1.02
15	15	73.100	75.821	3.915	-2.721	-0.79
16	16	26.300	23.694	4.067	2.606	0.79
17	17	22.600	19.272	4.067	3.328	1.01
18	18	18.200	17.167	3.018	1.033	0.24
19	19	45.100	39.480	3.915	5.620	1.62
20	20	74.900	72.337	3.915	2.563	0.74
21	21	15.600	17.221	4.067	-1.621	-0.49
22	22	4.500	8.796	4.067	-4.296	-1.31
23	23	26.900	21.606	3.993	5.294	1.57
24	24	45.500	42.442	3.993	3.058	0.91
25	25	41.200	43.124	3.993	-1.924	-0.57
26	26	38.400	42.561	3.993	-4.161	-1.23
27	27	24.000	17.167	3.018	6.833	1.60

Removal of Second Term

Response Surface Regression: wt.% Ni versus time, temp, grit, foil

The analysis was done using coded units.

Estimated Regression Coefficients for wt.% Ni

Term	Coef	SE Coef	T	P
Constant	15.667	2.977	5.264	0.000
time	6.108	1.488	4.103	0.001
temp	4.613	1.488	3.099	0.008
grit	5.367	1.484	3.616	0.003
foil	-21.450	1.484	-14.453	0.000
time*time	3.121	2.226	1.402	0.183
temp*temp	11.596	2.226	5.209	0.000
grit*grit	8.671	2.226	3.895	0.002
foil*foil	15.670	2.238	7.001	0.000
time*grit	5.075	2.571	1.974	0.068
time*foil	-10.321	2.567	-4.021	0.001
temp*grit	-5.350	2.571	-2.081	0.056
temp*foil	-6.824	2.567	-2.659	0.019

S = 5.14110 PRESS = 1541.75
R-Sq = 96.05% R-Sq(pred) = 83.52% R-Sq(adj) = 92.66%

Analysis of Variance for wt.% Ni

Source	DF	Seq SS	Adj SS	Adj MS	F	P
Regression	12	8986.8	8986.8	748.90	28.33	0.000
Linear	4	6481.7	6565.8	1641.45	62.10	0.000
Square	4	1673.4	1673.4	418.36	15.83	0.000

Interaction	4	831.7	831.7	207.92	7.87	0.002
Residual Error	14	370.0	370.0	26.43		
Lack-of-Fit	12	260.4	260.4	21.70	0.40	0.879
Pure Error	2	109.6	109.6	54.82		
Total	26	9356.8				

Obs	StdOrder	wt.% Ni	Fit	SE Fit	Residual	St Resid
1	1	20.800	20.019	2.969	0.781	0.19
2	2	30.400	33.611	2.969	-3.211	-0.77
3	3	32.100	30.156	2.969	1.944	0.46
4	4	42.300	43.748	2.969	-1.448	-0.34
5	5	50.800	56.092	2.968	-5.292	-1.26
6	6	70.200	66.825	2.968	3.375	0.80
7	7	13.000	13.192	2.968	-0.192	-0.05
8	8	24.100	23.925	2.968	0.175	0.04
9	9	9.300	17.167	2.968	-7.867	-1.87
10	10	17.200	21.871	3.927	-4.671	-1.41
11	11	27.200	25.313	3.927	1.887	0.57
12	12	20.400	22.454	3.927	-2.054	-0.62
13	13	50.700	46.196	3.927	4.504	1.36
14	14	49.400	52.946	3.850	-3.546	-1.04
15	15	73.100	75.821	3.850	-2.721	-0.80
16	16	26.300	23.694	4.000	2.606	0.81
17	17	22.600	19.272	4.000	3.328	1.03
18	18	18.200	17.167	2.968	1.033	0.25
19	19	45.100	39.480	3.850	5.620	1.65
20	20	74.900	72.337	3.850	2.563	0.75
21	21	15.600	17.221	4.000	-1.621	-0.50
22	22	4.500	8.796	4.000	-4.296	-1.33
23	23	26.900	21.648	3.927	5.252	1.58
24	24	45.500	42.485	3.927	3.015	0.91
25	25	41.200	43.082	3.927	-1.882	-0.57
26	26	38.400	42.518	3.927	-4.118	-1.24
27	27	24.000	17.167	2.968	6.833	1.63

Removal of Third Time

Response Surface Regression: wt.% Ni versus time, temp, grit, foil

The analysis was done using coded units.

Estimated Regression Coefficients for wt.% Ni

Term	Coef	SE Coef	T	P
Constant	18.446	2.291	8.052	0.000
time	6.108	1.536	3.978	0.001
temp	4.613	1.536	3.004	0.009
grit	5.367	1.531	3.505	0.003
foil	-21.450	1.531	-14.009	0.000
temp*temp	10.556	2.165	4.875	0.000
grit*grit	7.631	2.165	3.524	0.003
foil*foil	14.626	2.177	6.717	0.000
time*grit	5.075	2.652	1.914	0.075
time*foil	-10.321	2.648	-3.897	0.001
temp*grit	-5.350	2.652	-2.017	0.062
temp*foil	-6.824	2.648	-2.577	0.021

S = 5.30394 PRESS = 1462.44
R-Sq = 95.49% R-Sq(pred) = 84.37% R-Sq(adj) = 92.18%

Analysis of Variance for wt.% Ni

Source	DF	Seq SS	Adj SS	Adj MS	F	P
Regression	11	8934.8	8934.8	812.26	28.87	0.000
Linear	4	6481.7	6565.8	1641.45	58.35	0.000
Square	3	1621.5	1621.5	540.50	19.21	0.000
Interaction	4	831.7	831.7	207.92	7.39	0.002
Residual Error	15	422.0	422.0	28.13		
Lack-of-Fit	13	312.3	312.3	24.03	0.44	0.859
Pure Error	2	109.6	109.6	54.82		
Total	26	9356.8				

Obs	StdOrder	wt.% Ni	Fit	SE Fit	Residual	St Resid	
1	1	20.800	18.632	2.888	2.168	0.49	
2	2	30.400	32.224	2.888	-1.824	-0.41	
3	3	32.100	28.769	2.888	3.331	0.75	
4	4	42.300	42.361	2.888	-0.061	-0.01	
5	5	50.800	56.785	3.019	-5.985	-1.37	
6	6	70.200	67.519	3.019	2.681	0.61	
7	7	13.000	13.885	3.019	-0.885	-0.20	
8	8	24.100	24.619	3.019	-0.519	-0.12	
9	9	9.300	19.941	2.282	-10.641	-2.22	R
10	10	17.200	20.484	3.921	-3.284	-0.92	
11	11	27.200	23.926	3.921	3.274	0.92	
12	12	20.400	21.067	3.921	-0.667	-0.19	
13	13	50.700	44.809	3.921	5.891	1.65	
14	14	49.400	53.639	3.939	-4.239	-1.19	
15	15	73.100	76.514	3.939	-3.414	-0.96	
16	16	26.300	24.388	4.095	1.912	0.57	
17	17	22.600	19.966	4.095	2.634	0.78	
18	18	18.200	19.941	2.282	-1.741	-0.36	
19	19	45.100	38.093	3.839	7.007	1.91	
20	20	74.900	70.950	3.839	3.950	1.08	
21	21	15.600	15.834	3.998	-0.234	-0.07	
22	22	4.500	7.409	3.998	-2.909	-0.83	
23	23	26.900	22.342	4.019	4.558	1.32	
24	24	45.500	43.179	4.019	2.321	0.67	
25	25	41.200	43.775	4.019	-2.575	-0.74	
26	26	38.400	43.212	4.019	-4.812	-1.39	
27	27	24.000	19.941	2.282	4.059	0.85	

Removal of Fourth Term

Response Surface Regression: wt.% Ni versus time, temp, grit, foil

The analysis was done using coded units.

Estimated Regression Coefficients for wt.% Ni

Term	Coef	SE Coef	T	P
Constant	18.446	2.474	7.455	0.000
time	6.108	1.658	3.683	0.002
temp	4.613	1.658	2.782	0.013
grit	5.367	1.654	3.245	0.005
foil	-21.450	1.654	-12.972	0.000
temp*temp	10.556	2.339	4.514	0.000
grit*grit	7.631	2.339	3.263	0.005
foil*foil	14.626	2.352	6.219	0.000
time*foil	-10.321	2.860	-3.609	0.002
temp*grit	-5.350	2.864	-1.868	0.080

```
temp*foil   -6.824    2.860   -2.386  0.030


S = 5.72821    PRESS = 1509.63
R-Sq = 94.39%  R-Sq(pred) = 83.87%  R-Sq(adj) = 90.88%


Analysis of Variance for wt.% Ni

Source          DF  Seq SS  Adj SS   Adj MS      F      P
Regression      10  8831.8  8831.8   883.18  26.92  0.000
  Linear         4  6481.7  6565.8  1641.45  50.03  0.000
  Square         3  1621.5  1621.5   540.50  16.47  0.000
  Interaction    3   728.6   728.6   242.88   7.40  0.003
Residual Error  16   525.0   525.0    32.81
  Lack-of-Fit   14   415.4   415.4    29.67   0.54  0.806
  Pure Error     2   109.6   109.6    54.82
Total           26  9356.8


Obs  StdOrder  wt.% Ni     Fit  SE Fit  Residual  St Resid
  1         1   20.800  18.632   3.119     2.168      0.45
  2         2   30.400  32.224   3.119    -1.824     -0.38
  3         3   32.100  28.769   3.119     3.331      0.69
  4         4   42.300  42.361   3.119    -0.061     -0.01
  5         5   50.800  56.785   3.261    -5.985     -1.27
  6         6   70.200  67.519   3.261     2.681      0.57
  7         7   13.000  13.885   3.261    -0.885     -0.19
  8         8   24.100  24.619   3.261    -0.519     -0.11
  9         9    9.300  19.941   2.465   -10.641     -2.06 R
 10        10   17.200  15.409   3.119     1.791      0.37
 11        11   27.200  29.001   3.119    -1.801     -0.37
 12        12   20.400  26.142   3.119    -5.742     -1.20
 13        13   50.700  39.734   3.119    10.966      2.28 R
 14        14   49.400  53.639   4.255    -4.239     -1.11
 15        15   73.100  76.514   4.255    -3.414     -0.89
 16        16   26.300  24.388   4.422     1.912      0.53
 17        17   22.600  19.966   4.422     2.634      0.72
 18        18   18.200  19.941   2.465    -1.741     -0.34
 19        19   45.100  38.093   4.146     7.007      1.77
 20        20   74.900  70.950   4.146     3.950      1.00
 21        21   15.600  15.834   4.318    -0.234     -0.06
 22        22    4.500   7.409   4.318    -2.909     -0.77
 23        23   26.900  22.342   4.341     4.558      1.22
 24        24   45.500  43.179   4.341     2.321      0.62
 25        25   41.200  43.775   4.341    -2.575     -0.69
 26        26   38.400  43.212   4.341    -4.812     -1.29
 27        27   24.000  19.941   2.465     4.059      0.79

R denotes an observation with a large standardized residual.
```

Results after Fifth Term Removal

Response Surface Regression: wt.% Ni versus time, temp, grit, foil

The analysis was done using coded units.

Estimated Regression Coefficients for wt.% Ni

```
Term          Coef  SE Coef        T      P
Constant    18.446    2.649    6.963  0.000
time         6.108    1.776    3.440  0.003
```

temp	4.613	1.776	2.598	0.019
grit	5.367	1.771	3.031	0.008
foil	-21.450	1.771	-12.115	0.000
temp*temp	10.556	2.504	4.216	0.001
grit*grit	7.631	2.504	3.047	0.007
foil*foil	14.626	2.518	5.809	0.000
time*foil	-10.321	3.062	-3.370	0.004
temp*foil	-6.824	3.062	-2.229	0.040

S = 6.13327 PRESS = 1574.22
R-Sq = 93.17% R-Sq(pred) = 83.18% R-Sq(adj) = 89.55%

Analysis of Variance for wt.% Ni

Source	DF	Seq SS	Adj SS	Adj MS	F	P
Regression	9	8717.3	8717.3	968.59	25.75	0.000
Linear	4	6481.7	6565.8	1641.45	43.64	0.000
Square	3	1621.5	1621.5	540.50	14.37	0.000
Interaction	2	614.1	614.1	307.07	8.16	0.003
Residual Error	17	639.5	639.5	37.62		
Lack-of-Fit	15	529.8	529.8	35.32	0.64	0.756
Pure Error	2	109.6	109.6	54.82		
Total	26	9356.8				

Obs	StdOrder	wt.% Ni	Fit	SE Fit	Residual	St Resid	
1	1	20.800	18.632	3.340	2.168	0.42	
2	2	30.400	32.224	3.340	-1.824	-0.35	
3	3	32.100	28.769	3.340	3.331	0.65	
4	4	42.300	42.361	3.340	-0.061	-0.01	
5	5	50.800	56.785	3.492	-5.985	-1.19	
6	6	70.200	67.519	3.492	2.681	0.53	
7	7	13.000	13.885	3.492	-0.885	-0.18	
8	8	24.100	24.619	3.492	-0.519	-0.10	
9	9	9.300	19.941	2.639	-10.641	-1.92	
10	10	17.200	15.409	3.339	1.791	0.35	
11	11	27.200	29.001	3.339	-1.801	-0.35	
12	12	20.400	26.142	3.339	-5.742	-1.12	
13	13	50.700	39.734	3.339	10.966	2.13	R
14	14	49.400	53.639	4.555	-4.239	-1.03	
15	15	73.100	76.514	4.555	-3.414	-0.83	
16	16	26.300	24.388	4.735	1.912	0.49	
17	17	22.600	19.966	4.735	2.634	0.68	
18	18	18.200	19.941	2.639	-1.741	-0.31	
19	19	45.100	38.093	4.439	7.007	1.66	
20	20	74.900	70.950	4.439	3.950	0.93	
21	21	15.600	15.834	4.623	-0.234	-0.06	
22	22	4.500	7.409	4.623	-2.909	-0.72	
23	23	26.900	27.692	3.492	-0.792	-0.16	
24	24	45.500	37.829	3.492	7.671	1.52	
25	25	41.200	38.425	3.492	2.775	0.55	
26	26	38.400	48.562	3.492	-10.162	-2.02	R
27	27	24.000	19.941	2.639	4.059	0.73	

R denotes an observation with a large standardized residual.

Wt.% Cu Minitab Output

Response Surface Regression: wt. % Cu versus time, temp, grit, foil

The analysis was done using coded units.

Estimated Regression Coefficients for wt. % Cu

Term	Coef	SE Coef	T	P
Constant	75.559	2.903	26.027	0.000
time	-5.162	1.452	-3.556	0.004
temp	-2.682	1.452	-1.848	0.089
grit	-4.200	1.452	-2.893	0.014
foil	20.383	1.447	14.082	0.000
time*time	-5.225	2.171	-2.406	0.033
temp*temp	-9.538	2.171	-4.393	0.001
grit*grit	-9.562	2.171	-4.404	0.001
foil*foil	-15.051	2.183	-6.894	0.000
time*temp	-1.325	2.507	-0.528	0.607
time*grit	-5.975	2.507	-2.383	0.035
time*foil	7.971	2.503	3.184	0.008
temp*grit	5.800	2.507	2.313	0.039
temp*foil	8.462	2.503	3.380	0.005
grit*foil	4.313	2.503	1.723	0.111

S = 5.01427 PRESS = 1236.73
R-Sq = 96.29% R-Sq(pred) = 84.81% R-Sq(adj) = 91.97%

Analysis of Variance for wt. % Cu

Source	DF	Seq SS	Adj SS	Adj MS	F	P
Regression	14	7838.3	7838.3	559.88	22.27	0.000
Linear	4	5525.3	5599.9	1399.99	55.68	0.000
Square	4	1411.8	1411.8	352.96	14.04	0.000
Interaction	6	901.2	901.2	150.20	5.97	0.004
Residual Error	12	301.7	301.7	25.14		
Lack-of-Fit	10	159.5	159.5	15.95	0.22	0.959
Pure Error	2	142.2	142.2	71.12		
Total	26	8140.1				

Obs	StdOrder	wt. % Cu	Fit	SE Fit	Residual	St Resid
1	1	66.700	66.986	3.831	-0.286	-0.09
2	2	62.200	58.248	3.831	3.952	1.22
3	3	61.900	63.143	3.831	-1.243	-0.38
4	4	52.100	49.106	3.831	2.994	0.93
5	5	43.300	39.076	3.755	4.224	1.27
6	6	21.900	22.049	3.755	-0.149	-0.04
7	7	73.800	71.216	3.901	2.584	0.82
8	8	70.200	71.443	3.901	-1.243	-0.39
9	9	82.100	74.133	2.895	7.967	1.95
10	10	64.200	63.552	3.831	0.648	0.20
11	11	62.900	64.115	3.831	-1.215	-0.38
12	12	66.200	66.527	3.831	-0.327	-0.10
13	13	41.000	43.190	3.831	-2.190	-0.68
14	14	43.900	41.732	3.755	2.168	0.65
15	15	20.400	19.443	3.755	0.957	0.29
16	16	63.000	65.574	3.901	-2.574	-0.82
17	17	73.500	77.134	3.901	-3.634	-1.15
18	18	75.000	74.133	2.895	0.867	0.21
19	19	45.700	48.033	3.755	-2.333	-0.70
20	20	16.900	21.767	3.755	-4.867	-1.46
21	21	76.400	72.858	3.901	3.542	1.12
22	22	79.800	78.475	3.901	1.325	0.42
23	23	64.400	68.567	3.831	-4.167	-1.29
24	24	48.400	50.474	3.831	-2.074	-0.64

25	25	48.900	47.992	3.831	0.908	0.28
26	26	56.100	53.099	3.831	3.001	0.93
27	27	65.300	74.133	2.895	-8.833	-2.16 R

R denotes an observation with a large standardized residual.

After removal of first term

Response Surface Regression: wt. % Cu versus time, temp, grit, foil

The analysis was done using coded units.

Estimated Regression Coefficients for wt. % Cu

Term	Coef	SE Coef	T	P
Constant	75.559	2.821	26.780	0.000
time	-5.162	1.411	-3.659	0.003
temp	-2.682	1.411	-1.901	0.080
grit	-4.200	1.411	-2.977	0.011
foil	20.383	1.407	14.489	0.000
time*time	-5.225	2.110	-2.476	0.028
temp*temp	-9.538	2.110	-4.520	0.001
grit*grit	-9.562	2.110	-4.532	0.001
foil*foil	-15.051	2.122	-7.094	0.000
time*grit	-5.975	2.437	-2.452	0.029
time*foil	7.971	2.433	3.276	0.006
temp*grit	5.800	2.437	2.380	0.033
temp*foil	8.462	2.433	3.478	0.004
grit*foil	4.313	2.433	1.773	0.100

S = 4.87329 PRESS = 1160.41
R-Sq = 96.21% R-Sq(pred) = 85.74% R-Sq(adj) = 92.41%

Analysis of Variance for wt. % Cu

Source	DF	Seq SS	Adj SS	Adj MS	F	P
Regression	13	7831.3	7831.3	602.41	25.37	0.000
Linear	4	5525.3	5599.9	1399.99	58.95	0.000
Square	4	1411.8	1411.8	352.96	14.86	0.000
Interaction	5	894.2	894.2	178.83	7.53	0.002
Residual Error	13	308.7	308.7	23.75		
Lack-of-Fit	11	166.5	166.5	15.14	0.21	0.967
Pure Error	2	142.2	142.2	71.12		
Total	26	8140.1				

Obs	StdOrder	wt. % Cu	Fit	SE Fit	Residual	St Resid
1	1	66.700	68.311	2.815	-1.611	-0.40
2	2	62.200	56.923	2.815	5.277	1.33
3	3	61.900	61.818	2.815	0.082	0.02
4	4	52.100	50.431	2.815	1.669	0.42
5	5	43.300	39.076	3.650	4.224	1.31
6	6	21.900	22.049	3.650	-0.149	-0.05
7	7	73.800	71.216	3.791	2.584	0.84
8	8	70.200	71.443	3.791	-1.243	-0.41
9	9	82.100	74.133	2.814	7.967	2.00 R
10	10	64.200	63.552	3.723	0.648	0.21
11	11	62.900	64.115	3.723	-1.215	-0.39
12	12	66.200	66.527	3.723	-0.327	-0.10
13	13	41.000	43.190	3.723	-2.190	-0.70
14	14	43.900	41.732	3.650	2.168	0.67

15	15	20.400	19.443	3.650	0.957	0.30	
16	16	63.000	65.574	3.791	-2.574	-0.84	
17	17	73.500	77.134	3.791	-3.634	-1.19	
18	18	75.000	74.133	2.814	0.867	0.22	
19	19	45.700	48.033	3.650	-2.333	-0.72	
20	20	16.900	21.767	3.650	-4.867	-1.51	
21	21	76.400	72.858	3.791	3.542	1.16	
22	22	79.800	78.475	3.791	1.325	0.43	
23	23	64.400	68.567	3.723	-4.167	-1.33	
24	24	48.400	50.474	3.723	-2.074	-0.66	
25	25	48.900	47.992	3.723	0.908	0.29	
26	26	56.100	53.099	3.723	3.001	0.95	
27	27	65.300	74.133	2.814	-8.833	-2.22	R

R denotes an observation with a large standardized residual.

After Second Term Removal

Response Surface Regression: wt. % Cu versus time, temp, grit, foil

The analysis was done using coded units.

Estimated Regression Coefficients for wt. % Cu

Term	Coef	SE Coef	T	P
Constant	75.559	3.030	24.939	0.000
time	-5.162	1.515	-3.407	0.004
temp	-2.682	1.515	-1.770	0.098
grit	-4.392	1.511	-2.907	0.011
foil	20.383	1.511	13.493	0.000
time*time	-5.225	2.266	-2.306	0.037
temp*temp	-9.538	2.266	-4.209	0.001
grit*grit	-9.562	2.266	-4.220	0.001
foil*foil	-15.051	2.278	-6.606	0.000
time*grit	-5.975	2.616	-2.284	0.039
time*foil	7.971	2.613	3.051	0.009
temp*grit	5.800	2.616	2.217	0.044
temp*foil	8.462	2.613	3.239	0.006

S = 5.23298 PRESS = 1236.22
R-Sq = 95.29% R-Sq(pred) = 84.81% R-Sq(adj) = 91.25%

Analysis of Variance for wt. % Cu

Source	DF	Seq SS	Adj SS	Adj MS	F	P
Regression	12	7756.7	7756.7	646.39	23.60	0.000
Linear	4	5525.3	5621.0	1405.24	51.32	0.000
Square	4	1411.8	1411.8	352.96	12.89	0.000
Interaction	4	819.5	819.5	204.88	7.48	0.002
Residual Error	14	383.4	383.4	27.38		
Lack-of-Fit	12	241.1	241.1	20.09	0.28	0.938
Pure Error	2	142.2	142.2	71.12		
Total	26	8140.1				

Obs	StdOrder	wt. % Cu	Fit	SE Fit	Residual	St Resid
1	1	66.700	68.311	3.022	-1.611	-0.38
2	2	62.200	56.923	3.022	5.277	1.24
3	3	61.900	61.818	3.022	0.082	0.02
4	4	52.100	50.431	3.022	1.669	0.39
5	5	43.300	34.954	3.021	8.346	1.95

6	6	21.900	26.171	3.021	-4.271	-1.00
7	7	73.800	75.721	3.021	-1.921	-0.45
8	8	70.200	66.937	3.021	3.263	0.76
9	9	82.100	74.133	3.021	7.967	1.86
10	10	64.200	63.456	3.997	0.744	0.22
11	11	62.900	64.019	3.997	-1.119	-0.33
12	12	66.200	66.623	3.997	-0.423	-0.13
13	13	41.000	43.285	3.997	-2.285	-0.68
14	14	43.900	41.732	3.919	2.168	0.63
15	15	20.400	19.443	3.919	0.957	0.28
16	16	63.000	65.574	4.071	-2.574	-0.78
17	17	73.500	77.134	4.071	-3.634	-1.11
18	18	75.000	74.133	3.021	0.867	0.20
19	19	45.700	48.033	3.919	-2.333	-0.67
20	20	16.900	21.767	3.919	-4.867	-1.40
21	21	76.400	72.858	4.071	3.542	1.08
22	22	79.800	78.475	4.071	1.325	0.40
23	23	64.400	68.471	3.997	-4.071	-1.21
24	24	48.400	50.379	3.997	-1.979	-0.59
25	25	48.900	48.088	3.997	0.812	0.24
26	26	56.100	53.195	3.997	2.905	0.86
27	27	65.300	74.133	3.021	-8.833	-2.07 R

R denotes an observation with a large standardized residual.

Initial Strength Model

Response Surface Regression: Sigma versus time, temp, grit, foil

The analysis was done using coded units.

Estimated Regression Coefficients for Sigma

Term	Coef	SE Coef	T	P
Constant	17.398	5.441	3.197	0.008
time	-4.445	2.721	-1.634	0.128
temp	9.689	2.721	3.561	0.004
grit	-3.635	2.721	-1.336	0.206
foil	7.387	2.713	2.723	0.019
time*time	4.621	4.070	1.135	0.278
temp*temp	5.920	4.070	1.455	0.171
grit*grit	-1.122	4.070	-0.276	0.787
foil*foil	11.246	4.092	2.749	0.018
time*temp	3.528	4.699	0.751	0.467
time*grit	7.217	4.699	1.536	0.151
time*foil	-1.896	4.692	-0.404	0.693
temp*grit	6.512	4.699	1.386	0.191
temp*foil	6.997	4.692	1.491	0.162
grit*foil	9.247	4.692	1.971	0.072

S = 9.39828 PRESS = 5852.11
R-Sq = 79.37% R-Sq(pred) = 0.00% R-Sq(adj) = 55.29%

Analysis of Variance for Sigma

Source	DF	Seq SS	Adj SS	Adj MS	F	P
Regression	14	4076.66	4076.66	291.19	3.30	0.023
Linear	4	2199.00	2168.05	542.01	6.14	0.006
Square	4	896.05	896.05	224.01	2.54	0.095
Interaction	6	981.60	981.60	163.60	1.85	0.171
Residual Error	12	1059.93	1059.93	88.33		
Lack-of-Fit	10	993.83	993.83	99.38	3.01	0.275

Pure Error	2	66.10	66.10	33.05	
Total	26	5136.59			

Obs	StdOrder	Sigma	Fit	SE Fit	Residual	St Resid	
1	1	24.052	26.121	7.180	-2.069	-0.34	
2	2	9.200	10.427	7.180	-1.227	-0.20	
3	3	39.002	37.509	7.180	1.492	0.25	
4	4	38.262	35.927	7.180	2.335	0.38	
5	5	35.797	33.017	7.039	2.781	0.45	
6	6	11.858	7.253	7.039	4.605	0.74	
7	7	25.072	29.298	7.312	-4.225	-0.72	
8	8	37.892	40.521	7.312	-2.629	-0.45	
9	9	10.576	16.955	5.426	-6.379	-0.83	
10	10	32.887	36.241	7.180	-3.355	-0.55	
11	11	8.037	13.170	7.180	-5.133	-0.85	
12	12	19.378	13.305	7.180	6.073	1.00	
13	13	23.396	19.101	7.180	4.295	0.71	
14	14	19.612	24.485	7.039	-4.874	-0.78	
15	15	40.495	29.869	7.039	10.626	1.71	
16	16	16.549	25.266	7.312	-8.717	-1.48	
17	17	63.482	58.637	7.312	4.845	0.82	
18	18	21.736	16.955	5.426	4.781	0.62	
19	19	21.359	28.427	7.039	-7.068	-1.14	
20	20	17.258	23.328	7.039	-6.070	-0.97	
21	21	51.920	46.994	7.312	4.927	0.83	
22	22	40.111	34.311	7.312	5.800	0.98	
23	23	37.308	23.295	7.180	14.013	2.31	R
24	24	24.634	28.715	7.180	-4.080	-0.67	
25	25	4.642	1.768	7.180	2.874	0.47	
26	26	18.018	33.237	7.180	-15.218	-2.51	R
27	27	18.554	16.955	5.426	1.598	0.21	

R denotes an observation with a large standardized residual.

Removal of first term

Response Surface Regression: Sigma versus time, temp, grit, foil

The analysis was done using coded units.

Estimated Regression Coefficients for Sigma

Term	Coef	SE Coef	T	P
Constant	16.399	3.912	4.192	0.001
time	-4.445	2.623	-1.695	0.114
temp	9.689	2.623	3.694	0.003
grit	-3.635	2.623	-1.386	0.189
foil	7.387	2.615	2.825	0.014
time*time	4.995	3.698	1.351	0.200
temp*temp	6.294	3.698	1.702	0.113
foil*foil	11.622	3.719	3.125	0.008
time*temp	3.528	4.529	0.779	0.450
time*grit	7.217	4.529	1.593	0.135
time*foil	-1.896	4.522	-0.419	0.682
temp*grit	6.512	4.529	1.438	0.174
temp*foil	6.997	4.522	1.547	0.146
grit*foil	9.247	4.522	2.045	0.062

S = 9.05812 PRESS = 5198.73
R-Sq = 79.23% R-Sq(pred) = 0.00% R-Sq(adj) = 58.47%

Analysis of Variance for Sigma

Source	DF	Seq SS	Adj SS	Adj MS	F	P
Regression	13	4069.95	4069.95	313.07	3.82	0.011
Linear	4	2199.00	2168.05	542.01	6.61	0.004
Square	3	889.34	889.34	296.45	3.61	0.043
Interaction	6	981.60	981.60	163.60	1.99	0.140
Residual Error	13	1066.64	1066.64	82.05		
Lack-of-Fit	11	1000.54	1000.54	90.96	2.75	0.297
Pure Error	2	66.10	66.10	33.05		
Total	26	5136.59				

Obs	StdOrder	Sigma	Fit	SE Fit	Residual	St Resid	
1	1	24.052	25.872	6.865	-1.820	-0.31	
2	2	9.200	10.178	6.865	-0.978	-0.17	
3	3	39.002	37.260	6.865	1.742	0.29	
4	4	38.262	35.678	6.865	2.584	0.44	
5	5	35.797	33.515	6.556	2.282	0.37	
6	6	11.858	7.752	6.556	4.106	0.66	
7	7	25.072	29.796	6.828	-4.724	-0.79	
8	8	37.892	41.020	6.828	-3.128	-0.53	
9	9	10.576	15.958	3.898	-5.382	-0.66	
10	10	32.887	36.740	6.697	-3.853	-0.63	
11	11	8.037	13.668	6.697	-5.631	-0.92	
12	12	19.378	13.804	6.697	5.575	0.91	
13	13	23.396	19.599	6.697	3.797	0.62	
14	14	19.612	24.236	6.728	-4.624	-0.76	
15	15	40.495	29.619	6.728	10.876	1.79	
16	16	16.549	25.017	6.993	-8.468	-1.47	
17	17	63.482	58.388	6.993	5.095	0.88	
18	18	21.736	15.958	3.898	5.778	0.71	
19	19	21.359	28.178	6.728	-6.819	-1.12	
20	20	17.258	23.079	6.728	-5.821	-0.96	
21	21	51.920	46.745	6.993	5.176	0.90	
22	22	40.111	34.062	6.993	6.049	1.05	
23	23	37.308	23.794	6.697	13.514	2.22	R
24	24	24.634	29.213	6.697	-4.579	-0.75	
25	25	4.642	2.266	6.697	2.376	0.39	
26	26	18.018	33.735	6.697	-15.717	-2.58	R
27	27	18.554	15.958	3.898	2.596	0.32	

R denotes an observation with a large standardized residual.

<u>After Second term</u>

Response Surface Regression: Sigma versus time, temp, grit, foil

The analysis was done using coded units.

Estimated Regression Coefficients for Sigma

Term	Coef	SE Coef	T	P
Constant	16.399	3.795	4.321	0.001
time	-4.361	2.537	-1.719	0.108
temp	9.689	2.544	3.808	0.002
grit	-3.635	2.544	-1.429	0.175
foil	7.387	2.537	2.912	0.011
time*time	4.995	3.587	1.392	0.186
temp*temp	6.294	3.587	1.754	0.101
foil*foil	11.622	3.607	3.222	0.006

time*temp	3.528	4.394	0.803	0.435
time*grit	7.217	4.394	1.643	0.123
temp*grit	6.512	4.394	1.482	0.160
temp*foil	6.997	4.387	1.595	0.133
grit*foil	9.247	4.387	2.108	0.054

S = 8.78744 PRESS = 4756.17
R-Sq = 78.95% R-Sq(pred) = 7.41% R-Sq(adj) = 60.91%

Analysis of Variance for Sigma

Source	DF	Seq SS	Adj SS	Adj MS	F	P
Regression	12	4055.52	4055.52	337.96	4.38	0.005
Linear	4	2199.00	2160.53	540.13	6.99	0.003
Square	3	889.34	889.34	296.45	3.84	0.034
Interaction	5	967.18	967.18	193.44	2.51	0.081
Residual Error	14	1081.07	1081.07	77.22		
Lack-of-Fit	12	1014.96	1014.96	84.58	2.56	0.315
Pure Error	2	66.10	66.10	33.05		
Total	26	5136.59				

Obs	StdOrder	Sigma	Fit	SE Fit	Residual	St Resid	
1	1	24.052	25.914	6.659	-1.862	-0.32	
2	2	9.200	10.136	6.659	-0.936	-0.16	
3	3	39.002	37.302	6.659	1.700	0.30	
4	4	38.262	35.636	6.659	2.626	0.46	
5	5	35.797	33.515	6.360	2.282	0.38	
6	6	11.858	7.752	6.360	4.106	0.68	
7	7	25.072	29.796	6.624	-4.724	-0.82	
8	8	37.892	41.020	6.624	-3.128	-0.54	
9	9	10.576	15.958	3.782	-5.382	-0.68	
10	10	32.887	36.782	6.496	-3.896	-0.66	
11	11	8.037	13.626	6.496	-5.589	-0.94	
12	12	19.378	13.846	6.496	5.532	0.93	
13	13	23.396	19.557	6.496	3.839	0.65	
14	14	19.612	24.236	6.527	-4.624	-0.79	
15	15	40.495	29.619	6.527	10.876	1.85	
16	16	16.549	25.017	6.784	-8.468	-1.52	
17	17	63.482	58.388	6.784	5.095	0.91	
18	18	21.736	15.958	3.782	5.778	0.73	
19	19	21.359	29.990	5.002	-8.631	-1.19	
20	20	17.258	21.267	5.002	-4.009	-0.55	
21	21	51.920	44.764	5.002	7.156	0.99	
22	22	40.111	36.042	5.002	4.069	0.56	
23	23	37.308	23.794	6.496	13.514	2.28	R
24	24	24.634	29.213	6.496	-4.579	-0.77	
25	25	4.642	2.266	6.496	2.376	0.40	
26	26	18.018	33.735	6.496	-15.717	-2.66	R
27	27	18.554	15.958	3.782	2.596	0.33	

R denotes an observation with a large standardized residual.
After Third Term

Response Surface Regression: Sigma versus time, temp, grit, foil

The analysis was done using coded units.

Estimated Regression Coefficients for Sigma

Term	Coef	SE Coef	T	P

Constant	16.399	3.750	4.373	0.001
time	-4.361	2.506	-1.740	0.102
temp	9.689	2.514	3.854	0.002
grit	-3.635	2.514	-1.446	0.169
foil	7.387	2.506	2.947	0.010
time*time	4.995	3.545	1.409	0.179
temp*temp	6.294	3.545	1.776	0.096
foil*foil	11.622	3.564	3.260	0.005
time*grit	7.217	4.341	1.662	0.117
temp*grit	6.512	4.341	1.500	0.154
temp*foil	6.997	4.335	1.614	0.127
grit*foil	9.247	4.335	2.133	0.050

S = 8.68275 PRESS = 4818.19
R-Sq = 77.98% R-Sq(pred) = 6.20% R-Sq(adj) = 61.84%

Analysis of Variance for Sigma

Source	DF	Seq SS	Adj SS	Adj MS	F	P
Regression	11	4005.74	4005.74	364.16	4.83	0.003
Linear	4	2199.00	2160.53	540.13	7.16	0.002
Square	3	889.34	889.34	296.45	3.93	0.030
Interaction	4	917.39	917.39	229.35	3.04	0.051
Residual Error	15	1130.85	1130.85	75.39		
Lack-of-Fit	13	1064.75	1064.75	81.90	2.48	0.324
Pure Error	2	66.10	66.10	33.05		
Total	26	5136.59				

Obs	StdOrder	Sigma	Fit	SE Fit	Residual	St Resid	
1	1	24.052	22.386	4.944	1.666	0.23	
2	2	9.200	13.664	4.944	-4.463	-0.63	
3	3	39.002	40.830	4.944	-1.828	-0.26	
4	4	38.262	32.108	4.944	6.154	0.86	
5	5	35.797	33.515	6.285	2.282	0.38	
6	6	11.858	7.752	6.285	4.106	0.69	
7	7	25.072	29.796	6.545	-4.724	-0.83	
8	8	37.892	41.020	6.545	-3.128	-0.55	
9	9	10.576	15.958	3.736	-5.382	-0.69	
10	10	32.887	36.782	6.418	-3.896	-0.67	
11	11	8.037	13.626	6.418	-5.589	-0.96	
12	12	19.378	13.846	6.418	5.532	0.95	
13	13	23.396	19.557	6.418	3.839	0.66	
14	14	19.612	24.236	6.449	-4.624	-0.80	
15	15	40.495	29.619	6.449	10.876	1.87	
16	16	16.549	25.017	6.703	-8.468	-1.53	
17	17	63.482	58.388	6.703	5.095	0.92	
18	18	21.736	15.958	3.736	5.778	0.74	
19	19	21.359	29.990	4.943	-8.631	-1.21	
20	20	17.258	21.267	4.943	-4.009	-0.56	
21	21	51.920	44.764	4.943	7.156	1.00	
22	22	40.111	36.042	4.943	4.069	0.57	
23	23	37.308	23.794	6.419	13.514	2.31	R
24	24	24.634	29.213	6.419	-4.579	-0.78	
25	25	4.642	2.266	6.419	2.376	0.41	
26	26	18.018	33.735	6.419	-15.717	-2.69	R
27	27	18.554	15.958	3.736	2.596	0.33	

R denotes an observation with a large standardized residual.

After Fourth Term

Response Surface Regression: Sigma versus time, temp, grit, foil

The analysis was done using coded units.

Estimated Regression Coefficients for Sigma

Term	Coef	SE Coef	T	P
Constant	19.734	2.997	6.585	0.000
time	-4.361	2.583	-1.689	0.111
temp	9.689	2.590	3.741	0.002
grit	-3.635	2.590	-1.403	0.180
foil	7.387	2.583	2.860	0.011
temp*temp	5.045	3.536	1.427	0.173
foil*foil	10.368	3.556	2.915	0.010
time*grit	7.217	4.473	1.613	0.126
temp*grit	6.512	4.473	1.456	0.165
temp*foil	6.997	4.466	1.567	0.137
grit*foil	9.247	4.466	2.070	0.055

S = 8.94617 PRESS = 4845.69
R-Sq = 75.07% R-Sq(pred) = 5.66% R-Sq(adj) = 59.49%

Analysis of Variance for Sigma

Source	DF	Seq SS	Adj SS	Adj MS	F	P
Regression	10	3856.05	3856.05	385.60	4.82	0.003
Linear	4	2199.00	2160.53	540.13	6.75	0.002
Square	2	739.65	739.65	369.83	4.62	0.026
Interaction	4	917.39	917.39	229.35	2.87	0.058
Residual Error	16	1280.54	1280.54	80.03		
Lack-of-Fit	14	1214.44	1214.44	86.75	2.62	0.310
Pure Error	2	66.10	66.10	33.05		
Total	26	5136.59				

Obs	StdOrder	Sigma	Fit	SE Fit	Residual	St Resid
1	1	24.052	19.472	4.627	4.580	0.60
2	2	9.200	10.750	4.627	-1.550	-0.20
3	3	39.002	37.917	4.627	1.085	0.14
4	4	38.262	29.194	4.627	9.068	1.18
5	5	35.797	35.596	6.294	0.201	0.03
6	6	11.858	9.833	6.294	2.025	0.32
7	7	25.072	31.878	6.570	-6.805	-1.12
8	8	37.892	43.101	6.570	-5.209	-0.86
9	9	10.576	19.288	2.982	-8.712	-1.03
10	10	32.887	35.117	6.500	-2.231	-0.36
11	11	8.037	11.961	6.500	-3.924	-0.64
12	12	19.378	12.181	6.500	7.197	1.17
13	13	23.396	17.892	6.500	5.504	0.90
14	14	19.612	25.068	6.617	-5.457	-0.91
15	15	40.495	30.452	6.617	10.043	1.67
16	16	16.549	25.849	6.880	-9.300	-1.63
17	17	63.482	59.220	6.880	4.262	0.75
18	18	21.736	19.288	2.982	2.448	0.29
19	19	21.359	27.076	4.626	-5.717	-0.75
20	20	17.258	18.354	4.626	-1.095	-0.14
21	21	51.920	41.851	4.626	10.070	1.32
22	22	40.111	33.128	4.626	6.983	0.91
23	23	37.308	25.875	6.436	11.433	1.84
24	24	24.634	31.294	6.436	-6.660	-1.07
25	25	4.642	4.347	6.436	0.295	0.05

26	26	18.018	35.816	6.436	-17.798	-2.86 R
27	27	18.554	19.288	2.982	-0.734	-0.09

R denotes an observation with a large standardized residual.

After Fifth Term

Response Surface Regression: Sigma versus time, temp, grit, foil

The analysis was done using coded units.

Estimated Regression Coefficients for Sigma

Term	Coef	SE Coef	T	P
Constant	22.430	2.396	9.359	0.000
time	-4.361	2.660	-1.640	0.119
temp	9.689	2.668	3.632	0.002
grit	-3.635	2.668	-1.362	0.191
foil	7.387	2.660	2.777	0.013
foil*foil	9.354	3.589	2.606	0.018
time*grit	7.217	4.607	1.566	0.136
temp*grit	6.512	4.607	1.413	0.176
temp*foil	6.997	4.600	1.521	0.147
grit*foil	9.247	4.600	2.010	0.061

S = 9.21462 PRESS = 4452.10
R-Sq = 71.90% R-Sq(pred) = 13.33% R-Sq(adj) = 57.02%

Analysis of Variance for Sigma

Source	DF	Seq SS	Adj SS	Adj MS	F	P
Regression	9	3693.13	3693.13	410.35	4.83	0.003
Linear	4	2199.00	2160.53	540.13	6.36	0.003
Square	1	576.74	576.74	576.74	6.79	0.018
Interaction	4	917.39	917.39	229.35	2.70	0.066
Residual Error	17	1443.46	1443.46	84.91		
Lack-of-Fit	15	1377.35	1377.35	91.82	2.78	0.296
Pure Error	2	66.10	66.10	33.05		
Total	26	5136.59				

Obs	StdOrder	Sigma	Fit	SE Fit	Residual	St Resid
1	1	24.052	17.118	4.452	6.934	0.86
2	2	9.200	8.395	4.452	0.805	0.10
3	3	39.002	35.562	4.452	3.440	0.43
4	4	38.262	26.840	4.452	11.422	1.42
5	5	35.797	37.278	6.368	-1.481	-0.22
6	6	11.858	11.515	6.368	0.343	0.05
7	7	25.072	33.559	6.657	-8.487	-1.33
8	8	37.892	44.783	6.657	-6.891	-1.08
9	9	10.576	21.979	2.379	-11.403	-1.28
10	10	32.887	37.808	6.407	-4.921	-0.74
11	11	8.037	14.652	6.407	-6.615	-1.00
12	12	19.378	14.872	6.407	4.507	0.68
13	13	23.396	20.583	6.407	2.813	0.42
14	14	19.612	21.705	6.368	-2.093	-0.31
15	15	40.495	27.088	6.368	13.407	2.01 R
16	16	16.549	22.486	6.657	-5.937	-0.93
17	17	63.482	55.857	6.657	7.626	1.20
18	18	21.736	21.979	2.379	-0.243	-0.03

19	19	21.359	28.758	4.607	-7.399	-0.93	
20	20	17.258	20.035	4.607	-2.777	-0.35	
21	21	51.920	43.532	4.607	8.388	1.05	
22	22	40.111	34.810	4.607	5.301	0.66	
23	23	37.308	23.520	6.408	13.787	2.08	R
24	24	24.634	28.940	6.408	-4.306	-0.65	
25	25	4.642	1.993	6.408	2.649	0.40	
26	26	18.018	33.462	6.408	-15.444	-2.33	R
27	27	18.554	21.979	2.379	-3.425	-0.38	

R denotes an observation with a large standardized residual.

After Sixth Term

Response Surface Regression: Sigma versus time, temp, grit, foil

The analysis was done using coded units.

Estimated Regression Coefficients for Sigma

Term	Coef	SE Coef	T	P
Constant	22.430	2.462	9.110	0.000
time	-4.361	2.733	-1.596	0.128
temp	9.689	2.741	3.535	0.002
grit	-3.635	2.741	-1.326	0.201
foil	7.387	2.733	2.703	0.015
foil*foil	9.354	3.687	2.537	0.021
time*grit	7.217	4.733	1.525	0.145
temp*foil	6.997	4.726	1.480	0.156
grit*foil	9.247	4.726	1.956	0.066

S = 9.46660 PRESS = 3811.13
R-Sq = 68.60% R-Sq(pred) = 25.80% R-Sq(adj) = 54.64%

Analysis of Variance for Sigma

Source	DF	Seq SS	Adj SS	Adj MS	F	P
Regression	8	3523.49	3523.49	440.44	4.91	0.002
Linear	4	2199.00	2160.53	540.13	6.03	0.003
Square	1	576.74	576.74	576.74	6.44	0.021
Interaction	3	747.75	747.75	249.25	2.78	0.071
Residual Error	18	1613.10	1613.10	89.62		
Lack-of-Fit	16	1547.00	1547.00	96.69	2.93	0.284
Pure Error	2	66.10	66.10	33.05		
Total	26	5136.59				

Obs	StdOrder	Sigma	Fit	SE Fit	Residual	St Resid
1	1	24.052	17.118	4.574	6.934	0.84
2	2	9.200	8.395	4.574	0.805	0.10
3	3	39.002	35.562	4.574	3.440	0.42
4	4	38.262	26.840	4.574	11.422	1.38
5	5	35.797	37.278	6.542	-1.481	-0.22
6	6	11.858	11.515	6.542	0.343	0.05
7	7	25.072	33.559	6.839	-8.487	-1.30
8	8	37.892	44.783	6.839	-6.891	-1.05
9	9	10.576	21.979	2.444	-11.403	-1.25
10	10	32.887	37.808	6.582	-4.921	-0.72
11	11	8.037	14.652	6.582	-6.615	-0.97
12	12	19.378	14.872	6.582	4.507	0.66

13	13	23.396	20.583	6.582	2.813	0.41
14	14	19.612	21.705	6.542	-2.093	-0.31
15	15	40.495	27.088	6.542	13.407	1.96
16	16	16.549	22.486	6.839	-5.937	-0.91
17	17	63.482	55.857	6.839	7.626	1.17
18	18	21.736	21.979	2.444	-0.243	-0.03
19	19	21.359	28.758	4.733	-7.399	-0.90
20	20	17.258	20.035	4.733	-2.777	-0.34
21	21	51.920	43.532	4.733	8.388	1.02
22	22	40.111	34.810	4.733	5.301	0.65
23	23	37.308	17.008	4.575	20.300	2.45 R
24	24	24.634	35.452	4.575	-10.818	-1.31
25	25	4.642	8.505	4.575	-3.863	-0.47
26	26	18.018	26.950	4.575	-8.931	-1.08
27	27	18.554	21.979	2.444	-3.425	-0.37

R denotes an observation with a large standardized residual.

After Seventh Term

Response Surface Regression: Sigma versus time, temp, grit, foil

The analysis was done using coded units.

Estimated Regression Coefficients for Sigma

Term	Coef	SE Coef	T	P
Constant	22.430	2.538	8.837	0.000
time	-4.361	2.817	-1.548	0.138
temp	9.378	2.817	3.329	0.004
grit	-3.635	2.825	-1.286	0.214
foil	7.387	2.817	2.622	0.017
foil*foil	9.354	3.801	2.461	0.024
time*grit	7.217	4.879	1.479	0.156
grit*foil	9.247	4.872	1.898	0.073

S = 9.75893 PRESS = 3569.21
R-Sq = 64.77% R-Sq(pred) = 30.51% R-Sq(adj) = 51.79%

Analysis of Variance for Sigma

Source	DF	Seq SS	Adj SS	Adj MS	F	P
Regression	7	3327.09	3327.09	475.30	4.99	0.002
Linear	4	2199.00	2096.00	524.00	5.50	0.004
Square	1	576.74	576.74	576.74	6.06	0.024
Interaction	2	551.35	551.35	275.67	2.89	0.080
Residual Error	19	1809.50	1809.50	95.24		
Lack-of-Fit	17	1743.40	1743.40	102.55	3.10	0.271
Pure Error	2	66.10	66.10	33.05		
Total	26	5136.59				

Obs	StdOrder	Sigma	Fit	SE Fit	Residual	St Resid
1	1	24.052	16.962	4.714	7.090	0.83
2	2	9.200	8.240	4.714	0.960	0.11
3	3	39.002	35.718	4.714	3.284	0.38
4	4	38.262	26.995	4.714	11.267	1.32
5	5	35.797	37.278	6.744	-1.481	-0.21
6	6	11.858	11.515	6.744	0.343	0.05
7	7	25.072	33.559	7.050	-8.487	-1.26
8	8	37.892	44.783	7.050	-6.891	-1.02
9	9	10.576	21.979	2.520	-11.403	-1.21

10	10	32.887	37.808	6.785	-4.921	-0.70	
11	11	8.037	14.652	6.785	-6.615	-0.94	
12	12	19.378	14.872	6.785	4.507	0.64	
13	13	23.396	20.583	6.785	2.813	0.40	
14	14	19.612	15.019	4.879	4.593	0.54	
15	15	40.495	33.774	4.879	6.721	0.80	
16	16	16.549	29.793	4.879	-13.245	-1.57	
17	17	63.482	48.549	4.879	14.933	1.77	
18	18	21.736	21.979	2.520	-0.243	-0.03	
19	19	21.359	28.758	4.879	-7.399	-0.88	
20	20	17.258	20.035	4.879	-2.777	-0.33	
21	21	51.920	43.532	4.879	8.388	0.99	
22	22	40.111	34.810	4.879	5.301	0.63	
23	23	37.308	16.852	4.715	20.455	2.39	R
24	24	24.634	35.608	4.715	-10.973	-1.28	
25	25	4.642	8.350	4.715	-3.708	-0.43	
26	26	18.018	27.105	4.715	-9.087	-1.06	
27	27	18.554	21.979	2.520	-3.425	-0.36	

R denotes an observation with a large standardized residual.

Estimated Regression Coefficients for Sigma using data in uncoded units

Term	Coef
Constant	22.4297
time	-4.36116
temp	9.37764
grit	-3.63490
foil	7.38729
foil*foil	9.35416
time*grit	7.21682
grit*foil	9.24670

After Eighth Term

Response Surface Regression: Sigma versus time, temp, grit, foil

The analysis was done using coded units.

Estimated Regression Coefficients for Sigma

Term	Coef	SE Coef	T	P
Constant	22.430	2.612	8.586	0.000
time	-4.361	2.900	-1.504	0.148
temp	9.378	2.900	3.234	0.004
grit	-3.635	2.908	-1.250	0.226
foil	7.387	2.900	2.548	0.019
foil*foil	9.354	3.912	2.391	0.027
grit*foil	9.247	5.015	1.844	0.080

S = 10.0445 PRESS = 3726.93
R-Sq = 60.72% R-Sq(pred) = 27.44% R-Sq(adj) = 48.93%

Analysis of Variance for Sigma

Source	DF	Seq SS	Adj SS	Adj MS	F	P
Regression	6	3118.76	3118.76	519.79	5.15	0.002
Linear	4	2199.00	2096.00	524.00	5.19	0.005
Square	1	576.74	576.74	576.74	5.72	0.027

Interaction	1	343.02	343.02	343.02	3.40	0.080
Residual Error	20	2017.83	2017.83	100.89		
Lack-of-Fit	18	1951.73	1951.73	108.43	3.28	0.259
Pure Error	2	66.10	66.10	33.05		
Total	26	5136.59				

Obs	StdOrder	Sigma	Fit	SE Fit	Residual	St Resid	
1	1	24.052	16.962	4.852	7.090	0.81	
2	2	9.200	8.240	4.852	0.960	0.11	
3	3	39.002	35.718	4.852	3.284	0.37	
4	4	38.262	26.995	4.852	11.267	1.28	
5	5	35.797	37.278	6.942	-1.481	-0.20	
6	6	11.858	11.515	6.942	0.343	0.05	
7	7	25.072	33.559	7.256	-8.487	-1.22	
8	8	37.892	44.783	7.256	-6.891	-0.99	
9	9	10.576	21.979	2.593	-11.403	-1.18	
10	10	32.887	30.591	4.853	2.295	0.26	
11	11	8.037	21.869	4.853	-13.832	-1.57	
12	12	19.378	22.089	4.853	-2.710	-0.31	
13	13	23.396	13.366	4.853	10.030	1.14	
14	14	19.612	15.019	5.022	4.593	0.53	
15	15	40.495	33.774	5.022	6.721	0.77	
16	16	16.549	29.793	5.022	-13.245	-1.52	
17	17	63.482	48.549	5.022	14.933	1.72	
18	18	21.736	21.979	2.593	-0.243	-0.03	
19	19	21.359	28.758	5.022	-7.399	-0.85	
20	20	17.258	20.035	5.022	-2.777	-0.32	
21	21	51.920	43.532	5.022	8.388	0.96	
22	22	40.111	34.810	5.022	5.301	0.61	
23	23	37.308	16.852	4.853	20.455	2.33	R
24	24	24.634	35.608	4.853	-10.973	-1.25	
25	25	4.642	8.350	4.853	-3.708	-0.42	
26	26	18.018	27.105	4.853	-9.087	-1.03	
27	27	18.554	21.979	2.593	-3.425	-0.35	

R denotes an observation with a large standardized residual.

Estimated Regression Coefficients for Sigma using data in uncoded units

Term	Coef
Constant	22.4297
time	-4.36116
temp	9.37764
grit	-3.63490
foil	7.38729
foil*foil	9.35416
grit*foil	9.24670

After ninth Term

Response Surface Regression: Sigma versus time, temp, grit, foil

The analysis was done using coded units.

Estimated Regression Coefficients for Sigma

Term	Coef	SE Coef	T	P
Constant	22.430	2.758	8.134	0.000
time	-4.361	3.061	-1.425	0.169
temp	9.378	3.061	3.064	0.006

grit	-4.046	3.061	-1.322	0.200
foil	7.387	3.061	2.414	0.025
foil*foil	9.354	4.130	2.265	0.034

S = 10.6029 PRESS = 4021.33
R-Sq = 54.04% R-Sq(pred) = 21.71% R-Sq(adj) = 43.10%

Analysis of Variance for Sigma

Source	DF	Seq SS	Adj SS	Adj MS	F	P
Regression	5	2775.74	2775.74	555.149	4.94	0.004
Linear	4	2199.00	2134.81	533.703	4.75	0.007
Square	1	576.74	576.74	576.738	5.13	0.034
Residual Error	21	2360.85	2360.85	112.421		
Lack-of-Fit	19	2294.74	2294.74	120.776	3.65	0.236
Pure Error	2	66.10	66.10	33.052		
Total	26	5136.59				

Obs	StdOrder	Sigma	Fit	SE Fit	Residual	St Resid	
1	1	24.052	16.962	5.122	7.090	0.76	
2	2	9.200	8.240	5.122	0.960	0.10	
3	3	39.002	35.718	5.122	3.284	0.35	
4	4	38.262	26.995	5.122	11.267	1.21	
5	5	35.797	28.442	5.301	7.355	0.80	
6	6	11.858	20.351	5.301	-8.492	-0.92	
7	7	25.072	43.217	5.301	-18.145	-1.98	
8	8	37.892	35.125	5.301	2.767	0.30	
9	9	10.576	21.979	2.738	-11.403	-1.11	
10	10	32.887	30.386	5.122	2.501	0.27	
11	11	8.037	21.663	5.122	-13.627	-1.47	
12	12	19.378	22.294	5.122	-2.916	-0.31	
13	13	23.396	13.572	5.122	9.824	1.06	
14	14	19.612	15.019	5.301	4.593	0.50	
15	15	40.495	33.774	5.301	6.721	0.73	
16	16	16.549	29.793	5.301	-13.245	-1.44	
17	17	63.482	48.549	5.301	14.933	1.63	
18	18	21.736	21.979	2.738	-0.243	-0.02	
19	19	21.359	28.758	5.301	-7.399	-0.81	
20	20	17.258	20.035	5.301	-2.777	-0.30	
21	21	51.920	43.532	5.301	8.388	0.91	
22	22	40.111	34.810	5.301	5.301	0.58	
23	23	37.308	16.647	5.122	20.661	2.23	R
24	24	24.634	35.402	5.122	-10.768	-1.16	
25	25	4.642	8.555	5.122	-3.913	-0.42	
26	26	18.018	27.311	5.122	-9.292	-1.00	
27	27	18.554	21.979	2.738	-3.425	-0.33	

R denotes an observation with a large standardized residual.

Estimated Regression Coefficients for Sigma using data in uncoded units

Term	Coef
Constant	22.4297
time	-4.36116
temp	9.37764
grit	-4.04587
foil	7.38729
foil*foil	9.35416

After Tenth Term

Response Surface Regression: Sigma versus time, temp, foil

The analysis was done using coded units.

Estimated Regression Coefficients for Sigma

Term	Coef	SE Coef	T	P
Constant	22.430	2.804	7.999	0.000
time	-4.361	3.112	-1.401	0.175
temp	9.378	3.112	3.013	0.006
foil	7.387	3.112	2.374	0.027
foil*foil	9.354	4.199	2.227	0.036

S = 10.7815 PRESS = 3839.49
R-Sq = 50.21% R-Sq(pred) = 25.25% R-Sq(adj) = 41.16%

Analysis of Variance for Sigma

Source	DF	Seq SS	Adj SS	Adj MS	F	P
Regression	4	2579.31	2579.31	644.828	5.55	0.003
Linear	3	2002.58	1938.38	646.128	5.56	0.005
Square	1	576.74	576.74	576.738	4.96	0.036
Residual Error	22	2557.28	2557.28	116.240		
Lack-of-Fit	14	1357.87	1357.87	96.991	0.65	0.773
Pure Error	8	1199.41	1199.41	149.926		
Total	26	5136.59				

Obs	StdOrder	Sigma	Fit	SE Fit	Residual	St Resid	
1	1	24.052	16.962	5.208	7.090	0.75	
2	2	9.200	8.240	5.208	0.960	0.10	
3	3	39.002	35.718	5.208	3.284	0.35	
4	4	38.262	26.995	5.208	11.267	1.19	
5	5	35.797	24.397	4.402	11.401	1.16	
6	6	11.858	24.397	4.402	-12.538	-1.27	
7	7	25.072	39.171	4.402	-14.099	-1.43	
8	8	37.892	39.171	4.402	-1.279	-0.13	
9	9	10.576	21.979	2.784	-11.403	-1.09	
10	10	32.887	26.340	4.176	6.547	0.66	
11	11	8.037	17.618	4.176	-9.581	-0.96	
12	12	19.378	26.340	4.176	-6.962	-0.70	
13	13	23.396	17.618	4.176	5.778	0.58	
14	14	19.612	15.019	5.391	4.593	0.49	
15	15	40.495	33.774	5.391	6.721	0.72	
16	16	16.549	29.793	5.391	-13.245	-1.42	
17	17	63.482	48.549	5.391	14.933	1.60	
18	18	21.736	21.979	2.784	-0.243	-0.02	
19	19	21.359	28.758	5.391	-7.399	-0.79	
20	20	17.258	20.035	5.391	-2.777	-0.30	
21	21	51.920	43.532	5.391	8.388	0.90	
22	22	40.111	34.810	5.391	5.301	0.57	
23	23	37.308	12.601	4.176	24.706	2.49	R
24	24	24.634	31.356	4.176	-6.722	-0.68	
25	25	4.642	12.601	4.176	-7.959	-0.80	
26	26	18.018	31.356	4.176	-13.338	-1.34	
27	27	18.554	21.979	2.784	-3.425	-0.33	

R denotes an observation with a large standardized residual.

Estimated Regression Coefficients for Sigma using data in uncoded units

Term	Coef
Constant	22.4297
time	-4.36116
temp	9.37764
foil	7.38729
foil*foil	9.35416

After Eleventh Term

Response Surface Regression: Sigma versus temp, foil

The analysis was done using coded units.

Estimated Regression Coefficients for Sigma

Term	Coef	SE Coef	T	P
Constant	22.430	2.862	7.837	0.000
temp	9.378	3.177	2.952	0.007
foil	7.387	3.177	2.325	0.029
foil*foil	9.354	4.287	2.182	0.040

S = 11.0050 PRESS = 3968.55
R-Sq = 45.77% R-Sq(pred) = 22.74% R-Sq(adj) = 38.70%

Analysis of Variance for Sigma

Source	DF	Seq SS	Adj SS	Adj MS	F	P
Regression	3	2351.08	2351.08	783.692	6.47	0.002
Linear	2	1774.34	1710.15	855.073	7.06	0.004
Square	1	576.74	576.74	576.738	4.76	0.040
Residual Error	23	2785.51	2785.51	121.109		
Lack-of-Fit	5	711.86	711.86	142.372	1.24	0.333
Pure Error	18	2073.65	2073.65	115.203		
Total	26	5136.59				

Obs	StdOrder	Sigma	Fit	SE Fit	Residual	St Resid
1	1	24.052	12.601	4.262	11.451	1.13
2	2	9.200	12.601	4.262	-3.401	-0.34
3	3	39.002	31.356	4.262	7.645	0.75
4	4	38.262	31.356	4.262	6.905	0.68
5	5	35.797	24.397	4.493	11.401	1.13
6	6	11.858	24.397	4.493	-12.538	-1.25
7	7	25.072	39.171	4.493	-14.099	-1.40
8	8	37.892	39.171	4.493	-1.279	-0.13
9	9	10.576	21.979	2.841	-11.403	-1.07
10	10	32.887	21.979	2.841	10.908	1.03
11	11	8.037	21.979	2.841	-13.942	-1.31
12	12	19.378	21.979	2.841	-2.600	-0.24
13	13	23.396	21.979	2.841	1.417	0.13
14	14	19.612	15.019	5.502	4.593	0.48
15	15	40.495	33.774	5.502	6.721	0.71
16	16	16.549	29.793	5.502	-13.245	-1.39
17	17	63.482	48.549	5.502	14.933	1.57
18	18	21.736	21.979	2.841	-0.243	-0.02
19	19	21.359	24.397	4.493	-3.038	-0.30
20	20	17.258	24.397	4.493	-7.138	-0.71

21	21	51.920	39.171	4.493	12.749	1.27
22	22	40.111	39.171	4.493	0.940	0.09
23	23	37.308	12.601	4.262	24.706	2.44 R
24	24	24.634	31.356	4.262	-6.722	-0.66
25	25	4.642	12.601	4.262	-7.959	-0.78
26	26	18.018	31.356	4.262	-13.338	-1.31
27	27	18.554	21.979	2.841	-3.425	-0.32

R denotes an observation with a large standardized residual.

Strength Model After Area Analysis

Response Surface Regression: S versus time, temp, grit, foil

The analysis was done using coded units.

Estimated Regression Coefficients for S

Term	Coef	SE Coef	T	P
Constant	67.8519	24.31	2.791	0.016
time	-0.4591	12.16	-0.038	0.970
temp	26.6976	12.16	2.196	0.049
grit	-5.2315	12.16	-0.430	0.675
foil	27.4594	12.12	2.265	0.043
time*time	22.4542	18.18	1.235	0.241
temp*temp	9.0253	18.18	0.496	0.629
grit*grit	-16.5373	18.18	-0.909	0.381
foil*foil	-3.8569	18.28	-0.211	0.836
time*temp	17.5501	21.00	0.836	0.420
time*grit	26.1935	21.00	1.247	0.236
time*foil	-18.7164	20.97	-0.893	0.390
temp*grit	6.3145	21.00	0.301	0.769
temp*foil	30.0473	20.97	1.433	0.177
grit*foil	8.1713	20.97	0.390	0.704

S = 41.9944 PRESS = 119776
R-Sq = 61.11% R-Sq(pred) = 0.00% R-Sq(adj) = 15.75%

Analysis of Variance for S

Source	DF	Seq SS	Adj SS	Adj MS	F	P
Regression	14	33257.9	33257.9	2375.6	1.35	0.306
Linear	4	17000.8	17880.2	4470.0	2.53	0.095
Square	4	6825.8	6825.8	1706.5	0.97	0.460
Interaction	6	9431.2	9431.2	1571.9	0.89	0.531
Residual Error	12	21162.3	21162.3	1763.5		
Lack-of-Fit	10	20906.1	20906.1	2090.6	16.31	0.059
Pure Error	2	256.3	256.3	128.1		
Total	26	54420.2				

Obs	StdOrder	S	Fit	SE Fit	Residual	St Resid
1	1	44.824	89.551	32.081	-44.726	-1.65
2	2	87.599	56.028	32.081	31.571	1.17
3	3	78.423	103.839	32.081	-25.416	-0.94
4	4	191.398	140.517	32.081	50.881	1.88
5	5	54.901	33.401	31.452	21.499	0.77
6	6	17.083	6.596	31.452	10.487	0.38
7	7	66.956	71.977	32.671	-5.021	-0.19
8	8	63.200	77.857	32.671	-14.657	-0.56
9	9	62.070	66.004	24.245	-3.934	-0.11

10	10	118.699	103.102	32.081	15.597	0.58	
11	11	28.699	52.292	32.081	-23.593	-0.87	
12	12	93.890	39.163	32.081	54.727	2.02	R
13	13	108.664	93.127	32.081	15.537	0.57	
14	14	48.999	48.911	31.452	0.088	0.00	
15	15	73.323	42.211	31.452	31.112	1.12	
16	16	45.695	43.735	32.671	1.960	0.07	
17	17	186.331	157.225	32.671	29.106	1.10	
18	18	57.176	66.004	24.245	-8.828	-0.26	
19	19	28.929	40.733	31.452	-11.803	-0.42	
20	20	25.863	77.247	31.452	-51.384	-1.85	
21	21	144.706	133.084	32.671	11.622	0.44	
22	22	71.722	94.733	32.671	-23.011	-0.87	
23	23	65.845	45.888	32.081	19.956	0.74	
24	24	54.210	82.648	32.081	-28.438	-1.05	
25	25	12.857	21.707	32.081	-8.850	-0.33	
26	26	26.480	83.725	32.081	-57.245	-2.11	R
27	27	78.766	66.004	24.245	12.762	0.37	

R denotes an observation with a large standardized residual.

Estimated Regression Coefficients for S using data in uncoded units

Term	Coef
Constant	67.8519
time	-0.459136
temp	26.6976
grit	-5.23150
foil	27.4594
time*time	22.4542
temp*temp	9.02527
grit*grit	-16.5373
foil*foil	-3.85691
time*temp	17.5501
time*grit	26.1935
time*foil	-18.7164
temp*grit	6.31454
temp*foil	30.0473
grit*foil	8.17128

After First Term

Response Surface Regression: S versus time, temp, grit, foil

The analysis was done using coded units.

Estimated Regression Coefficients for S

Term	Coef	SE Coef	T	P
Constant	64.4208	17.39	3.703	0.003
time	-0.4591	11.70	-0.039	0.969
temp	26.6976	11.70	2.281	0.040
grit	-5.2315	11.70	-0.447	0.662
foil	27.3459	11.66	2.346	0.036
time*time	23.7316	16.50	1.438	0.174
temp*temp	10.3027	16.50	0.624	0.543
grit*grit	-15.2599	16.50	-0.925	0.372
time*temp	17.5501	20.21	0.868	0.401
time*grit	26.1935	20.21	1.296	0.218
time*foil	-18.7164	20.18	-0.927	0.371
temp*grit	6.3145	20.21	0.312	0.760

```
temp*foil   30.0473    20.18   1.489  0.160
grit*foil    8.1713    20.18   0.405  0.692


S = 40.4216    PRESS = 110800
R-Sq = 60.97%  R-Sq(pred) = 0.00%  R-Sq(adj) = 21.94%


Analysis of Variance for S

Source          DF   Seq SS   Adj SS  Adj MS      F      P
Regression      13  33179.4  33179.4  2552.3   1.56  0.216
  Linear         4  17000.8  17823.2  4455.8   2.73  0.076
  Square         3   6747.4   6747.4  2249.1   1.38  0.294
  Interaction    6   9431.2   9431.2  1571.9   0.96  0.487
Residual Error  13  21240.8  21240.8  1633.9
  Lack-of-Fit   11  20984.5  20984.5  1907.7  14.89  0.065
  Pure Error     2    256.3    256.3   128.1
Total           26  54420.2


Obs  StdOrder        S       Fit  SE Fit  Residual  St Resid
  1         1   44.824   88.699  30.634   -43.875     -1.66
  2         2   87.599   55.176  30.634    32.422      1.23
  3         3   78.423  102.988  30.634   -24.565     -0.93
  4         4  191.398  139.665  30.634    51.732      1.96
  5         5   54.901   35.218  29.117    19.683      0.70
  6         6   17.083    8.412  29.117     8.671      0.31
  7         7   66.956   73.567  30.599    -6.611     -0.25
  8         8   63.200   79.447  30.599   -16.246     -0.62
  9         9   62.070   62.598  17.408    -0.528     -0.01
 10        10  118.699  102.251  30.634    16.449      0.62
 11        11   28.699   51.441  30.634   -22.742     -0.86
 12        12   93.890   38.311  30.634    55.579      2.11 R
 13        13  108.664   92.275  30.634    16.388      0.62
 14        14   48.999   50.727  29.117    -1.728     -0.06
 15        15   73.323   44.028  29.117    29.296      1.04
 16        16   45.695   45.324  30.599     0.371      0.01
 17        17  186.331  158.814  30.599    27.517      1.04
 18        18   57.176   62.598  17.408    -5.422     -0.15
 19        19   28.929   42.549  29.117   -13.620     -0.49
 20        20   25.863   79.064  29.117   -53.201     -1.90
 21        21  144.706  134.674  30.599    10.032      0.38
 22        22   71.722   96.323  30.599   -24.601     -0.93
 23        23   65.845   45.037  30.634    20.808      0.79
 24        24   54.210   81.797  30.634   -27.587     -1.05
 25        25   12.857   20.855  30.634    -7.998     -0.30
 26        26   26.480   82.873  30.634   -56.393     -2.14 R
 27        27   78.766   62.598  17.408    16.169      0.44

R denotes an observation with a large standardized residual.


Estimated Regression Coefficients for S using data in uncoded units

Term            Coef
Constant     64.4208
time        -0.459136
temp         26.6976
grit        -5.23150
foil         27.3459
time*time    23.7316
temp*temp    10.3027
```

```
grit*grit   -15.2599
time*temp    17.5501
time*grit    26.1935
time*foil   -18.7164
temp*grit    6.31454
temp*foil    30.0473
grit*foil    8.17128
```

After Second Term

Response Surface Regression: S versus time, temp, grit, foil

The analysis was done using coded units.

Estimated Regression Coefficients for S

Term	Coef	SE Coef	T	P
Constant	64.4208	16.82	3.829	0.002
time	-0.4591	11.32	-0.041	0.968
temp	26.6976	11.32	2.359	0.033
grit	-5.2315	11.32	-0.462	0.651
foil	27.3459	11.28	2.425	0.029
time*time	23.7316	15.96	1.487	0.159
temp*temp	10.3027	15.96	0.645	0.529
grit*grit	-15.2599	15.96	-0.956	0.355
time*temp	17.5501	19.55	0.898	0.384
time*grit	26.1935	19.55	1.340	0.202
time*foil	-18.7164	19.52	-0.959	0.354
temp*foil	30.0473	19.52	1.539	0.146
grit*foil	8.1713	19.52	0.419	0.682

S = 39.0972 PRESS = 96376.5
R-Sq = 60.68% R-Sq(pred) = 0.00% R-Sq(adj) = 26.97%

Analysis of Variance for S

Source	DF	Seq SS	Adj SS	Adj MS	F	P
Regression	12	33019.9	33019.9	2751.7	1.80	0.147
Linear	4	17000.8	17823.2	4455.8	2.91	0.060
Square	3	6747.4	6747.4	2249.1	1.47	0.265
Interaction	5	9271.7	9271.7	1854.3	1.21	0.353
Residual Error	14	21400.3	21400.3	1528.6		
Lack-of-Fit	12	21144.0	21144.0	1762.0	13.75	0.070
Pure Error	2	256.3	256.3	128.1		
Total	26	54420.2				

Obs	StdOrder	S	Fit	SE Fit	Residual	St Resid	
1	1	44.824	88.699	29.630	-43.875	-1.72	
2	2	87.599	55.176	29.630	32.422	1.27	
3	3	78.423	102.988	29.630	-24.565	-0.96	
4	4	191.398	139.665	29.630	51.732	2.03	R
5	5	54.901	35.218	28.163	19.683	0.73	
6	6	17.083	8.412	28.163	8.671	0.32	
7	7	66.956	73.567	29.596	-6.611	-0.26	
8	8	63.200	79.447	29.596	-16.246	-0.64	
9	9	62.070	62.598	16.838	-0.528	-0.01	
10	10	118.699	102.251	29.630	16.449	0.64	
11	11	28.699	51.441	29.630	-22.742	-0.89	
12	12	93.890	38.311	29.630	55.579	2.18	R
13	13	108.664	92.275	29.630	16.388	0.64	

14	14	48.999	50.727	28.163	-1.728	-0.06
15	15	73.323	44.028	28.163	29.296	1.08
16	16	45.695	45.324	29.596	0.371	0.01
17	17	186.331	158.814	29.596	27.517	1.08
18	18	57.176	62.598	16.838	-5.422	-0.15
19	19	28.929	42.549	28.163	-13.620	-0.50
20	20	25.863	79.064	28.163	-53.201	-1.96
21	21	144.706	134.674	29.596	10.032	0.39
22	22	71.722	96.323	29.596	-24.601	-0.96
23	23	65.845	38.722	22.266	27.123	0.84
24	24	54.210	88.111	22.266	-33.901	-1.05
25	25	12.857	27.170	22.266	-14.313	-0.45
26	26	26.480	76.559	22.266	-50.078	-1.56
27	27	78.766	62.598	16.838	16.169	0.46

R denotes an observation with a large standardized residual.

Estimated Regression Coefficients for S using data in uncoded units

Term	Coef
Constant	64.4208
time	-0.459136
temp	26.6976
grit	-5.23150
foil	27.3459
time*time	23.7316
temp*temp	10.3027
grit*grit	-15.2599
time*temp	17.5501
time*grit	26.1935
time*foil	-18.7164
temp*foil	30.0473
grit*foil	8.17128

After Third Term

Response Surface Regression: S versus time, temp, grit, foil

The analysis was done using coded units.

Estimated Regression Coefficients for S

Term	Coef	SE Coef	T	P
Constant	64.4208	16.36	3.939	0.001
time	-0.4591	11.00	-0.042	0.967
temp	26.6976	11.00	2.426	0.028
grit	-5.5947	10.97	-0.510	0.618
foil	27.3459	10.96	2.495	0.025
time*time	23.7316	15.52	1.529	0.147
temp*temp	10.3027	15.52	0.664	0.517
grit*grit	-15.2599	15.52	-0.983	0.341
time*temp	17.5501	19.00	0.924	0.370
time*grit	26.1935	19.00	1.378	0.188
time*foil	-18.7164	18.98	-0.986	0.340
temp*foil	30.0473	18.98	1.583	0.134

S = 38.0072 PRESS = 94661.1
R-Sq = 60.18% R-Sq(pred) = 0.00% R-Sq(adj) = 30.98%

Analysis of Variance for S

Source	DF	Seq SS	Adj SS	Adj MS	F	P
Regression	11	32752.1	32752.1	2977.5	2.06	0.096
Linear	4	17000.8	17872.3	4468.1	3.09	0.048
Square	3	6747.4	6747.4	2249.1	1.56	0.241
Interaction	4	9003.9	9003.9	2251.0	1.56	0.236
Residual Error	15	21668.2	21668.2	1444.5		
Lack-of-Fit	13	21411.9	21411.9	1647.1	12.85	0.074
Pure Error	2	256.3	256.3	128.1		
Total	26	54420.2				

Obs	StdOrder	S	Fit	SE Fit	Residual	St Resid	
1	1	44.824	88.699	28.804	-43.875	-1.77	
2	2	87.599	55.176	28.804	32.422	1.31	
3	3	78.423	102.988	28.804	-24.565	-0.99	
4	4	191.398	139.665	28.804	51.732	2.09	R
5	5	54.901	27.410	20.512	27.491	0.86	
6	6	17.083	16.220	20.512	0.862	0.03	
7	7	66.956	82.101	20.857	-15.145	-0.48	
8	8	63.200	70.912	20.857	-7.712	-0.24	
9	9	62.070	62.598	16.369	-0.528	-0.02	
10	10	118.699	102.069	28.801	16.630	0.67	
11	11	28.699	51.259	28.801	-22.560	-0.91	
12	12	93.890	38.493	28.801	55.397	2.23	R
13	13	108.664	92.457	28.801	16.207	0.65	
14	14	48.999	50.727	27.378	-1.728	-0.07	
15	15	73.323	44.028	27.378	29.296	1.11	
16	16	45.695	45.324	28.771	0.371	0.01	
17	17	186.331	158.814	28.771	27.517	1.11	
18	18	57.176	62.598	16.369	-5.422	-0.16	
19	19	28.929	42.549	27.378	-13.620	-0.52	
20	20	25.863	79.064	27.378	-53.201	-2.02	R
21	21	144.706	134.674	28.771	10.032	0.40	
22	22	71.722	96.323	28.771	-24.601	-0.99	
23	23	65.845	38.541	21.641	27.304	0.87	
24	24	54.210	87.930	21.641	-33.720	-1.08	
25	25	12.857	27.351	21.641	-14.494	-0.46	
26	26	26.480	76.740	21.641	-50.260	-1.61	
27	27	78.766	62.598	16.369	16.169	0.47	

R denotes an observation with a large standardized residual.

Estimated Regression Coefficients for S using data in uncoded units

Term	Coef
Constant	64.4208
time	-0.459136
temp	26.6976
grit	-5.59467
foil	27.3459
time*time	23.7316
temp*temp	10.3027
grit*grit	-15.2599
time*temp	17.5501
time*grit	26.1935
time*foil	-18.7164
temp*foil	30.0473

After Fourth Term

Response Surface Regression: S versus time, temp, grit, foil

The analysis was done using coded units.

Estimated Regression Coefficients for S

Term	Coef	SE Coef	T	P
Constant	71.2867	12.45	5.727	0.000
time	-0.4591	10.81	-0.042	0.967
temp	26.6976	10.81	2.470	0.025
grit	-5.5947	10.78	-0.519	0.611
foil	27.2316	10.77	2.529	0.022
time*time	21.1540	14.76	1.433	0.171
grit*grit	-17.8374	14.76	-1.209	0.244
time*temp	17.5501	18.67	0.940	0.361
time*grit	26.1935	18.67	1.403	0.180
time*foil	-18.7164	18.64	-1.004	0.330
temp*foil	30.0473	18.64	1.612	0.127

S = 37.3371 PRESS = 86322.3
R-Sq = 59.01% R-Sq(pred) = 0.00% R-Sq(adj) = 33.40%

Analysis of Variance for S

Source	DF	Seq SS	Adj SS	Adj MS	F	P
Regression	10	32115.3	32115.3	3211.5	2.30	0.066
Linear	4	17000.8	17799.6	4449.9	3.19	0.042
Square	2	6110.7	6110.7	3055.3	2.19	0.144
Interaction	4	9003.9	9003.9	2251.0	1.61	0.219
Residual Error	16	22304.9	22304.9	1394.1		
Lack-of-Fit	14	22048.6	22048.6	1574.9	12.29	0.078
Pure Error	2	256.3	256.3	128.1		
Total	26	54420.2				

Obs	StdOrder	S	Fit	SE Fit	Residual	St Resid	
1	1	44.824	82.692	26.864	-37.868	-1.46	
2	2	87.599	49.169	26.864	38.429	1.48	
3	3	78.423	96.981	26.864	-18.558	-0.72	
4	4	191.398	133.658	26.864	57.739	2.23	R
5	5	54.901	31.812	19.069	23.088	0.72	
6	6	17.083	20.623	19.069	-3.540	-0.11	
7	7	66.956	86.276	19.536	-19.319	-0.61	
8	8	63.200	75.086	19.536	-11.886	-0.37	
9	9	62.070	69.471	12.455	-7.401	-0.21	
10	10	118.699	103.787	28.178	14.912	0.61	
11	11	28.699	52.978	28.178	-24.279	-0.99	
12	12	93.890	40.211	28.178	53.679	2.19	R
13	13	108.664	94.175	28.178	14.488	0.59	
14	14	48.999	47.405	26.442	1.594	0.06	
15	15	73.323	40.705	26.442	32.618	1.24	
16	16	45.695	41.773	27.771	3.922	0.16	
17	17	186.331	155.263	27.771	31.068	1.24	
18	18	57.176	69.471	12.455	-12.295	-0.35	
19	19	28.929	46.952	26.094	-18.023	-0.67	
20	20	25.863	83.466	26.094	-57.603	-2.16	R
21	21	144.706	138.848	27.581	5.858	0.23	
22	22	71.722	100.497	27.581	-28.775	-1.14	
23	23	65.845	32.534	19.313	33.311	1.04	
24	24	54.210	81.923	19.313	-27.713	-0.87	
25	25	12.857	21.345	19.313	-8.488	-0.27	
26	26	26.480	70.734	19.313	-44.253	-1.38	

27	27	78.766	69.471	12.455	9.295	0.26

R denotes an observation with a large standardized residual.

Estimated Regression Coefficients for S using data in uncoded units

Term	Coef
Constant	71.2867
time	-0.459136
temp	26.6976
grit	-5.59467
foil	27.2316
time*time	21.1540
grit*grit	-17.8374
time*temp	17.5501
time*grit	26.1935
time*foil	-18.7164
temp*foil	30.0473

After Fifth Term

Response Surface Regression: S versus time, temp, grit, foil

The analysis was done using coded units.

Estimated Regression Coefficients for S

Term	Coef	SE Coef	T	P
Constant	71.2867	12.41	5.746	0.000
time	-0.4591	10.77	-0.043	0.967
temp	26.6976	10.77	2.478	0.024
grit	-5.5947	10.74	-0.521	0.609
foil	27.2316	10.73	2.538	0.021
time*time	21.1540	14.71	1.438	0.169
grit*grit	-17.8374	14.71	-1.213	0.242
time*grit	26.1935	18.60	1.408	0.177
time*foil	-18.7164	18.58	-1.007	0.328
temp*foil	30.0473	18.58	1.617	0.124

S = 37.2092 PRESS = 72582.9
R-Sq = 56.75% R-Sq(pred) = 0.00% R-Sq(adj) = 33.85%

Analysis of Variance for S

Source	DF	Seq SS	Adj SS	Adj MS	F	P
Regression	9	30883.3	30883.3	3431.5	2.48	0.051
Linear	4	17000.8	17799.6	4449.9	3.21	0.039
Square	2	6110.7	6110.7	3055.3	2.21	0.141
Interaction	3	7771.8	7771.8	2590.6	1.87	0.173
Residual Error	17	23536.9	23536.9	1384.5		
Lack-of-Fit	15	23280.6	23280.6	1552.0	12.11	0.079
Pure Error	2	256.3	256.3	128.1		
Total	26	54420.2				

Obs	StdOrder	S	Fit	SE Fit	Residual	St Resid
1	1	44.824	65.142	19.251	-20.318	-0.64
2	2	87.599	66.719	19.251	20.879	0.66
3	3	78.423	114.531	19.251	-36.108	-1.13

4	4	191.398	116.108	19.251	75.289	2.36	R
5	5	54.901	31.812	19.003	23.088	0.72	
6	6	17.083	20.623	19.003	-3.540	-0.11	
7	7	66.956	86.276	19.469	-19.319	-0.61	
8	8	63.200	75.086	19.469	-11.886	-0.37	
9	9	62.070	69.471	12.412	-7.401	-0.21	
10	10	118.699	103.787	28.082	14.912	0.61	
11	11	28.699	52.978	28.082	-24.279	-0.99	
12	12	93.890	40.211	28.082	53.679	2.20	R
13	13	108.664	94.175	28.082	14.488	0.59	
14	14	48.999	47.405	26.351	1.594	0.06	
15	15	73.323	40.705	26.351	32.618	1.24	
16	16	45.695	41.773	27.676	3.922	0.16	
17	17	186.331	155.263	27.676	31.068	1.25	
18	18	57.176	69.471	12.412	-12.295	-0.35	
19	19	28.929	46.952	26.005	-18.023	-0.68	
20	20	25.863	83.466	26.005	-57.603	-2.16	R
21	21	144.706	138.848	27.486	5.858	0.23	
22	22	71.722	100.497	27.486	-28.775	-1.15	
23	23	65.845	32.534	19.246	33.311	1.05	
24	24	54.210	81.923	19.246	-27.713	-0.87	
25	25	12.857	21.345	19.246	-8.488	-0.27	
26	26	26.480	70.734	19.246	-44.253	-1.39	
27	27	78.766	69.471	12.412	9.295	0.26	

R denotes an observation with a large standardized residual.

Estimated Regression Coefficients for S using data in uncoded units

Term	Coef
Constant	71.2867
time	-0.459136
temp	26.6976
grit	-5.59467
foil	27.2316
time*time	21.1540
grit*grit	-17.8374
time*grit	26.1935
time*foil	-18.7164
temp*foil	30.0473

After Sixth Term

Response Surface Regression: S versus time, temp, grit, foil

The analysis was done using coded units.

Estimated Regression Coefficients for S

Term	Coef	SE Coef	T	P
Constant	71.2867	12.41	5.744	0.000
time	0.3727	10.75	0.035	0.973
temp	26.6976	10.78	2.477	0.023
grit	-5.5947	10.75	-0.521	0.609
foil	27.2316	10.73	2.537	0.021
time*time	21.1540	14.72	1.438	0.168
grit*grit	-17.8374	14.72	-1.212	0.241
time*grit	26.1935	18.61	1.407	0.176
temp*foil	30.0473	18.58	1.617	0.123

S = 37.2248 PRESS = 65256.5
R-Sq = 54.17% R-Sq(pred) = 0.00% R-Sq(adj) = 33.80%

Analysis of Variance for S

Source	DF	Seq SS	Adj SS	Adj MS	F	P
Regression	8	29478.0	29478.0	3684.7	2.66	0.040
Linear	4	17000.8	17798.7	4449.7	3.21	0.037
Square	2	6110.7	6110.7	3055.3	2.20	0.139
Interaction	2	6366.5	6366.5	3183.2	2.30	0.129
Residual Error	18	24942.3	24942.3	1385.7		
Lack-of-Fit	16	24686.0	24686.0	1542.9	12.04	0.079
Pure Error	2	256.3	256.3	128.1		
Total	26	54420.2				

Obs	StdOrder	S	Fit	SE Fit	Residual	St Resid	
1	1	44.824	65.558	19.255	-20.734	-0.65	
2	2	87.599	66.303	19.255	21.295	0.67	
3	3	78.423	114.947	19.255	-36.524	-1.15	
4	4	191.398	115.692	19.255	75.705	2.38	R
5	5	54.901	31.812	19.011	23.088	0.72	
6	6	17.083	20.623	19.011	-3.540	-0.11	
7	7	66.956	86.276	19.477	-19.319	-0.61	
8	8	63.200	75.086	19.477	-11.886	-0.37	
9	9	62.070	69.471	12.417	-7.401	-0.21	
10	10	118.699	104.203	28.091	14.496	0.59	
11	11	28.699	52.562	28.091	-23.863	-0.98	
12	12	93.890	40.627	28.091	53.263	2.18	R
13	13	108.664	93.759	28.091	14.904	0.61	
14	14	48.999	47.405	26.362	1.594	0.06	
15	15	73.323	40.705	26.362	32.618	1.24	
16	16	45.695	41.773	27.688	3.922	0.16	
17	17	186.331	155.263	27.688	31.068	1.25	
18	18	57.176	69.471	12.417	-12.295	-0.35	
19	19	28.929	64.836	19.011	-35.907	-1.12	
20	20	25.863	65.582	19.011	-39.719	-1.24	
21	21	144.706	119.300	19.477	25.406	0.80	
22	22	71.722	120.045	19.477	-48.323	-1.52	
23	23	65.845	32.534	19.255	33.311	1.05	
24	24	54.210	81.923	19.255	-27.713	-0.87	
25	25	12.857	21.345	19.255	-8.488	-0.27	
26	26	26.480	70.734	19.255	-44.253	-1.39	
27	27	78.766	69.471	12.417	9.295	0.26	

R denotes an observation with a large standardized residual.

Estimated Regression Coefficients for S using data in uncoded units

Term	Coef
Constant	71.2867
time	0.372703
temp	26.6976
grit	-5.59467
foil	27.2316
time*time	21.1540
grit*grit	-17.8374
time*grit	26.1935
temp*foil	30.0473

After Seventh Term

Response Surface Regression: S versus time, temp, grit, foil

The analysis was done using coded units.

Estimated Regression Coefficients for S

Term	Coef	SE Coef	T	P
Constant	61.7783	9.735	6.346	0.000
time	0.3727	10.878	0.034	0.973
temp	26.6976	10.910	2.447	0.024
grit	-5.5947	10.878	-0.514	0.613
foil	27.3898	10.865	2.521	0.021
time*time	24.7236	14.595	1.694	0.107
time*grit	26.1935	18.841	1.390	0.181
temp*foil	30.0473	18.813	1.597	0.127

S = 37.6817 PRESS = 61360.2
R-Sq = 50.43% R-Sq(pred) = 0.00% R-Sq(adj) = 32.16%

Analysis of Variance for S

Source	DF	Seq SS	Adj SS	Adj MS	F	P
Regression	7	27441.9	27441.9	3920.3	2.76	0.037
Linear	4	17000.8	17904.0	4476.0	3.15	0.038
Square	1	4074.6	4074.6	4074.6	2.87	0.107
Interaction	2	6366.5	6366.5	3183.2	2.24	0.134
Residual Error	19	26978.3	26978.3	1419.9		
Lack-of-Fit	17	26722.0	26722.0	1571.9	12.27	0.078
Pure Error	2	256.3	256.3	128.1		
Total	26	54420.2				

Obs	StdOrder	S	Fit	SE Fit	Residual	St Resid	
1	1	44.824	59.609	18.847	-14.784	-0.45	
2	2	87.599	60.354	18.847	27.244	0.83	
3	3	78.423	108.998	18.847	-30.575	-0.94	
4	4	191.398	109.743	18.847	81.654	2.50	R
5	5	54.901	39.983	17.994	14.917	0.45	
6	6	17.083	28.794	17.994	-11.711	-0.35	
7	7	66.956	94.763	18.398	-27.806	-0.85	
8	8	63.200	83.573	18.398	-20.373	-0.62	
9	9	62.070	59.952	9.737	2.118	0.06	
10	10	118.699	116.091	26.646	2.608	0.10	
11	11	28.699	64.450	26.646	-35.751	-1.34	
12	12	93.890	52.515	26.646	41.375	1.55	
13	13	108.664	105.647	26.646	3.016	0.11	
14	14	48.999	37.738	25.436	11.261	0.41	
15	15	73.323	31.039	25.436	42.285	1.52	
16	16	45.695	32.423	26.918	13.272	0.50	
17	17	186.331	145.913	26.918	40.418	1.53	
18	18	57.176	59.952	9.737	-2.776	-0.08	
19	19	28.929	58.739	18.559	-29.810	-0.91	
20	20	25.863	59.485	18.559	-33.622	-1.03	
21	21	144.706	113.519	19.116	31.187	0.96	
22	22	71.722	114.264	19.116	-42.542	-1.31	
23	23	65.845	40.853	18.211	24.992	0.76	
24	24	54.210	90.241	18.211	-36.032	-1.09	
25	25	12.857	29.663	18.211	-16.806	-0.51	
26	26	26.480	79.052	18.211	-52.572	-1.59	

27	27	78.766	59.952	9.737	18.814	0.52

R denotes an observation with a large standardized residual.

Estimated Regression Coefficients for S using data in uncoded units

Term	Coef
Constant	61.7783
time	0.372703
temp	26.6976
grit	-5.59467
foil	27.3898
time*time	24.7236
time*grit	26.1935
temp*foil	30.0473

After Eighth Term

Response Surface Regression: S versus time, temp, grit, foil

The analysis was done using coded units.

Estimated Regression Coefficients for S

Term	Coef	SE Coef	T	P
Constant	61.7783	9.960	6.203	0.000
time	0.3727	11.129	0.033	0.974
temp	26.6976	11.161	2.392	0.027
grit	-5.5947	11.129	-0.503	0.621
foil	27.3898	11.115	2.464	0.023
time*time	24.7236	14.931	1.656	0.113
temp*foil	30.0473	19.247	1.561	0.134

S = 38.5504 PRESS = 59558.5
R-Sq = 45.38% R-Sq(pred) = 0.00% R-Sq(adj) = 29.00%

Analysis of Variance for S

Source	DF	Seq SS	Adj SS	Adj MS	F	P
Regression	6	24697.5	24697.5	4116.3	2.77	0.040
Linear	4	17000.8	17904.0	4476.0	3.01	0.043
Square	1	4074.6	4074.6	4074.6	2.74	0.113
Interaction	1	3622.1	3622.1	3622.1	2.44	0.134
Residual Error	20	29722.7	29722.7	1486.1		
Lack-of-Fit	18	29466.4	29466.4	1637.0	12.77	0.075
Pure Error	2	256.3	256.3	128.1		
Total	26	54420.2				

Obs	StdOrder	S	Fit	SE Fit	Residual	St Resid	
1	1	44.824	59.609	19.282	-14.784	-0.44	
2	2	87.599	60.354	19.282	27.244	0.82	
3	3	78.423	108.998	19.282	-30.575	-0.92	
4	4	191.398	109.743	19.282	81.654	2.45	R
5	5	54.901	39.983	18.409	14.917	0.44	
6	6	17.083	28.794	18.409	-11.711	-0.35	
7	7	66.956	94.763	18.822	-27.806	-0.83	
8	8	63.200	83.573	18.822	-20.373	-0.61	
9	9	62.070	59.952	9.962	2.118	0.06	

10	10	118.699	89.898	19.277	28.801	0.86
11	11	28.699	90.643	19.277	-61.944	-1.86
12	12	93.890	78.709	19.277	15.181	0.45
13	13	108.664	79.454	19.277	29.210	0.87
14	14	48.999	37.738	26.022	11.261	0.40
15	15	73.323	31.039	26.022	42.285	1.49
16	16	45.695	32.423	27.539	13.272	0.49
17	17	186.331	145.913	27.539	40.418	1.50
18	18	57.176	59.952	9.962	-2.776	-0.07
19	19	28.929	58.739	18.987	-29.810	-0.89
20	20	25.863	59.485	18.987	-33.622	-1.00
21	21	144.706	113.519	19.557	31.187	0.94
22	22	71.722	114.264	19.557	-42.542	-1.28
23	23	65.845	40.853	18.631	24.992	0.74
24	24	54.210	90.241	18.631	-36.032	-1.07
25	25	12.857	29.663	18.631	-16.806	-0.50
26	26	26.480	79.052	18.631	-52.572	-1.56
27	27	78.766	59.952	9.962	18.814	0.51

R denotes an observation with a large standardized residual.

Estimated Regression Coefficients for S using data in uncoded units

Term	Coef
Constant	61.7783
time	0.372703
temp	26.6976
grit	-5.59467
foil	27.3898
time*time	24.7236
temp*foil	30.0473

After Ninth Term

Response Surface Regression: S versus time, temp, foil

The analysis was done using coded units.

Estimated Regression Coefficients for S

Term	Coef	SE Coef	T	P
Constant	61.7783	9.781	6.316	0.000
time	0.3727	10.929	0.034	0.973
temp	26.6976	10.961	2.436	0.024
foil	27.3898	10.916	2.509	0.020
time*time	24.7236	14.663	1.686	0.107
temp*foil	30.0473	18.901	1.590	0.127

S = 37.8583 PRESS = 56014.4
R-Sq = 44.69% R-Sq(pred) = 0.00% R-Sq(adj) = 31.52%

Analysis of Variance for S

Source	DF	Seq SS	Adj SS	Adj MS	F	P
Regression	5	24322	24322	4864.4	3.39	0.021
Linear	3	16625	17528	5842.8	4.08	0.020
Square	1	4075	4075	4074.6	2.84	0.107
Interaction	1	3622	3622	3622.1	2.53	0.127
Residual Error	21	30098	30098	1433.3		

Lack-of-Fit	13	23827	23827	1832.8	2.34	0.116
Pure Error	8	6272	6272	784.0		
Total	26	54420				

Obs	StdOrder	S	Fit	SE Fit	Residual	St Resid	
1	1	44.824	59.609	18.935	-14.784	-0.45	
2	2	87.599	60.354	18.935	27.244	0.83	
3	3	78.423	108.998	18.935	-30.575	-0.93	
4	4	191.398	109.743	18.935	81.654	2.49	R
5	5	54.901	34.389	14.402	20.512	0.59	
6	6	17.083	34.389	14.402	-17.306	-0.49	
7	7	66.956	89.168	14.908	-22.212	-0.64	
8	8	63.200	89.168	14.908	-25.968	-0.75	
9	9	62.070	59.952	9.783	2.118	0.06	
10	10	118.699	84.303	15.457	34.396	1.00	
11	11	28.699	85.049	15.457	-56.350	-1.63	
12	12	93.890	84.303	15.457	9.586	0.28	
13	13	108.664	85.049	15.457	23.615	0.68	
14	14	48.999	37.738	25.555	11.261	0.40	
15	15	73.323	31.039	25.555	42.285	1.51	
16	16	45.695	32.423	27.044	13.272	0.50	
17	17	186.331	145.913	27.044	40.418	1.53	
18	18	57.176	59.952	9.783	-2.776	-0.08	
19	19	28.929	58.739	18.646	-29.810	-0.90	
20	20	25.863	59.485	18.646	-33.622	-1.02	
21	21	144.706	113.519	19.206	31.187	0.96	
22	22	71.722	114.264	19.206	-42.542	-1.30	
23	23	65.845	35.258	14.674	30.587	0.88	
24	24	54.210	84.647	14.674	-30.437	-0.87	
25	25	12.857	35.258	14.674	-22.401	-0.64	
26	26	26.480	84.647	14.674	-58.167	-1.67	
27	27	78.766	59.952	9.783	18.814	0.51	

R denotes an observation with a large standardized residual.

Estimated Regression Coefficients for S using data in uncoded units

Term	Coef
Constant	61.7783
time	0.372703
temp	26.6976
foil	27.3898
time*time	24.7236
temp*foil	30.0473

After Tenth Term

Response Surface Regression: S versus time, temp, foil

The analysis was done using coded units.

Estimated Regression Coefficients for S

Term	Coef	SE Coef	T	P
Constant	61.7783	10.11	6.108	0.000
time	0.3727	11.30	0.033	0.974
temp	25.3622	11.30	2.244	0.035
foil	27.3898	11.29	2.426	0.024
time*time	24.7236	15.16	1.630	0.117

S = 39.1503 PRESS = 54535.2
R-Sq = 38.04% R-Sq(pred) = 0.00% R-Sq(adj) = 26.77%

Analysis of Variance for S

Source	DF	Seq SS	Adj SS	Adj MS	F	P
Regression	4	20699.9	20699.9	5174.97	3.38	0.027
Linear	3	16625.2	16744.3	5581.44	3.64	0.028
Square	1	4074.6	4074.6	4074.64	2.66	0.117
Residual Error	22	33720.4	33720.4	1532.74		
Lack-of-Fit	14	27448.7	27448.7	1960.62	2.50	0.098
Pure Error	8	6271.7	6271.7	783.96		
Total	26	54420.2				

Obs	StdOrder	S	Fit	SE Fit	Residual	St Resid	
1	1	44.824	58.941	19.577	-14.117	-0.42	
2	2	87.599	59.686	19.577	27.912	0.82	
3	3	78.423	109.665	19.577	-31.242	-0.92	
4	4	191.398	110.411	19.577	80.987	2.39	R
5	5	54.901	34.389	14.893	20.512	0.57	
6	6	17.083	34.389	14.893	-17.306	-0.48	
7	7	66.956	89.168	15.416	-22.212	-0.62	
8	8	63.200	89.168	15.416	-25.968	-0.72	
9	9	62.070	59.952	10.117	2.118	0.06	
10	10	118.699	84.303	15.985	34.396	0.96	
11	11	28.699	85.049	15.985	-56.350	-1.58	
12	12	93.890	84.303	15.985	9.586	0.27	
13	13	108.664	85.049	15.985	23.615	0.66	
14	14	48.999	9.026	18.696	39.973	1.16	
15	15	73.323	59.751	18.696	13.573	0.39	
16	16	45.695	63.806	19.115	-18.111	-0.53	
17	17	186.331	114.530	19.115	71.801	2.10	R
18	18	57.176	59.952	10.117	-2.776	-0.07	
19	19	28.929	58.739	19.282	-29.810	-0.87	
20	20	25.863	59.485	19.282	-33.622	-0.99	
21	21	144.706	113.519	19.861	31.187	0.92	
22	22	71.722	114.264	19.861	-42.542	-1.26	
23	23	65.845	34.590	15.168	31.255	0.87	
24	24	54.210	85.315	15.168	-31.105	-0.86	
25	25	12.857	34.590	15.168	-21.733	-0.60	
26	26	26.480	85.315	15.168	-58.834	-1.63	
27	27	78.766	59.952	10.117	18.814	0.50	

R denotes an observation with a large standardized residual.

Estimated Regression Coefficients for S using data in uncoded units

Term	Coef
Constant	61.7783
time	0.372703
temp	25.3622
foil	27.3898
time*time	24.7236

<u>After Eleventh Term</u>

Response Surface Regression: S versus time, temp, foil

The analysis was done using coded units.

Estimated Regression Coefficients for S

Term	Coef	SE Coef	T	P
Constant	72.7598	7.813	9.312	0.000
time	0.3727	11.702	0.032	0.975
temp	25.3622	11.702	2.167	0.041
foil	27.2071	11.688	2.328	0.029

S = 40.5372 PRESS = 54625.4
R-Sq = 30.55% R-Sq(pred) = 0.00% R-Sq(adj) = 21.49%

Analysis of Variance for S

Source	DF	Seq SS	Adj SS	Adj MS	F	P
Regression	3	16625	16625	5541.7	3.37	0.036
Linear	3	16625	16625	5541.7	3.37	0.036
Residual Error	23	37795	37795	1643.3		
Lack-of-Fit	15	31523	31523	2101.6	2.68	0.081
Pure Error	8	6272	6272	784.0		
Total	26	54420				

Obs	StdOrder	S	Fit	SE Fit	Residual	St Resid	
1	1	44.824	45.211	18.299	-0.387	-0.01	
2	2	87.599	45.957	18.299	41.642	1.15	
3	3	78.423	95.936	18.299	-17.512	-0.48	
4	4	191.398	96.681	18.299	94.717	2.62	R
5	5	54.901	45.553	13.694	9.348	0.25	
6	6	17.083	45.553	13.694	-28.470	-0.75	
7	7	66.956	99.967	14.414	-33.011	-0.87	
8	8	63.200	99.967	14.414	-36.767	-0.97	
9	9	62.070	70.946	7.809	-8.876	-0.22	
10	10	118.699	70.573	14.068	48.126	1.27	
11	11	28.699	71.319	14.068	-42.620	-1.12	
12	12	93.890	70.573	14.068	23.316	0.61	
13	13	108.664	71.319	14.068	37.345	0.98	
14	14	48.999	20.191	18.013	28.808	0.79	
15	15	73.323	70.915	18.013	2.409	0.07	
16	16	45.695	74.605	18.566	-28.910	-0.80	
17	17	186.331	125.329	18.566	61.002	1.69	
18	18	57.176	70.946	7.809	-13.770	-0.35	
19	19	28.929	45.180	18.013	-16.251	-0.45	
20	20	25.863	45.925	18.013	-20.062	-0.55	
21	21	144.706	99.594	18.566	45.112	1.25	
22	22	71.722	100.340	18.566	-28.618	-0.79	
23	23	65.845	45.584	14.068	20.261	0.53	
24	24	54.210	96.308	14.068	-42.098	-1.11	
25	25	12.857	45.584	14.068	-32.727	-0.86	
26	26	26.480	96.308	14.068	-69.828	-1.84	
27	27	78.766	70.946	7.809	7.820	0.20	

R denotes an observation with a large standardized residual.

Estimated Regression Coefficients for S using data in uncoded units

Term	Coef
Constant	72.7598
time	0.372703

temp 25.3622
foil 27.2071

After Twelfth Term

Response Surface Regression: S versus temp, foil

The analysis was done using coded units.

Estimated Regression Coefficients for S

Term	Coef	SE Coef	T	P
Constant	72.76	7.649	9.512	0.000
temp	25.36	11.456	2.214	0.037
foil	27.21	11.442	2.378	0.026

S = 39.6845 PRESS = 49187.8
R-Sq = 30.55% R-Sq(pred) = 9.61% R-Sq(adj) = 24.76%

Analysis of Variance for S

Source	DF	Seq SS	Adj SS	Adj MS	F	P
Regression	2	16624	16624	8312	5.28	0.013
Linear	2	16624	16624	8312	5.28	0.013
Residual Error	24	37797	37797	1575		
Lack-of-Fit	6	7756	7756	1293	0.77	0.600
Pure Error	18	30041	30041	1669		
Total	26	54420				

Obs	StdOrder	S	Fit	SE Fit	Residual	St Resid	
1	1	44.824	45.584	13.772	-0.759	-0.02	
2	2	87.599	45.584	13.772	42.015	1.13	
3	3	78.423	96.308	13.772	-17.885	-0.48	
4	4	191.398	96.308	13.772	95.089	2.55	R
5	5	54.901	45.553	13.406	9.348	0.25	
6	6	17.083	45.553	13.406	-28.470	-0.76	
7	7	66.956	99.967	14.111	-33.011	-0.89	
8	8	63.200	99.967	14.111	-36.767	-0.99	
9	9	62.070	70.946	7.645	-8.876	-0.23	
10	10	118.699	70.946	7.645	47.753	1.23	
11	11	28.699	70.946	7.645	-42.247	-1.08	
12	12	93.890	70.946	7.645	22.944	0.59	
13	13	108.664	70.946	7.645	37.718	0.97	
14	14	48.999	20.191	17.634	28.808	0.81	
15	15	73.323	70.915	17.634	2.409	0.07	
16	16	45.695	74.605	18.176	-28.910	-0.82	
17	17	186.331	125.329	18.176	61.002	1.73	
18	18	57.176	70.946	7.645	-13.770	-0.35	
19	19	28.929	45.553	13.406	-16.624	-0.45	
20	20	25.863	45.553	13.406	-19.690	-0.53	
21	21	144.706	99.967	14.111	44.739	1.21	
22	22	71.722	99.967	14.111	-28.245	-0.76	
23	23	65.845	45.584	13.772	20.261	0.54	
24	24	54.210	96.308	13.772	-42.098	-1.13	
25	25	12.857	45.584	13.772	-32.727	-0.88	
26	26	26.480	96.308	13.772	-69.828	-1.88	
27	27	78.766	70.946	7.645	7.820	0.20	

R denotes an observation with a large standardized residual.

Estimated Regression Coefficients for S using data in uncoded units

Term	Coef
Constant	72.7598
temp	25.3622
foil	27.2071

Summary of Final Models

Wt.% Ni Model

Estimated Regression Coefficients for wt.% Ni

Term	Coef	SE Coef	T	P
Constant	18.446	2.649	6.963	0.000
time	6.108	1.776	3.440	0.003
temp	4.613	1.776	2.598	0.019
grit	5.367	1.771	3.031	0.008
foil	-21.450	1.771	-12.115	0.000
temp*temp	10.556	2.504	4.216	0.001
grit*grit	7.631	2.504	3.047	0.007
foil*foil	14.626	2.518	5.809	0.000
time*foil	-10.321	3.062	-3.370	0.004
temp*foil	-6.824	3.062	-2.229	0.040

Wt.% Cu Model

Estimated Regression Coefficients for wt. % Cu

Term	Coef	SE Coef	T	P
Constant	75.559	3.030	24.939	0.000
time	-5.162	1.515	-3.407	0.004
temp	-2.682	1.515	-1.770	0.098
grit	-4.392	1.511	-2.907	0.011
foil	20.383	1.511	13.493	0.000
time*time	-5.225	2.266	-2.306	0.037
temp*temp	-9.538	2.266	-4.209	0.001
grit*grit	-9.562	2.266	-4.220	0.001
foil*foil	-15.051	2.278	-6.606	0.000
time*grit	-5.975	2.616	-2.284	0.039
time*foil	7.971	2.613	3.051	0.009
temp*grit	5.800	2.616	2.217	0.044
temp*foil	8.462	2.613	3.239	0.006

Initial Strength Model

Estimated Regression Coefficients for Sigma

Term	Coef	SE Coef	T	P
Constant	22.430	2.862	7.837	0.000
temp	9.378	3.177	2.952	0.007
foil	7.387	3.177	2.325	0.029
foil*foil	9.354	4.287	2.182	0.040

Final Strength Model

Estimated Regression Coefficients for S

Term	Coef	SE Coef	T	P
Constant	72.76	7.649	9.512	0.000
temp	25.36	11.456	2.214	0.037
foil	27.21	11.442	2.378	0.026

REFERENCES

1. Rahman, A.H.M.E.; Cavalli, M.N.*Diffusion Bonding of Commercailly Pure Ni using Cu Interlayer.* Materials Characterization. 2012, 69, 90-96.
2. Eagar, T.W. *Challenges in Joining Emerging Materials.* Proceedings from International Institute of Welding Conference held in Montreal, Canada, Pergamon Press, Oxford (1990)
3. *Fundamentals of Diffusion Bonding*, Welding Fundamentals and Processes, Vol 6A, ASM Handbook, ASM International, 2001, P217-221.
4. Joseph Fernandus, M., Senthilkumar, T., Balasubramanian, V., Rajakumar, S. Optimizing Diffusion Bonding Parameters to Maximize the Strength of AA6061 Aluminum and AZ31B Magnesium Alloy Joints. *Materials and Design*, 2012, 33 (1), pp. 31-41.
5. Juan, Wang; Yajiang, Li; Peng, Liu; Haoran, Geng. Microstructure and XRD analysis in the interface zone of Mg/Al Diffusion Bonding. Journal of Materials Processing Technology. 2008, 205, 146-150.
6. Shackelford, James F. *Introduction to Materials Science for Engineers*. 6th ed. Upper Saddle River, NJ: Pearson/Prentice Hall, 2005. Print.
7. Shirzadi, Amir. "Diffusion Bonding." *Diffusion Bonding*. University of Cambridge, n.d. Web. 01 Dec. 2012. http://www.msm.cam.ac.uk/phase-trans/2005/Amir/bond.html.
8. Tsakiris, V., Kappel, W., Alecu, G. Solid state diffusion welding of Cu-Fe/Al/Ag and Al-Ni dissimilar metals. *Journal of Optoelectronics and Advanced Materials*, 2011, 13 (9), pp. 1176-1180.
9. Gale, W. F., and D. A. Butts. "Transient Liquid Phase Bonding." *Science and Technology of Welding and Joining* 9.4 (2004): 283-300. *SCOPUS.* Web. 24 May 2012.
10. Cook III, G.O., Sorensen, C.D.Overview of transient liquid phase and partial transient liquid phase bonding. *Journal of Materials Science*, 2011, 46 (16), pp. 5305-5323.
11. Kay, W.D. Diffusion Brazin, Welding, Brazing, and Soldering, Vol 6, ASM Handbook, ASM International, 1993, 343-344.

12. Pardon, T.; Khan, T.I.; Kabir, M.J. Modelling the Transient Liquid Phase Bonding Behaviour of a Duplex Stainless Steel Using Copper Interlayers. Materials Scient and Engineering. 2004, A 385, 220-228.
13. Shinmura, Toshiyasu; Ohsasa, Kenichi; Narita, Toshio. Isothermal Solidification Behavior During the Transient Liquid Phase Bonding Process of Nickel Using Binary Filler Metals. Materials Tranactions. 2001, 42(2) pp. 292-297.
14. Li, J., Han, Z., Xiong, J., Zhang, F., Li, W.-Y.Study on microstructure and strength of AgNi alloy/pure Al vacuum diffusion bonded joints. *Materials and Design*. 2009, 30 (8), pp. 3265-3268.
15. Lemus-Ruiz, J., et al. "Joining of Tungsten Carbide to Nickel by Direct Diffusion Bonding and using a Cu-Zn Alloy." *Journal of Materials Science* 43.18 (2008): 6296-300. *SCOPUS.* Web. 24 May 2012.
16. Cooke, K.O.[a] , Khan, T.I.[a] , Oliver, G.D.[b] Transient liquid phase diffusion bonding Al-6061 using nano-dispersed Ni coatings. *Materials and Design*. 2012, 33 (1), pp. 469-475.
17. Torun, O.; Celikyurek, I. Diffusion Bonding of Nickel Aluminide $Ni_{75}Al_{25}$ Using a Pure Nickel Interlayer. Intermetallics. 2008, 16, pp. 406-409.
18. Sabetghadam, H.; Zarei Hanzaki, A.; Araee, A. Diffusion Bonding of 410 Stainless Steel to Copper Using a Nickel Interlayer. Materials Characterization. 2010, 61, pp. 626-634.
19. Wu, Horng-Yu; Lee, Shyong; Wang, Jian-Yih. Solid-State Bonding of Iron-Based Alloys, Steel-Brass, and Aluminum Alloys. Journal of Materials Processing Technology. 1998, 75, pp. 173-179.
20. Goin, R. D. "Applications for Solid-State Joints in the Chemical Process Industry." *JOM* 60.11 (2008): 35-9. *SCOPUS.* Web. 24 May 2012.
21. Kong, T.-F., Chan, L.-C., Lee, T.-C. Weld diffusion analysis of forming bimetallic components using statistical experimental methods. *Materials and Manufacturing Processes*. 2009, 24 (4), pp. 422-430.
22. Wang, Carol Y. "Rapid Manufacturing." *CSA - Discovery Guides*. N.p., Sept. 2002. Web. 20 Nov. 2012. <http://www.csa.com/discoveryguides/rapidman/editor.php>.
23. Mishra, Rajiv S., and Murray W. Mahoney. *Friction Stir Welding and Processing*. Materials Park, OH: ASM International, 2007.
24. Groover, Mikell P. "Electron-Beam Welding." *Fundamentals of Modern Manufacturing.* 3rd ed. Hoboken, NJ: Wiley, 2007. 727.
25. Mankins, W.L.; Lamb, S. Nickel and Nickel Alloys, properties and selection: Nonferrous Alloys and Special-Purpose Materials, Vol 2 ASM Handbook, ASM International, 1990, pp. 428-445.
26. ASTM Standard E8 Standard Test Methods for Tension Testing of Metallic Materials. ASTM International. 2008.

27. Lawson, John, and John Erjavec. *Modern Statistics for Engineering and Quality Improvement*. Pacific Grove, CA: Brooks/Cole-Thomson Learning, 2000.
28. Box, G.E.P., and D. W. Behnken. "Some New Level Designs for the Study of Quantitative Variables." *Technometrics* 2.4 (1960): 455-75.
29. Shen, Zhenliang. Colour Differentiation in Digital Images. Victoria University of Technology, 2003.
30. Bhadeshia, H.K.D.H. "The Kirkendall Effect." *The Kirkendall Effect*. N.p., n.d. Web. 01 Dec. 2012. http://www.msm.cam.ac.uk/phase-trans/kirkendall.html.
31. Kejanli, Haluk, Mustafa Taşkin, Sedat Kolukisa, and Polat Topuz. "Transient Liquid Phase (tlp) Diffusion Bonding of Ti45Ni49Cu6 P/M Components Using Cu Interlayer." *The International Journal of Advanced Manufacturing Technology* 44.7-8 (2009): 695-99.
32. Aydin, Kemal, Yakup Kaya, and Nizamettin Kahraman. "Experimental Study of Diffusion Welding/Bonding of Titanium to Copper." *Experimental Study of Diffusion Welding/Bonding of Titanium to Copper* 37 (2012): 356-68.
33. Simões, Sónia, Filomena Viana, Volker Ventzke, Mustafa Koçak, A. Sofia Ramos, M. Teresa Vieira, and Manuel F. Vieira. "Diffusion Bonding of TiAl Using Ni/Al Multilayers." *Journal of Materials Science* 45.16 (2010): 4351-357.
34. Meyers, Marc A., and Krishan Kumar Chawla. *Mechanical Behavior of Materials*. 2nd ed. Cambridge: Cambridge UP, 2009.